Xsuite physics manual

CERN - Geneva, Switzerland

Contents

1 Xtrack **7**

1.1 Notation and reference frame . . . 7
1.2 Hamiltonian and particle coordinates . . . 8
1.3 Cavity time, energy errors and acceleration . . . 10
1.3.1 Implementing energy errors . . . 10
1.3.2 Acceleration . . . 11
1.4 Beam elements . . . 11
1.4.1 Drift . . . 11
1.4.1.1 Expanded Drift . . . 12
1.4.1.2 Exact Drift . . . 12
1.4.1.3 Polar Drift . . . 12
1.4.2 Dipole . . . 13
1.4.2.1 Thin dipole . . . 13
1.4.2.2 Thick dipole . . . 13
1.4.2.3 Dipole Edge effects . . . 14
1.4.2.4 Fringe field . . . 14
1.4.2.5 MAD8 fringe . . . 17
1.4.3 Combined dipole quadrupole . . . 18
1.4.4 Thin Multipole . . . 19
1.4.5 Accelerating Cavity . . . 20
1.4.6 RF-Multipole . . . 20
1.4.7 Solenoid . . . 21
1.4.8 AC-dipole . . . 22
1.4.9 Wire . . . 22
1.4.10 Misalignment . . . 24
1.4.11 Electron Lens . . . 24
1.4.11.1 Hollow electron lens - uniform annular profile . . . 24
1.5 Linear optics calculations . . . 25
1.5.1 Diagonalisation of one-turn matrix . . . 26
1.5.2 Normalisation of eigenvectors . . . 27
1.5.3 Conversion to normalized coordinates . . . 28
1.5.4 Twiss parameters . . . 30
1.5.5 Transformation to normalized coordinates . . . 32
1.5.6 Crab dispersion . . . 32
1.6 Synchrotron motion . . . 33
1.6.1 Linearized motion . . . 34

1.6.2 Smooth approximation 34

2 Xfields **37**
2.1 Fields generated by a bunch of particles 37
2.1.1 2.5D approximation 39
2.1.2 Modulated 2D 39
2.2 Lorentz force 40
2.3 Space charge 41
2.4 Beam-beam interaction (4D model) 42
2.5 Longitudinal profiles 43
2.5.1 Gaussian profile 43
2.5.2 q-Gaussian 43
2.6 FFT Poisson solver 44
2.6.1 Notation for Discrete Fourier Transform 44
2.6.2 FFT convolution - 1D case 45
2.6.3 Extension to multiple dimensionss 49
2.6.4 Green functions for 2D and 3D Poisson problems 50
2.6.4.1 3D Poisson problem, free space boundary conditions . 50
2.6.4.2 2D Poisson problem, free space boundary conditions . 52

3 "6D" beam-beam interaction **53**
3.1 Introduction 53
3.2 Direct Lorentz boost (for the weak beam) 53
3.3 Syncrho-beam mapping 55
3.3.1 Propagation of the strong beam to the collision point 56
3.3.2 Forces and kicks on weak beam particles 62
3.4 Inverse Lorentz boost (for the weak beam) 65
3.5 Bhabha scattering 66
3.5.1 Luminosity Computation 67
3.5.2 Virtual Photon Generation 68
3.5.3 Inverse Compton Scattering of Virtual Photons 69
3.6 Beamstrahlung 69
Appendices 73
A1 Detailed explanation of "the boost" transformation 73
A2 Constant charge slicing 74
A3 Considerations on the Σ-matrix description 75

4 Configuration of beam-beam lenses **77**
4.1 Introduction 77
4.2 Identification of the beam position and direction 77
4.3 Computation of beam-beam separations 78
4.4 Crossing plane and crossing angle 79
4.4.1 The crossing plane 79
4.4.2 The crossing angle 81
4.5 Transformations for the counterclockwise beam (B4) 82
4.6 Crab crossing 83
4.6.1 Configuration of beam-beam lenses for beam 1 86

4.6.2 Configuration of beam-beam lenses for beam 2 86
4.6.3 Crab bump from MAD-X twiss 87
4.7 Step-by-step configuration procedure 87
References 88

Chapter 1

Xtrack

XTrack is a 6D single particle symplectic tracking code used to compute the trajectories of individual relativistic charged particles in circular accelerators. It has been developed based on SixTrack.
The physical models are collected from the main references [1, 2, 3, 4, 5, 6, 7], which contain more details of the derivation of the maps.

1.1 Notation and reference frame

The speed, momentum, energy, rest mass, charge of a particle are indicated by v, P, E, m and q, respectively. These quantities are related by the following equations:

$$v = \beta c \qquad E^2 - P^2c^2 = m^2c^4 \qquad E = \gamma mc^2 \qquad Pc = \beta E \tag{1.1}$$

where β and γ are the relativistic factors.
In a curvilinear reference frame defined by a constant curvature h_x in the $\hat{X}, \hat{Z}$ plane and parameterized by s, the position of the particle at a time t can be written as:

$$\mathbf{Q}(t) = \mathbf{r}(s) + x\,\hat{x}(s) + y\,\hat{y}(s), \tag{1.2}$$

and therefore identified by the coordinates s, x, y, t in the reference frame defined by $\hat{x}(s)$ and $\hat{y}(s)$. In particle tracking, s is normally used as independent parameter and t as a coordinate.
The electromagnetic fields $\mathbf{E}$ and $\mathbf{B}$ can be derived in a curvilinear reference frame from the potentials $V(x, y, s, t)$ and $\mathbf{A}(x, y, s, t)$, where

$$\mathbf{A}(x, y, s, t) = A_x(x, y, s, t)\hat{x}(s) + A_y(x, y, s, t)\hat{y}(s) + A_s(x, y, s, t)\hat{z}(s) \tag{1.3}$$

and for which:

$$\mathbf{E} = -\nabla V - \frac{\partial \mathbf{A}}{\partial t} = -\partial_x V\hat{x} - \partial_y V\hat{y} - \frac{1}{1+hx}\partial_s V\hat{z} - \partial_t \mathbf{A} \tag{1.4}$$

$$\mathbf{B} = \nabla \times \mathbf{A} = \left(\partial_y A_s - \frac{\partial_s A_y}{1+hx}\right)\hat{x} + \left(\frac{\partial_s A_x - \partial_x(1+hx)A_s}{1+hx}\right)\hat{y} \tag{1.5}$$

$$+ \quad \left(\partial_x A_y - \partial_y A_x\right)\hat{z}. \tag{1.6}$$

In this reference frame the canonical momenta are:

$$P_x = m\gamma\dot{x} + qA_x, \quad P_y = m\gamma\dot{y} + qA_y, \quad P_s = m\gamma\dot{s}(1+hx)^2 + q(1+hx)A_s. \tag{1.7}$$

and the energy of a particle and the field is

$$E = qV + c\sqrt{(mc)^2 + \frac{(P_s - qA_s(1+hx))^2}{(1+hx)^2} + (P_x - qA_x)^2 + (P_x - qA_x)^2}. \tag{1.8}$$

1.2 Hamiltonian and particle coordinates

If $s(t)$ is monotonically increasing, it is possible to derive the equations of motion using s as the independent parameter, $(-t, E)$ as conjugate coordinates and $-P_s$ as Hamiltonian.

$$P_s = (1+hx)\left(\sqrt{\frac{(E-q\phi)^2}{c^2} - (mc)^2 - (P_x - qA_x)^2 - (P_y - qA_y)^2} + qA_s\right) \tag{1.9}$$

Since in accelerators the orbits of the particles are often a perturbation of the reference trajectory followed by a particle with rest mass m_0, charge q_0, speed $\beta_0 c$ and momentum P_0, one could use the following derived quantities that usually assume small values:

$$p(x,y) = \frac{m_0}{m}\frac{P(x,y)}{P_0} \qquad \chi = \frac{q}{q_0}\frac{m_0}{m} \qquad a(x,y,s) = \frac{q_0}{P_0}A(x,y,s) \tag{1.10}$$

Note that here m is used to indicate the rest mass of particles of species different from the reference particle (which has mass m_0) and not the relativistic mass. Further rescaling the energy and charge density as

$$e(x,y,s) = \frac{m_0}{m}\frac{E(x,y,s)}{P_0} \qquad \varphi(x,y,s) = \frac{q_0}{P_0 c}\phi(x,y,s)\,, \tag{1.11}$$

and as all canonical momenta scale with the same factor, we can define a new Hamiltonian $\tilde{H}$ that still satisfies the same equations of motion:

$$\begin{aligned}\tilde{H}(x,y,-t,p_x,p_y,e) &= \frac{m_0}{m}\frac{1}{P_0}H(x,y,-t,P_x,P_y,E)\\ \tilde{H} &= -(1+hx)\left(\sqrt{\left(\frac{e}{c} - \chi\varphi\right)^2 - \frac{1}{\beta_0^2\gamma_0^2} - (p_x - \chi a_x)^2 - (p_y - \chi a_y)^2} + \chi a_s\right)\end{aligned} \tag{1.12}$$

Different sets of longitudinal variables can be used:

$$\xi = s\frac{\beta}{\beta_0} - \beta c t \qquad \tau = \frac{s}{\beta_0} - ct \qquad \zeta = s - \beta_0 c t \tag{1.13}$$

$$\delta = \frac{P\frac{m_0}{m} - P_0}{P_0} \qquad p_\tau = \frac{1}{\beta_0}\frac{E\frac{m_0}{m} - E_0}{E_0} \qquad p_\zeta = \frac{1}{\beta_0^2}\frac{E\frac{m_0}{m} - E_0}{E_0} \tag{1.14}$$

where variables in the same columns are canonically conjugate.
The different variables can be easily related to each other:

$$\xi = \beta\tau = \frac{\beta}{\beta_0}\zeta \tag{1.15}$$

$$\delta = \beta p_\tau + \frac{\beta - \beta_0}{\beta_0} = \beta\beta_0 p_\zeta + \frac{\beta - \beta_0}{\beta_0} \tag{1.16}$$

The conjugate pairs can be generated by the following generating functions [1]

$$F_2 = x p_x + y p_y + \left(\frac{s}{\beta_0} - ct\right)\frac{1+\delta}{\beta} \tag{1.17}$$

$$F_2 = x p_x + y p_y + \left(\frac{s}{\beta_0} - ct\right)\left(p_\tau + \frac{1}{\beta_0}\right) \tag{1.18}$$

$$F_2 = x p_x + y p_y + \left(\frac{s}{\beta_0} - ct\right)\left(\beta_0 p_\zeta + \frac{1}{\beta_0}\right) \tag{1.19}$$

The Hamiltonians are then:

$$H_\delta = \frac{1+\delta}{\beta\beta_0} - (1+hx)\left(\sqrt{\left(\frac{1+\delta}{\beta} - \chi\varphi\right)^2 - \frac{1}{\beta_0^2\gamma_0^2} - (p_x - \chi a_x)^2 - (p_y - \chi a_y)^2} + \chi a_s\right)$$

$$H_\tau = \frac{p_\tau}{\beta_0} - (1+hx)\left(\sqrt{\left(p_\tau + \frac{1}{\beta_0} - \chi\varphi\right)^2 - \frac{1}{\beta_0^2\gamma_0^2} - (p_x - \chi a_x)^2 - (p_y - \chi a_y)^2} + \chi a_s\right)$$

$$H_\zeta = p_\zeta - (1+hx)\left(\sqrt{\left(\beta_0 p_\zeta + \frac{1}{\beta_0} - \chi\varphi\right)^2 - \frac{1}{\beta_0^2\gamma_0^2} - (p_x - \chi a_x)^2 - (p_y - \chi a_y)^2} + \chi a_s\right)$$

Note that things get complicated when using the pair (ξ, δ), as then the Hamiltonian contains terms in β, which in turn depends on the energy. In particular:

$$\frac{\partial\beta}{\partial\delta} = \beta\,\frac{1-\beta^2}{1+\delta} \tag{1.20}$$

For this reason we prefer using H_τ when deriving the equations of motion. Note that when $\varphi = 0$, the Hamiltonian simplifies into:

$$H_\tau = \frac{p_\tau}{\beta_0} - (1+hx)\left(\sqrt{(1+\delta)^2 - (p_x - \chi a_x)^2 - (p_y - \chi a_y)^2} + \chi a_s\right) \tag{1.21}$$

The following identities are useful to derive the equations of motion:

[1] $F_2(-t, p_{\text{new}}, s)$, $e = \frac{\partial F_2}{\partial(-t)}$, $q_{\text{new}} = \frac{\partial F_2}{\partial p_{\text{new}}}$, $H_{\text{new}} = H + \frac{\partial F_2}{\partial s}$

$$\delta = \sqrt{p_\tau^2 + 2p_\tau/\beta_0 + 1} - 1 \tag{1.22}$$

$$\frac{\partial \delta}{\partial p_\tau} = \frac{p_\tau + 1/\beta_0}{1+\delta} = \frac{1}{\beta} \tag{1.23}$$

$$\frac{\partial}{\partial \delta}\left(\frac{1+\delta}{\beta\beta_0}\right) = \frac{\beta}{\beta_0} \tag{1.24}$$

1.3 Cavity time, energy errors and acceleration

A cavity kick depends on:

$$\sin(2\pi f T + \phi) \tag{1.25}$$

where T is laboratory time.
For the most general case:

$$\sin(2\pi f T + \phi) = \sin\left(2\pi f \frac{s-\zeta}{\beta_0 c} + \phi\right) \tag{1.26}$$

Most codes drop the term $2\pi f s/(\beta_0 c)$ that is

$$\sin(2\pi f T + \phi) \to \sin\left(-2\pi f \frac{\zeta}{\beta_0 c} + \phi\right) \tag{1.27}$$

to make sure that a particle that is syncrhonous to the reference trajectory is in phase with the cavity.

1.3.1 Implementing energy errors

One can define

$$\begin{aligned} s &= s_0 + n(L_0 - L) + nL \\ f_{\text{rev}} &= \beta_0 c/L \\ f &= h f_{\text{rev}} \end{aligned} \tag{1.28}$$

where s_0 is the path length at the cavity turn at 0, L_0 is the design circumference, n is the turn number, h is the harmonic number, L is the new path length with an energy error. Indeed one could write $L = L_0(1 + \eta\delta_s)$ where η is a constant property of the lattice.
Multiple cavities can have their own defined L.
Using these definitions, then

$$\sin(2\pi f T + \phi) = \sin\left(2\pi h f_{\text{rev}} \frac{s_0 + n(L_0 - L) - \zeta}{\beta_0 c} + \phi\right) \tag{1.29}$$

$$= \sin\left(2\pi h f_{\text{rev}} \frac{n(L_0 - L) - \zeta}{\beta_0 c} + \phi'\right) \tag{1.30}$$

where $\phi' = \frac{2\pi h s_0}{L} + \phi$.
In MAD-X twiss and MAD8, indeed the longitudinal coordinates is directly $\zeta' = n(L_0 - L) - \zeta$ and the term $n(L_0 - L)$ is added smoothly in each thick element. This forces all the cavities to share the same L or $f_{\rm rev}$.
In SixTrack or MAD-X track, one could simply define a turn dependent phase

$$\phi = \phi_0 + 2\pi h f_{\rm rev} n(L_0 - L) \tag{1.31}$$

which is very general or in alternative add a special element that perform at each turn the following transformation:

$$\zeta_{\rm new} = (L_0 - L) - \zeta_{\rm old} \tag{1.32}$$

1.3.2 Acceleration

Accelaration can be achieved by renormalized the relative variables using a new momentum reference. This has the side effect that the fields of the magnets (expressed in normalized strength) follow the energy ramp and that the cavity frequency (if expressed in terms of the harmonic number (NB we should perhaps change this in the Xtrack interface) is updated.
The re-normalization if done once at each turn is:

$$p_{x,\rm new} = p_{x,\rm old}\frac{P_{0,\rm old}}{P_{0,\rm new}} \qquad p_{y,\rm new} = p_{y,\rm old}\frac{P_{0,\rm old}}{P_{0,\rm new}} \tag{1.33}$$

$$\delta_{\rm new} = (\delta_{\rm old} + 1)\frac{P_{0,\rm old}}{P_{0,\rm new}} - 1 \qquad p_{\tau,\rm new} = \frac{p_{\tau,\rm old}\, P_{0,\rm old}\, c + E_{0,\rm old} - E_{0,\rm new}}{P_{0,\rm new} c} \tag{1.34}$$

$$\zeta_{\rm new} = s\beta_0\left(\frac{1}{\beta_{0,\rm new}} - \frac{1}{\beta_{0,\rm old}}\right) - \zeta_{\rm old} \qquad \tau_{\rm new} = s\left(\frac{1}{\beta_{0,\rm new}} - \frac{1}{\beta_{0,\rm old}}\right) - \tau_{\rm old} \tag{1.35}$$

$$\tag{1.36}$$

1.4 Beam elements

1.4.1 Drift

A drift is a straight, field-free region ($h(x,y) = 0$, $V = 0$ and $\mathbf{A} = 0$). The exact and expanded Hamiltonian for a drift space are

$$H_\tau = \frac{p_\tau}{\beta_0} - \sqrt{(1+\delta)^2 - p_x^2 - p_y^2} \approx \frac{p_\tau}{\beta_0} - \delta + \frac{1}{2}\frac{p_x^2 + p_y^2}{1+\delta}. \tag{1.37}$$

The map is given by solving the equations of motion:

$$\frac{{\rm d}p_i}{{\rm d}s} = -\frac{\partial H}{\partial q_i} \qquad \frac{{\rm d}q_i}{{\rm d}s} = \frac{\partial H}{\partial p_i} \tag{1.38}$$

As there is no explicit dependency on the position coordinates in the Hamiltonian, the momenta remain unchanged in a drift.
For the position coordinates, we get:

$$(x)' = \frac{p_x}{p_z} \approx \frac{p_x}{1+\delta} \tag{1.39}$$

$$(y)' = \frac{p_y}{p_z} \approx \frac{p_y}{1+\delta} \tag{1.40}$$

$$(\tau)' = \frac{1}{\beta_0} - \frac{1}{\beta}\frac{1+\delta}{p_z} \approx \frac{1}{\beta_0} - \frac{1}{\beta} - \frac{1}{\beta}\frac{p_x^2+p_y^2}{2} \tag{1.41}$$

$$p_z = \sqrt{(1+\delta)^2 - p_x^2 - p_y^2} \tag{1.42}$$

1.4.1.1 Expanded Drift

The map relative to the expanded Hamiltonian is then

$$x_p = \frac{p_x}{1+\delta} \qquad y_p = \frac{p_y}{1+\delta} \tag{1.43}$$

$$x \leftarrow x + x_p l \qquad y \leftarrow y + y_p l \tag{1.44}$$

$$\zeta \leftarrow \zeta + l\left(1 - \frac{\beta_0}{\beta}\left(1 + \frac{x_p^2+y_p^2}{2}\right)\right) \tag{1.45}$$

1.4.1.2 Exact Drift

The map relative to the exact Hamiltonian is then

$$x \leftarrow x + \frac{p_x}{p_z} l \qquad y \leftarrow y + \frac{p_x}{p_z} l \tag{1.46}$$

$$\zeta \leftarrow \zeta + l\left(1 - \frac{\beta_0}{\beta}\frac{1+\delta}{p_z}\right) \tag{1.47}$$

1.4.1.3 Polar Drift

It is possible to define a "polar" drift that has the effect of rotating the reference frame [8] for instance in the x-z plane

$$p_x \leftarrow p_x \cos\theta + p_z \sin\theta \qquad p_z \leftarrow -p_x \sin\theta + p_z \cos\theta \tag{1.48}$$

$$z = -x \sin\theta \qquad x' = p_x/p_z \qquad y' = p_y/p_z \tag{1.49}$$

$$x \leftarrow x\cos\theta - x'z \qquad y \leftarrow y - x'z \qquad \tau \leftarrow \tau + z\frac{1}{\beta}\frac{1+\delta}{p_z}. \tag{1.50}$$

where θ is the angle bringing the new $\hat{x}$ towards the old $\hat{z}$. The map can be also generated by combining a rotation with a $-x\sin(\theta)$-length drift. In case of an $\hat{x}$ rotation the role of x and y are interchanged.

1.4.2 Dipole

In a curvilinear reference system with a constant curvature h in the horizontal plane a uniform magnetic field can be derived by the vector potential:

$$A_x = 0, \qquad A_y = 0, \qquad A_s = -B_y \left(x - \frac{hx^2}{2(1+hx)} \right). \tag{1.51}$$

With the following normalization $k_0 = \frac{q_0}{p} B_y$ is the inverse of the bending radius of the reference particle.

The exact and expanded Hamiltonian for a horizontal bending magnet is (eq. 2.12 in [2])

$$H = \frac{p_\tau}{\beta_0} - (1+hx)\sqrt{(1+\delta)^2 - p_x^2 - p_y^2} + \chi k_0 \left(x + \frac{hx^2}{2} \right) \tag{1.52}$$

$$\simeq \frac{p_\tau}{\beta_0} + \frac{1}{2}\frac{p_x^2 + p_y^2}{1+\delta} - (1+hx)(1+\delta) + \chi k_0 \left(x + \frac{hx^2}{2} \right) \tag{1.53}$$

1.4.2.1 Thin dipole

The map for a thin dipole kick (horizontal or vertical) from the expanded Hamiltonian is (eq. 4.12 in [4]):

$$p_x \leftarrow p_x + (h_x l - \chi k_0 l) + h_x l \delta - \chi k_0 l h_x x \tag{1.54}$$

$$p_y \leftarrow p_y - (h_y l - \chi \hat{k}_0 l) - h_y l \delta + \chi \hat{k}_0 l h_y y \tag{1.55}$$

$$\tau \leftarrow \tau - \frac{h_x x - h_y y}{\beta} l. \tag{1.56}$$

1.4.2.2 Thick dipole

Defining the following quantities,

$$G_x = \chi \frac{k_0 h_x}{1+\delta}, \qquad G_y = \chi \frac{\hat{k}_0 h_y}{1+\delta} \tag{1.57}$$

$$C_{x,y} = \cos(\sqrt{G_{x,y}} L), \qquad S_{x,y} = \sin(\sqrt{G_{x,y}} L) \tag{1.58}$$

the map relative to the expanded Hamiltonian is (eq. 4.11 in [2])

$$x \leftarrow C_x \cdot x + \frac{S_x}{\sqrt{G_x}} \frac{1}{1+\delta} \cdot p_x + \frac{\delta}{h_x}(1 - C_x) \tag{1.59}$$

$$p_x \leftarrow -\sqrt{G_x}(1+\delta) \cdot S_x \cdot x + C_x \cdot p_x + \delta\sqrt{1+\delta} \cdot S_x \tag{1.60}$$

$$y \leftarrow C_y \cdot y + \frac{S_y}{\sqrt{G_y}} \frac{1}{1+\delta} \cdot p_y + \frac{\delta}{h_y}(1 - C_y) \tag{1.61}$$

$$p_y \leftarrow -\sqrt{G_y}(1+\delta) \cdot S_y \cdot y + C_y \cdot p_y + \delta\sqrt{1+\delta} \cdot S_y \tag{1.62}$$

$$\zeta \leftarrow \zeta + L\left(1 - \frac{\beta_0}{\beta}\right) \tag{1.63}$$

$$- \frac{\beta_0}{\beta}\left[\frac{h_x S_x}{\sqrt{G_x}} \cdot x + \frac{1 - C_x}{h_x} \cdot p_x + \frac{h_y S_y}{\sqrt{G_y}} \cdot y + \frac{1 - C_y}{h_y} \cdot p_y + \delta\left(2L - \frac{S_x}{\sqrt{G_x}} - \frac{S_y}{\sqrt{G_y}}\right)\right] \tag{1.64}$$

$$- \frac{1}{4}\frac{\beta_0}{\beta}\left[G_x\left(L - \frac{C_x S_x}{\sqrt{G_x}}\right)\left(x - \frac{\delta}{h_x}\right)^2 + \left(L + \frac{C_x S_x}{\sqrt{G_x}}\right)\frac{p_x^2}{(1+\delta)^2} - \left(x - \frac{\delta}{h_x}\right)\frac{2S_x^2}{1+\delta} \cdot p_x\right. \tag{1.65}$$

$$\left. + G_y\left(L - \frac{C_y S_y}{\sqrt{G_y}}\right)\left(y - \frac{\delta}{h_y}\right)^2 + \left(L + \frac{C_y S_y}{\sqrt{G_y}}\right)\frac{p_y^2}{(1+\delta)^2} - \left(y - \frac{\delta}{h_y}\right)\frac{2S_y^2}{1+\delta} \cdot p_y\right]. \tag{1.66}$$

1.4.2.3 Dipole Edge effects

Considering the dipole edge effects from a dipole of length L and bending angle θ, the map is

$$p_x \to p_x + \frac{1+\delta}{\rho}\tan(\alpha) \cdot x$$
$$p_y \to p_y - \frac{1+\delta}{\rho}\tan(\alpha) \cdot y,$$

where the bending radius ρ and α are defined as

$$\rho^{-1} = \frac{h_x}{\sqrt{1+\delta}} \qquad\qquad \alpha = \frac{1}{2}\frac{L}{\rho} = \frac{\theta}{2}.$$

1.4.2.4 Fringe field

Based on: `https://cds.cern.ch/record/2857004`

The map of the fringe field of a bending magnet can be written as:

$$y^f = \frac{2y}{1+\sqrt{1-2\frac{\partial\Phi}{\partial p_y}y}} \tag{1.67}$$

$$x^f = x + \frac{1}{2}\frac{\partial\Phi}{\partial p_x}y^{f2} \tag{1.68}$$

$$p_y^f = p_y - \Phi y^f \tag{1.69}$$

$$\zeta^f = \zeta + \frac{\beta_0}{\beta}\frac{1}{2}\frac{\partial\Phi}{\partial\delta}y^{f2} \tag{1.70}$$

where:

$$\Phi\left(p_x, p_y, \delta\right) = \frac{k_0 x'}{1+y'^2} - gk_0^2 f_{\text{int}}\left(\frac{(1+\delta)^2 - p_y^2}{p_z^3} + x'^2\frac{(1+\delta)^2 - p_x^2}{p_z^3}\right) \tag{1.71}$$

We define:

$$\phi_0(x', y') = \frac{x'}{1+y'^2} \tag{1.72}$$

$$\phi_x(p_x, p_y, \delta) = \frac{(1+\delta)^2 - p_x^2}{p_z^3} \tag{1.73}$$

$$\phi_y(p_x, p_y, \delta) = \frac{(1+\delta)^2 - p_y^2}{p_z^3} \tag{1.74}$$

So we can rewrite:

$$\Phi\left(p_x, p_y, \delta\right) = \frac{k_0 x'}{1+y'^2} - gk_0^2 f_{\text{int}}\left(\frac{(1+\delta)^2 - p_y^2}{p_z^3} + x'^2\frac{(1+\delta)^2 - p_x^2}{p_z^3}\right) \tag{1.75}$$

so we can rewrite:

$$\Phi\left(p_x, p_y, \delta\right) = k_0\phi_0(x', y') - gk_0^2 f_{\text{int}}\left(\phi_y(p_x, p_y, \delta) + x'^2\phi_x(p_x, p_y, \delta)\right) \tag{1.76}$$

The derivatives can be written as:

$$\frac{\partial\Phi}{\partial p_x} = k_0\left(\frac{\partial\phi_0}{\partial x'}\frac{\partial x'}{\partial p_x} + \frac{\partial\phi_0}{\partial y'}\frac{\partial y'}{\partial p_x}\right) - gk_0^2 f_{\text{int}}\left(\frac{\partial\phi_y}{\partial p_x} + 2x'\frac{\partial x'}{\partial p_x}\phi_x + x'^2\frac{\partial\phi_x}{\partial p_x}\right) \tag{1.77}$$

$$\frac{\partial\Phi}{\partial p_y} = k_0\left(\frac{\partial\phi_0}{\partial x'}\frac{\partial x'}{\partial p_y} + \frac{\partial\phi_0}{\partial y'}\frac{\partial y'}{\partial p_y}\right) - gk_0^2 f_{\text{int}}\left(\frac{\partial\phi_y}{\partial p_y} + 2x'\frac{\partial x'}{\partial p_y}\phi_x + x'^2\frac{\partial\phi_x}{\partial p_y}\right) \tag{1.78}$$

$$\frac{\partial\Phi}{\partial\delta} = k_0\left(\frac{\partial\phi_0}{\partial x'}\frac{\partial x'}{\partial\delta} + \frac{\partial\phi_0}{\partial y'}\frac{\partial y'}{\partial\delta}\right) - gk_0^2 f_{\text{int}}\left(\frac{\partial\phi_y}{\partial\delta} + 2x'\frac{\partial x'}{\partial\delta}\phi_x + x'^2\frac{\partial\phi_x}{\partial\delta}\right) \tag{1.79}$$

Expression of all other quantities needed for the calculation:

$$x' = \frac{p_x}{p_z} \tag{1.80}$$
$$\frac{\partial x'}{\partial p_x} = -\frac{p_x}{p_z^2}\frac{\partial p_z}{\partial p_x} + \frac{1}{p_z} \tag{1.81}$$
$$\frac{\partial x'}{\partial p_y} = -\frac{p_x}{p_z^2}\frac{\partial p_z}{\partial p_x} \tag{1.82}$$
$$\frac{\partial x'}{\partial \delta} = -\frac{p_x}{p_z^2}\frac{\partial p_z}{\partial \delta} \tag{1.83}$$

$$y' = \frac{p_y}{p_z} \tag{1.84}$$
$$\frac{\partial y'}{\partial p_y} = -\frac{p_y}{p_z^2}\frac{\partial p_z}{\partial p_y} \tag{1.85}$$
$$\frac{\partial y'}{\partial p_y} = -\frac{p_y}{p_z^2}\frac{\partial p_z}{\partial p_y} + \frac{1}{p_z} \tag{1.86}$$
$$\frac{\partial y'}{\partial \delta} = -\frac{p_y}{p_z^2}\frac{\partial p_z}{\partial \delta} \tag{1.87}$$

$$p_z = \sqrt{(1+\delta)^2 - p_x^2 - p_y^2} \tag{1.88}$$
$$\frac{\partial p_z}{\partial p_x} = -\frac{p_x}{p_z} = -x' \tag{1.89}$$
$$\frac{\partial p_z}{\partial p_y} = -\frac{p_y}{p_z} = -y' \tag{1.90}$$
$$\frac{\partial p_z}{\partial \delta} = \frac{1+\delta}{p_z} \tag{1.91}$$

$$\phi_x = \frac{(1+\delta)^2 - p_x^2}{p_z^3} \tag{1.92}$$
$$\frac{\partial \phi_x}{\partial p_x} = -\frac{3}{p_z^4}\frac{\partial p_z}{\partial p_x}\left((1+\delta)^2 - p_x^2\right) - 2\frac{p_x}{p_z^3} \tag{1.93}$$
$$\frac{\partial \phi_x}{\partial p_y} = -\frac{3}{p_z^4}\frac{\partial p_z}{\partial p_y}\left((1+\delta)^2 - p_x^2\right) \tag{1.94}$$
$$\frac{\partial \phi_x}{\partial \delta} = -\frac{3}{p_z^4}\frac{\partial p_z}{\partial \delta}\left((1+\delta)^2 - p_x^2\right) + 2\frac{(1+\delta)}{p_z^3} \tag{1.95}$$

$$\phi_y = \frac{(1+\delta)^2 - p_y^2}{p_z^3} \tag{1.96}$$

$$\frac{\partial \phi_y}{\partial p_x} = -\frac{3}{p_z^4}\frac{\partial p_z}{\partial p_x}\left((1+\delta)^2 - p_y^2\right) \tag{1.97}$$

$$\frac{\partial \phi_y}{\partial p_y} = -\frac{3}{p_z^4}\frac{\partial p_z}{\partial p_y}\left((1+\delta)^2 - p_y^2\right) - 2\frac{p_y}{p_z^3} \tag{1.98}$$

$$\frac{\partial \phi_x}{\partial \delta} = -\frac{3}{p_z^4}\frac{\partial p_z}{\partial \delta}\left((1+\delta)^2 - p_x^2\right) + 2\frac{(1+\delta)}{p_z^3} \tag{1.99}$$

$$\phi_0 = \frac{x'}{1+y'^2} \tag{1.100}$$

$$\frac{\partial \phi_0}{\partial x'} = \frac{1}{1+y'^2} \tag{1.101}$$

$$\frac{\partial \phi_0}{\partial y'} = -\frac{2x'y'}{(1+y'^2)^2} \tag{1.102}$$

1.4.2.5 MAD8 fringe

Again nased on: `https://cds.cern.ch/record/2857004` (eq. 37)
The map of the fringe field of a bending magnet can be written as:

$$y^f = \frac{2y}{1+\sqrt{1-2\frac{\partial \Psi}{\partial p_y}y}} \tag{1.103}$$

$$x^f = x + \frac{1}{2}\frac{\partial \Psi}{\partial p_x}y^{f2} \tag{1.104}$$

$$p_y^f = p_y - \Psi y^f \tag{1.105}$$

$$\zeta^f = \zeta + \frac{\beta_0}{\beta}\frac{1}{2}\frac{\partial \Psi}{\partial \delta}y^{f2} \tag{1.106}$$

where:

$$\Psi\left(p_x, p_y, \delta\right) = k_0 \tan^{-1}\left(\frac{x'}{1+y'^2}\right) - gk_0^2 f_{\text{int}} p_z\left(1 + x'^2\left(2 + y'^2\right)\right) \tag{1.107}$$

We define:

$$\phi_0(x', y') = \frac{x'}{1+y'^2} \tag{1.108}$$

$$\phi_1(x', y') = 1 + 2x'^2 + x'^2 y'^2 \tag{1.109}$$

so we can write

$$\Psi = k_0 \tan^{-1}\left(\phi_0\right) - gk_0^2 f_{\text{int}} p_z \phi_1 \tag{1.110}$$

from which:

$$\frac{\partial \Psi}{\partial p_x} = k_0 \frac{1}{1+\phi_0^2}\frac{\partial \phi_0}{\partial p_x} - g k_0^2 f_{\text{int}} \left(\phi_1 \frac{\partial p_z}{\partial p_x} + p_z \frac{\phi_1}{\partial p_x} \right) \tag{1.111}$$

$$\frac{\partial \Psi}{\partial p_y} = k_0 \frac{1}{1+\phi_0^2}\frac{\partial \phi_0}{\partial p_y} - g k_0^2 f_{\text{int}} \left(\phi_1 \frac{\partial p_z}{\partial p_y} + p_z \frac{\phi_1}{\partial p_y} \right) \tag{1.112}$$

$$\frac{\partial \Psi}{\partial \delta} = k_0 \frac{1}{1+\phi_0^2}\frac{\partial \phi_0}{\partial \delta} - g k_0^2 f_{\text{int}} \left(\phi_1 \frac{\partial p_z}{\partial p_y} + p_z \frac{\phi_1}{\partial \delta} \right) \tag{1.113}$$

$$\tag{1.114}$$

$$\frac{\partial \phi_{0,1}}{\partial p_x} = \frac{\partial \phi_{0,1}}{\partial x'}\frac{\partial x'}{\partial p_x} + \frac{\partial \phi_{0,1}}{\partial y'}\frac{\partial y'}{\partial p_x} \tag{1.115}$$

$$\frac{\partial \phi_{0,1}}{\partial p_y} = \frac{\partial \phi_{0,1}}{\partial x'}\frac{\partial x'}{\partial p_y} + \frac{\partial \phi_{0,1}}{\partial y'}\frac{\partial y'}{\partial p_y} \tag{1.116}$$

$$\frac{\partial \phi_{0,1}}{\partial \delta} = \frac{\partial \phi_{0,1}}{\partial x'}\frac{\partial x'}{\partial \delta} + \frac{\partial \phi_{0,1}}{\partial y'}\frac{\partial y'}{\partial \delta} \tag{1.117}$$

$$\phi_0 = \frac{x'}{1+y'^2} \tag{1.118}$$

$$\frac{\partial \phi_0}{\partial x'} = \frac{1}{1+y'^2} \tag{1.119}$$

$$\frac{\partial \phi_0}{\partial y'} = -\frac{2x'y'}{(1+y'^2)^2} \tag{1.120}$$

$$\phi_1 = 1 + 2x'^2 + x'^2 y'^2 \tag{1.121}$$

$$\frac{\partial \phi_1}{\partial x'} = 4x' + 2x'y'^2 \tag{1.122}$$

$$\frac{\partial \phi_1}{\partial y'} = 2x'^2 y' \tag{1.123}$$

1.4.3 Combined dipole quadrupole

The following vector potential in curvilinear coordinates

$$A_s = -\frac{g}{1+hx}\left(\frac{x^2}{2} - \frac{y^2}{2} + \frac{hx^3}{3} \right) \tag{1.124}$$

produce a field

$$B_x = g\left(y + \frac{hxy}{1+hx} \right) \qquad B_y = gx \tag{1.125}$$

The following vector potential in curvilinear coordinates

$$A_s = -\frac{g}{1+hx}\left(\frac{x^2}{2} - \frac{y^2}{2} + \frac{hx^3}{3} - \frac{hxy^2}{2}\right) \tag{1.126}$$

produce a field

$$B_x = gy \qquad\qquad B_y = g\left(x + \frac{hy^2}{2+2hx}\right) \tag{1.127}$$

1.4.4 Thin Multipole

The effect of a thin multipole can be approximated by the following Hamiltonian
A longitudinally uniform static magnetic field can be described by the following equations

$$B_y + iB_x = \sum_{n=1} \frac{B_n + iA_n}{r_0^{n-1}}(x+iy)^{n-1} \tag{1.128}$$

$$= B_N \sum_{n=N} \frac{b_n + ia_n}{r_0^{n-1}}(x+iy)^{n-1}. \tag{1.129}$$

Usually multipole are expressed as relative to
A thin multiple idealize the effect of the field by taking the limit of the integration length going to zero while keeping constant the integrated strength. The Hamiltonian is:

$$H = -\delta(s)\chi L \Re\left[\sum_{n=0}(k_n + i\hat{k}_n)(x+iy)^{n+1}\right]. \tag{1.130}$$

where

$$k_n = n!\frac{q_0}{p_0}\frac{B_{n+1}}{r_0^n} \qquad\qquad \hat{k}_n = n!\frac{q_0}{p_0}\frac{A_{n+1}}{r_0^n}. \tag{1.131}$$

The corresponding map is:

$$p_x \leftarrow p_x - \chi L \cdot \Re\left[\sum_{n=0}\frac{1}{n!}(k_n + i\hat{k}_n)(x+iy)^n\right], \tag{1.132}$$

$$p_y \leftarrow p_y + \chi L \cdot \Im\left[\sum_{n=0}\frac{1}{n!}(k_n + i\hat{k}_n)(x+iy)^n\right], \tag{1.133}$$

In case a curvature h, the vector potential become:

$$f(x,y) = \int B_x(x,y)dy \tag{1.134}$$

$$g(x,y) = \int \partial x B_x(x,y)dy \tag{1.135}$$

$$a_s(x,y) = \frac{c_1}{1+hx} + f(x,y) - \frac{\int_1^x (1+h\tilde{x})(g(\tilde{x},y)+\tilde{x}) + hf(x,y)\,d\tilde{x}}{1+hx} \tag{1.136}$$

$$\frac{\int_1^x \left(-h\tilde{x}\left(g(x,y)\right) - \int \mathrm{bx}^{(1,0)}(\tilde{x},y)\,dy - h\int \mathrm{bx}(\tilde{x},y)\,dy - h\tilde{x}\mathrm{by}(\tilde{x},y) - \mathrm{by}(\tilde{x},y)\right)\,d\tilde{x}}{hx+1} \tag{1.137}$$

1.4.5 Accelerating Cavity

The approximated energy gain of a particle passing through an electric field of frequency $f = \frac{k}{2\pi c}$ for which:

$$V\sin(\phi - k\tau) = \int_{-l/2}^{l/2} E_s(0,0,t,s)\,\mathrm{d}s. \tag{1.138}$$

An equivalent vector potential can be derived and normalized as

$$A_s = -\frac{V}{\omega}\cos(\phi - k\tau) \qquad\qquad V_n = \frac{q_0}{P_0 c}V \tag{1.139}$$

from which one can derive the following map

$$p_\tau \leftarrow p_\tau + \chi V_n \sin(\phi - k\tau + k\frac{s-s_0}{\beta_0}), \tag{1.140}$$

where the additional terms in the phase is added in case harmonic number is not exactly integer and the phase is unlocked phase). The new δ can be updated from the new p_τ.

1.4.6 RF-Multipole

The RF-multipole generalizes the interaction of a particle with an electromagnetic field by assuming that

$$\Delta E(x,y,\tau) = q\int_{-L/2}^{L/2} E_z(x,y,t)\,\mathrm{d}s \tag{1.141}$$

$$\Delta P_x(x,y,\tau) = q\int_{-L/2}^{L/2} E_x(x,y,t) + \beta c B_y(x,y,t)\,\mathrm{d}s \tag{1.142}$$

$$\Delta P_y(x,y,\tau) = q\int_{-L/2}^{L/2} E_y(x,y,t) - \beta c B_x(x,y,t)\,\mathrm{d}s. \tag{1.143}$$

are harmonic in x, y and periodic in τ of frequency $f = \frac{k}{2\pi c}$ such that:

$$a_s(x,y,\tau) = \Re\left[\sum_{n=1}^{N}\left(k_n\cos(\phi_n - k\tau) + i\hat{k}_n\cos(\hat{\phi}_n - k\tau)\right)(x+iy)^n\right], \tag{1.144}$$

The map then follows:

$$\Delta p_x = -\sum_{n=1}^{N} \frac{\chi}{n!} \Re\left[(k_n C_n + i\hat{k}_n \hat{C}_n)(x+iy)^{(n-1)}\right], \tag{1.145}$$

$$\Delta p_y = \sum_{n=1}^{N} \frac{\chi}{n!} \Im\left[(k_n C_n + i\hat{k}_n \hat{C}_n)(x+iy)^{(n-1)}\right], \tag{1.146}$$

$$\Delta p_\tau = -\chi k \sum_{n=1}^{N} \Re\left[(k_n S_n + ik_n \hat{S}_n)(x+iy)^n\right], \tag{1.147}$$

where

$$C_n = \cos(\phi_n - \omega\Delta t) \qquad \hat{C}_n = \cos(\hat{\phi}_n - \omega\Delta t) \tag{1.148}$$

$$S_n = \sin(\phi_n - \omega\Delta t) \qquad \hat{S}_n = \sin(\hat{\phi}_n - \omega\Delta t). \tag{1.149}$$

1.4.7 Solenoid

The expanded Hamiltonian for a particle in a solenoid is

$$H = p_\zeta + \frac{1}{2}\frac{(p_x + R\cdot y)^2 + (p_y - R\cdot x)}{1+\delta},$$

where $R = \frac{1}{2}\frac{q}{P_0 c}\mathbf{B}(0,0,s)$. The map for a solenoid of length L in the thin lens approximation with the expanded Hamiltonian (eq. 4.35 in [4])

$$\begin{aligned}
x &\to \quad C\cdot x + S\cdot y \\
p_x &\to -\theta R\cdot C\cdot x + C\cdot p_x - \theta R\cdot S\cdot y + S\cdot p_y \\
y &\to -S\cdot x + C\cdot y \\
p_y &\to \quad \theta R\cdot S\cdot x - S\cdot p_x - \theta R\cdot C\cdot y + C\cdot p_y \\
\zeta &\to \zeta - \frac{\beta_0}{\beta}\frac{\theta}{1+\delta}\left(\frac{1}{2}R(x^2+y^2) + (p_x y - p_y x)\right)
\end{aligned}$$

where $R \equiv R(s_0)$, $\theta = \frac{R}{1+\delta}$, $C = \cos(\theta)$ and $S = \sin(\theta)$.

The map for a thick solenoid is (eq. 3.47, 3.48 in [1])

$$\begin{aligned}
x &\to C^2\cdot x + \frac{1}{R}\cdot S\cdot C\cdot p_x + S\cdot C\cdot y + \frac{1}{R}\cdot S^2\cdot p_y \\
p_x &\to -R\cdot S\cdot C\cdot x + C^2\cdot p_x - R\cdot S^2\cdot y + S\cdot C\cdot p_y \\
y &\to -S\cdot C\cdot x - \frac{1}{R}\cdot S^2\cdot p_x + C^2\cdot y + \frac{1}{R}\cdot S\cdot C\cdot p_y \\
p_y &\to R\cdot S^2\cdot x - S\cdot C\cdot p_x - R\cdot S\cdot C\cdot y + C^2\cdot p_y \\
\zeta &\to \zeta - \frac{L}{2}\left[R^2(x^2+y^2) + 2R\left(\frac{p_x}{1+\delta}y - \frac{p_y}{1+\delta}x\right) + \frac{p_x^2+p_y^2}{(1+\delta)^2}\right]
\end{aligned}$$

where $\theta = R\cdot L$, $C = \cos\theta$ and $S = \sin\theta$.

1.4.8 AC-dipole

The excitation amplitude of the AC-dipole is denoted by A [Tm], the excitation frequency by q_d [2π] and the phase of the excitation by ϕ. The map presented here is for a purely horizontal dipole, the map for a vertical dipole is obtained by replacing $p_x \to p_y$.
The effect of the AC-dipole is split into four stages. The turn number is denoted by n.

1. A number of free turns n_{free}, in which the AC-dipole has no effect on the motion.

2. Ramp-up of the voltage from 0 to the excitation amplitude A for $n_{\text{ramp-up}}$ turns.

$$n' = \frac{n - n_{\text{free}}}{n_{\text{ramp-up}}}$$
$$p_x \to p_x + n' \cdot \frac{A}{pc} \cdot (1+\delta) \sin\left(2\pi q_d \cdot (n - n_{\text{free}}) + \phi\right)$$

3. Constant excitation amplitude for n_{flat} turns.

$$p_x \to p_x + \frac{A}{pc} \cdot (1+\delta) \sin\left(2\pi q_d \cdot (n - n_{\text{free}}) + \phi\right)$$

4. Ramp-down of the voltage from the excitation amplitude A to 0 for $n_{\text{ramp-down}}$ turns.

$$n' = \frac{n - n_{\text{free}} - n_{\text{ramp-up}} - n_{\text{flat}} - n_{\text{ramp-down}}}{n_{\text{ramp-down}}}$$
$$p_x \to p_x + n' \cdot \frac{A}{p} \cdot (1+\delta) \sin\left(2\pi q_d \cdot (n - n_{\text{free}}) + \phi\right)$$

1.4.9 Wire

For each part we define $p_z = \sqrt{(1+\delta)^2 - x'^2 - y'^2}$, using the current values for x' and y'.
Step 1. Initial backwards drift of length $L = \frac{embl}{2}$.

$$x \to x - L \cdot \frac{x'}{p_z}$$
$$y \to y - L \cdot \frac{y'}{p_z}$$

Step 2.

$$
\begin{aligned}
y &\to y - \frac{x \cdot \sin(t_x)}{\cos\left(\arctan\left(\frac{x'}{p_z}\right) - t_x\right)} \cdot \frac{y'}{\sqrt{(1+\delta)^2 - y'^2}} \\
x &\to x \cdot \left[\cos(t_x) - \sin(t_x) \cdot \tan\left(\arctan\left(\frac{x'}{p_z}\right) - t_x\right)\right] \\
x' &\to \sqrt{(1+\delta)^2 - y'^2} \cdot \sin\left(\arctan\left(\frac{x'}{p_z}\right) - t_x\right) \\
x &\to x - \frac{y \cdot \sin(t_y)}{\cos\left(\arctan\left(\frac{y'}{p_z}\right) - t_y\right)} \cdot \frac{x'}{\sqrt{(1+\delta)^2 - x'^2}} \\
y &\to y \left[\cos(t_y) - \sin(t_y) \cdot \tan\left(\arctan\left(\frac{y'}{p_z}\right) - t_y\right)\right] \\
y' &\to \sqrt{(1+\delta)^2 - x'^2} \sin\left(\arctan\left(\frac{y'}{p_z}\right) - t_y\right)
\end{aligned}
$$

Step 3. Drift part of length $L = lin$.

$$
\begin{aligned}
x &\to x + L \cdot \frac{x'}{p_z} \\
y &\to y + L \cdot \frac{y'}{p_z}
\end{aligned}
$$

Step 4. Here $x_i = x - r_x$ and $y = y - r_y$.

$$
\begin{aligned}
x' &\to x' - \frac{\frac{cur \cdot 10^{-7}}{chi} \cdot x_i}{x_i^2 + y_i^2} \left[\sqrt{(lin + l)^2 + x_i^2 + y_i^2} - \sqrt{(lin - l)^2 + x_i^2 + y_i^2}\right] \\
y' &\to y' - \frac{\frac{cur \cdot 10^{-7}}{chi} \cdot y_i}{x_i^2 + y_i^2} \left[\sqrt{(lin + l)^2 + x_i^2 + y_i^2} - \sqrt{(lin - l)^2 + x_i^2 + y_i^2}\right]
\end{aligned}
$$

Step 5. Drift of length $L = leff - lin$.

$$
\begin{aligned}
x &\to x + L\frac{x'}{p_z} \\
y &\to y + L\frac{y'}{p_z}
\end{aligned}
$$

Step 6.

$$
\begin{aligned}
x &\to x - \frac{y \cdot \sin(-t_y)}{\cos\left(\arctan\left(\frac{y'}{p_z}\right) + t_y\right)} \cdot \frac{x'}{\sqrt{(1+\delta)^2 - x'^2}} \\
y &\to y \cdot \left[\cos(-t_y) - \sin(-t_y) \cdot \tan\left(\arctan\left(\frac{y'}{p_z}\right) + t_y\right)\right] \\
y' &\to \sqrt{(1+\delta)^2 - x'^2} \cdot \sin\left(\arctan\left(\frac{y'}{p_z}\right) + t_y\right) \\
y &\to y - \frac{x \cdot \sin(-t_x)}{\cos\left(\arctan\left(\frac{x'}{p_z}\right) + t_x\right)} \cdot \frac{y'}{\sqrt{(1+\delta)^2 - y'^2}} \\
x &\to x \left[\cos(-t_x) - \sin(-t_x) \cdot \tan\left(\arctan\left(\frac{x'}{p_z}\right) + t_x\right)\right] \\
x' &\to \sqrt{(1+\delta)^2 - y'^2} \cdot \sin\left(\arctan\left(\frac{x'}{p_z}\right) + t_x\right)
\end{aligned}
$$

Step 7. Shift.

$$
\begin{aligned}
x &\to x + embl \cdot \tan(t_x) \\
y &\to y + embl \cdot \frac{\tan(t_y)}{\cos(t_x)}
\end{aligned}
$$

Step 8. Negative drift of length $L = \frac{embl}{2}$.

$$
\begin{aligned}
x &\to x - L \cdot \frac{x'}{p_z} \\
y &\to y - L \cdot \frac{y'}{p_z}
\end{aligned}
$$

1.4.10 Misalignment

Misalignments of elements affects the coordinates at the entrance of an element as follows

$$
\begin{aligned}
x &\to (x - x_s) \cdot t_c + (y - y_s) \cdot t_s \\
y &\to -(x - x_s) \cdot t_s + (y - y_s) \cdot t_c,
\end{aligned}
$$

where x_s and y_s are the displacements in the horizontal and vertical directions, respectively. t_c and t_s are the cosine and sine of the tilt angle for the element.

1.4.11 Electron Lens

1.4.11.1 Hollow electron lens - uniform annular profile

For a uniform distribution of the electron beam between R_1 and R_2, the radial kick can be described by a shape function $f(r)$ and a maximum kick strength $\theta_{\max}$:

$$
\theta(r) = \frac{f(r)}{(r/R_2)} \cdot \theta_{\max} \tag{1.150}
$$

with $r = \sqrt{x^2 + y^2}$ and $\theta_{\max}$ independent of r. The shape function $f(r)$ is defined as

$$f(r) = \frac{I(r)}{I_T} = \frac{2\pi}{I_T} \int_0^r r\rho(r)dr \tag{1.151}$$

where I_T is the total electron beam current, $I(r)$ is the current enclosed in a radius r and $\rho(r)$ is the electron beam density distribution.
For a uniform profile one then obtains:

$$\begin{cases} 0 & , \quad r < R_1 \\ \frac{r^2 - R_1^2}{R_2^2 - R_1^2} & , \quad R_1 \leq r < R_2 \\ 1 & , \quad R_2 \leq r \end{cases} \tag{1.152}$$

and

$$\theta_{\max} = \theta(R_2) = \frac{2LI_T(1 \pm \beta_e\beta_p)}{4\pi\epsilon_0 (B\rho)_p \beta_e\beta_p c^2} \cdot \frac{1}{R_2} \tag{1.153}$$

where L is the length of the e-lens, I_T the total electron beam current, $\beta_{e/p}$ the relativistic β of electron/proton beam, $B\rho$ the magnetic rigidity, c the speed of light and ϵ_0 the vacuum permittivity. The $\pm$-sign represents the two cases of the electron beam traveling in the direction of the proton beam $(+)$ or in the opposite direction $(-)$. For hollow electron beam collimation, electron and proton beam travel in the same direction.
The kick in (x', y') can then be expressed as (note $\frac{x}{r} = \cos(\phi)$, $\frac{y}{r} = \sin(\phi)$):

$$x' = x' - \theta_{\max} \cdot \frac{r_2}{r^2} \cdot f(r) \cdot x \tag{1.154}$$

$$y' = y' - \theta_{\max} \cdot \frac{r_2}{r^2} \cdot f(r) \cdot y \tag{1.155}$$

If the electron lens is offset by $(x_{\text{offset}}, y_{\text{offset}})$, the coordinates (x, y) are simply transfered to:

$$\tilde{x} = x + x_{\text{offset}} \tag{1.156}$$

$$\tilde{y} = y + y_{\text{offset}} \tag{1.157}$$

$$\tilde{r} = \sqrt{\tilde{x}^2 + \tilde{y}^2} \tag{1.158}$$

and the kick is then given by:

$$x' = x' - \theta_{\max} \cdot \frac{r_2}{\tilde{r}^2} \cdot f(\tilde{r}) \cdot \tilde{x} \tag{1.159}$$

$$y' = y' - \theta_{\max} \cdot \frac{r_2}{\tilde{r}^2} \cdot f(\tilde{r}) \cdot \tilde{y} \tag{1.160}$$

1.5 Linear optics calculations

Optics calculation are needed to study the motion around the closed orbit. By defining z as the vector of $2k$ coordinates,

$$z = (z_1, \ldots, z_{2k})^T = (x - x_0, p_x - p_{x0}, y - y_0, p_y - p_{y0}, \tau - \tau_0, p_\tau - p_{\tau 0})^T \tag{1.161}$$

one can define linear transfer maps (e.g. $M_{1\to 2}$ that propagates coordinates between two points s_1, s_2) and the one-turn map (e.g. M_1 that combines the effects for one turn starting from s_1):

$$z(s_2) = M_{1\to 2} z(s_1) \qquad\qquad z(C + s_1) = M_1 z(s_1). \tag{1.162}$$

In the following we will describe the optics calculation based on the Ripken formalism described in [9]. A good summary is also given in the MAD8 physics manual [10].

1.5.1 Diagonalisation of one-turn matrix

Since the matrices derive from symplectic maps, the eigenvalue spectrum of the one-turn map M consists of $2k$ distinct eigenvalues and linearly independent eigenvectors. In addition, for the motion to be stable the eigenvalues $\lambda_k^{\pm}$ with eigenvectors $v_k^{\pm}$ have to be complex [9]:

$$M v_k^{\pm} = \lambda_k^{\pm} v_k^{\pm},\ k = 1, \ldots, 3 \tag{1.163}$$

$$v_k^{+} = (v_k^{-})^*, \quad \lambda_k^{+} = (\lambda_k^{-})^*, \quad |\lambda_k^{\pm}| = 1 \tag{1.164}$$

As the eigenvectors are linearly independent M can be diagonalized with

$$M = V \Lambda V^{-1}, \tag{1.165}$$

where V consists of the eigenvectors and Λ of the eigenvalues:

$$V = \begin{pmatrix} v_{1,1}^{+} & v_{1,1}^{-} & \cdots & v_{3,1}^{-} \\ v_{1,2}^{+} & v_{1,2}^{-} & \cdots & v_{3,2}^{-} \\ \vdots & \vdots & \vdots & \vdots \end{pmatrix} \qquad \Lambda = \begin{pmatrix} \lambda_1^{+} & & & \\ & \lambda_1^{-} & & \\ & & \ddots & \\ & & & \lambda_3^{-} \end{pmatrix} \tag{1.166}$$

for which $v_{i,j}^{\pm}$ is the component j of eigenvector $v_i^{\pm}$.
The same calculation can be carried out with real numbers by the following definitions:

$$v_k^{\pm} = a_k \pm i b_k, \qquad \lambda_k^{\pm} = \cos\mu_k \pm i \sin\mu_k, \qquad \mu_k, a_k, b_k \in \mathbb{R} \tag{1.167}$$

such that:

$$M = W R W^{-1} \tag{1.168}$$

with

$$R = R(\mu_k) = \begin{pmatrix} \cos\mu_1 & \sin\mu_1 & & & & \\ -\sin\mu_1 & \cos\mu_1 & & & & \\ & & \ddots & & & \\ & & & \cos\mu_3 & \sin\mu_3 & \\ & & & -\sin\mu_3 & \cos\mu_3 & \end{pmatrix}, \tag{1.169}$$

$$W = \begin{pmatrix} a_{1,1} & b_{1,1} & \cdots & a_{3,1} & b_{3,1} \\ a_{1,2} & b_{1,2} & \cdots & a_{3,2} & b_{3,2} \\ \vdots & \vdots & \vdots & \vdots & \\ a_{1,6} & b_{1,6} & \cdots & a_{3,6} & b_{3,6} \end{pmatrix} \tag{1.170}$$

Usually μ_k is written as $\mu_k = 2\pi Q_k$, where Q_k is then the tune of the mode k.

1.5.2 Normalisation of eigenvectors

By convention, the eigenvectors and values are normalized, sorted and rotated so that the following three conditions are fulfilled:

1. Plane 1 is associated with the horizontal, plane 2 with the vertical and plane 3 with the longitudinal plane. This is achieved by first normalizing the eigenvectors $v_k^{\pm}$ and then sorting them so that:

$$|v^+_{j,2j-1}| = |v^-_{j,2j-1}| = \max_{k=1,2,3} v_{k,j}, \quad j = 1,\ldots,3 \tag{1.171}$$

2. The eigenvectors are then rotated with a phase term ψ_k

$$v_k \to v_k \exp(i\psi_k) \tag{1.172}$$

such that

$$\text{angle}(v^+_{k,2k-1}) = 0 \leftrightarrow \psi_k = -\text{angle}(v^+_{k,2k-1}) \tag{1.173}$$

In real space, Eqn. 1.171 and 1.173 then become equivalent to:

$$|a_{j,2j-1}| = \max_{k=1,2,3} |a_{k,j}|, \qquad b_{j,2j-1} = 0, \qquad j = 1,\ldots,3 \tag{1.174}$$

This has the effect that a particle with $x = 0$ is transformed to $\tilde{x}$ in the normalized phase space.

3. The sign of $b_{k,j}$ is fixed by the symplectic condition on W

$$W^T S W = S \tag{1.175}$$

with S defined as

$$S = \begin{pmatrix} 0 & 1 & \\ -1 & 0 & \\ & & \ddots \end{pmatrix} \tag{1.176}$$

which is equivalent to:

$$\begin{aligned} &a_k^T \cdot S \cdot b_k = 1, \quad b_k^T \cdot S \cdot a_k = -1, && \text{for } k = l \\ &a_k^T \cdot S \cdot b_l = 0, && \text{for } k \neq l \\ &a_k^T \cdot S \cdot a_l = 0, \quad b_k^T \cdot S \cdot b_l = 0, && k, l = 1, \ldots, 3 \end{aligned} \tag{1.177}$$

Eqn. 1.177 yields that in phase space a_k is thus obtained by an anticlockwise rotation of b_k by $\pi/2$ and a scaling of its length with $|a_k| = \frac{1}{|b_k|}$.

1.5.3 Conversion to normalized coordinates

We will show in the following that in the normalized phase space the propagation of particle coordinates $z(s)$ from s_1 to s_2 is just a rotation by an angle ϕ_k in the $k = 1, \ldots, 3$ planes, while the amplitude I_k and initial phase $\phi_{k,0}$ stay constant, explicitly $z(s)$ is then given by:

$$z(s) = \sum_{k=1}^{3} \sqrt{2I_k} \left(a_k(s) \cos\left(\phi_{k,0} + \phi_k(s)\right) - b_k(s) \sin\left(\phi_{k,0} + \phi_k(s)\right)\right) \tag{1.178}$$

and

$$\begin{aligned} z(s_2) = W(s_2) R(\phi_k) W(s_1)^{-1} z(s_1), \\ \text{with } \phi_k = \phi_k(s_2) - \phi_k(s_1) \end{aligned} \tag{1.179}$$

This implies that one turn is simply a rotation by $\phi_k = 2\pi Q_k$ where Q_k is the tune of the mode k. In the transverse plane the tune ($Q_{I,II}$) is usually positive and the particles rotate clockwise, while in the longitudinal plane the tune (Q_{III}) is negative above γ_T leading to an anticlockwise rotation.
For the derivation the following steps are needed:

1. The effect of one turn on the normalized variable $\tilde{z}(s) = W^{-1}(s) z(s)$ is a rotation:

$$\tilde{z}(C + s) = W^{-1} z(s + C) \overset{\text{(Eqn.1.168)}}{=} W^{-1} W R W^{-1} z(s) = R\tilde{z}(s), \tag{1.180}$$

As M and R are symplectic also W is symplectic, and its inverse is thus given by

$S^{-1}W^TS$, explicitly:

$$W^{-1} = \begin{pmatrix} b_{12} & -b_{11} & b_{14} & -b_{13} & b_{16} & -b_{15} \\ -a_{12} & a_{11} & -a_{14} & a_{13} & -a_{16} & a_{15} \\ b_{22} & -b_{21} & b_{24} & -b_{23} & b_{26} & -b_{25} \\ -a_{22} & a_{21} & -a_{24} & a_{23} & -a_{26} & a_{25} \\ b_{32} & -b_{31} & b_{34} & -b_{33} & b_{36} & -b_{35} \\ -a_{32} & a_{31} & -a_{34} & a_{33} & -a_{36} & a_{35} \end{pmatrix} \tag{1.181}$$

2. The one-turn map and W-matrix can be propagated from s_1 to s_2 by

$$M_2 = M_{1\to 2} M_1 M_{1\to 2}^{-1} \qquad\qquad W_2 = M_{1\to 2} W_1 \tag{1.182}$$

As Eqn. 1.180 represents a similarity transformation, the eigenvalues are thus independent of the position s and as the rotation matrix R consists of the eigenvalues of M, the angle of the rotation $\mu_k = 2\pi Q_k$ is thus also independent of s.

3. As Eqn. 1.168 represents a basis transformation from the standard $\mathbb{R}^2$ basis to the eigenvector basis, the vectors a_k and b_k are projected onto (Eqn. 1.177):

$$\begin{aligned} \tilde{a}_1 = W^{-1}a_1 &= -SW^TSa_1 \\ &= -S(a_1Sa_1, b_1Sa_1, \ldots, b_3Sa_1)^T = (1,0,\ldots,0) \\ \tilde{b}_1 = W^{-1}b_1 &= -SW^TSb_1 \\ &= -S(a_1Sb_1, b_1Sb_1, \ldots, b_3Sb_1)^T = (0,1,\ldots,0) \\ &\ldots \\ \tilde{b}_3 = W^{-1}b_3 &= -SW^TSb_3 \\ &= -S(a_1Sb_3, b_1Sb_3, \ldots, b_3Sb_3)^T = (0,0,\ldots,1) \end{aligned} \tag{1.183}$$

in the normalized phase space.

4. From Eqn. 1.180 it follows that the amplitude I_k and initial phase ϕ_{k0} of $\tilde{z} = W^{-1}z = (\tilde{z}_{a_1}, \tilde{z}_{b_1}, \ldots, \tilde{z}_{b_3})$

$$I_k = \frac{(\tilde{z}_{a_k})^2 + (\tilde{z}_{b_k})^2}{2}, \quad k = 1,\ldots,3 \tag{1.184}$$

$$\tan\phi_{k0} = -\frac{\tilde{z}_{b_k}}{\tilde{z}_{a_k}} \tag{1.185}$$

are constants of the motion. The initial phase is defined with a minus sign in view of the definition of the Twiss parameters, where the initial phase is then added (and not subtracted) to the phase advance. The components of $\tilde{z}$ are then

explicitly given by:

$$\tilde{z}_{a_k} = \sum_{j=1}^{3} b_{k,2j} z_{2j-1} - b_{k,2j-1} z_{2j}, \quad k = 1, \ldots, 3 \tag{1.186}$$

$$\tilde{z}_{b_k} = \sum_{j=1}^{3} a_{k,2j-1} z_{2j} - a_{k,2j} z_{2j-1}, \quad k = 1, \ldots, 3. \tag{1.187}$$

An arbitrary vector $z(s)$ can thus be written in the following form:

$$\begin{aligned} z(s) &= W(s)\tilde{z}(s) \\ &= W(s) \left(\sum_{k=1}^{3} \tilde{z}_{a_k} \tilde{a}_k + \tilde{z}_{b_k} \tilde{b}_k \right) \\ &= \sum_{k=1}^{3} \tilde{z}_{a_k} W(s) \tilde{a}_k + \tilde{z}_{b_k} W(s) \tilde{b}_k \overset{\text{Eqn. 1.183}}{=} \sum_{k=1}^{3} \tilde{z}_{a_k} a_k + \tilde{z}_{b_k} b_k \\ &\overset{\text{Eqns. 1.184,1.185}}{=} \sum_{k=1}^{3} \sqrt{2I_k} \left(a_k \cos\phi_{k0} - b_k \sin\phi_{k0} \right) \end{aligned} \tag{1.188}$$

1.5.4 Twiss parameters

In the following the parameter k will always be used for the mode k and the parameter $j = 1, 2, 3$ for the horizontal (x, p_x), vertical (y, p_y) and longitudinal plane (ζ, δ) in the phase space. z_{2j-1} then stands for the coordinates (x, y, ζ) and z_{2j} for $(p_{x,y}, \delta)$.
The Twiss parameters can be introduced by writing the components of the eigenvector basis $(a_k(s), b_k(s))$ as the product of two envelope functions $\sqrt{\beta_{k,j}(s)}$, $\sqrt{\gamma_{k,j}(s)}$ and phase functions $\phi_{k,j}(s)$, $\bar{\phi}_{k,j}(s)$, also called Twiss parameters or lattice functions, with

$$\begin{aligned} a_{k,2j-1}(s) &= \sqrt{\beta_{k,j}(s)} \cos\phi_{k,j}(s), \\ b_{k,2j-1}(s) &= \sqrt{\beta_{k,j}(s)} \sin\phi_{k,j}(s), \; k, j = 1, \ldots, 3, \end{aligned} \tag{1.189}$$

$$\begin{aligned} a_{k,2j}(s) &= \sqrt{\gamma_{k,j}(s)} \cos\bar{\phi}_{k,j}(s), \\ b_{k,2j}(s) &= \sqrt{\gamma_{k,j}(s)} \sin\bar{\phi}_{k,j}(s), \; k, j = 1, \ldots, 3 \end{aligned} \tag{1.190}$$

where $\beta_{k,j}(s), \alpha_{k,j}(s), \gamma_{k,j}(s)$ represent the projection of the ellipse of mode k on the plane of coordinates $z_{2k-1} - z_{2k}$.
Using Eqns. 1.178, 1.189, 1.190 and $\cos(x + y) = \cos x \cos y - \sin x \sin y$, the coordinates $z(s)$ can be expressed by:

$$z_{2j-1}(s) = \sum_{k=1}^{3} \sqrt{2I_k \beta_{k,j}(s)} \cos\left(\phi_{k,j}(s) + \phi_{k,0}\right) \tag{1.191}$$

$$z_{2j}(s) = \sum_{k=1}^{3} \sqrt{2I_k \gamma_{k,j}(s)} \cos\left(\bar{\phi}_{k,j}(s) + \phi_{k,0}\right), \; j = 1, \ldots, 3 \tag{1.192}$$

Conversely the lattice functions can also be expressed by a_k and b_k with

$$\beta_{k,j}(s) = a_{k,2j-1}(s)^2 + b_{k,2j-1}(s)^2 \tag{1.193}$$
$$\alpha_{k,j}(s) = -a_{k,2j-1}(s)a_{k,2j}(s) - b_{k,2j-1}(s)b_{k,2j}(s) \tag{1.194}$$
$$\gamma_{k,j}(s) = a_{k,2j}(s)^2 + b_{k,2j}(s)^2, \tag{1.195}$$

The well known relations between the lattice functions

$$\sum_{j=1}^{3} \beta_{k,j}\phi'_{k,j} = 1 \tag{1.196}$$
$$\gamma_{k,j} = \frac{\beta_{k,j}^2\phi_{k,j}'^2 + \alpha_{k,j}^2}{\beta_{k,j}}, \text{ with} \tag{1.197}$$
$$\alpha_{k,j} := -\frac{1}{2}\beta'_{k,j} \tag{1.198}$$

can then be derived with the help of the normalization condition (Eqn. 1.177)

$$a_k^T S b_k = 1 \tag{1.199}$$

by the following steps:

1. As $x' = \frac{dx}{ds}$, $y' = \frac{dy}{ds}$ and $\delta = \frac{d\zeta}{ds}$ the following relations hold also for a_k and b_k:

$$a_{k,2j} = a'_{k,2j-1} = \frac{d}{ds}(a_{k,2j-1}), \tag{1.200}$$
$$b_{k,2j} = b'_{k,2j-1} = \frac{d}{ds}(b_{k,2j-1}),\ k,j = 1,\ldots,3 \tag{1.201}$$

2. The normalization condition Eqn. 1.177 can then be written as

$$\begin{aligned} a_k^T S b_k &= \sum_{j=1}^{3} \sqrt{\beta_{k,j}}\cos\phi_{k,j}\left(\sqrt{\beta_{k,j}}\sin\phi_{k,j}\right)' \\ &\quad - \left(\sqrt{\beta_{k,j}}\cos\phi_{k,j}\right)'\sqrt{\beta_{k,j}}\sin\phi_{k,j} \\ &= \sum_{j=1}^{3} \beta_{k,j}\phi'_{k,j} \\ &= 1 \end{aligned} \tag{1.202}$$

Note that Eqn. 1.202 yields the the following relation between the phase advance ϕ and β in 2D:

$$\phi(s) = \phi(0) + \int_{s_0}^{s} \frac{1}{\beta(\bar{s})} d\bar{s} \tag{1.203}$$

3. Using the abbreviation $\alpha_{k,j} := -\frac{1}{2}\beta_{k,j}$, one finds for each mode k and plane j

$$\sqrt{\gamma_{k,j}}\cos\phi_{k,j} = a_{k,2j} = a'_{k,2j-1} = (\sqrt{\beta_{k,j}}\cos\phi_{k,j})' \tag{1}$$

$$\sqrt{\gamma_{k,j}}\sin\phi_{k,j} = b_{k,2j} = b'_{k,2j-1} = (\sqrt{\beta_{k,j}}\sin\phi_{k,j})' \tag{2}$$

$$\overset{(1)^2+(2)^2}{\Rightarrow} \gamma_{k,j} = \frac{\beta_{k,j}^2\phi_{k,j}'^2 + \alpha_{k,j}^2}{\beta_{k,j}}, \quad k,j = 1,\ldots,3 \tag{1.204}$$

which simplifies in the 2D case to:

$$\gamma \overset{\text{Eqn. 1.202}}{=} \frac{1+\alpha^2}{\beta} \tag{1.205}$$

1.5.5 Transformation to normalized coordinates

The W matrix can be used to transform normalized coordinate into physical coordinates and viceversa:

$$\begin{pmatrix} x \\ p_x \\ y \\ p_y \\ \zeta \\ p_\zeta \end{pmatrix} = W \begin{pmatrix} \sqrt{\varepsilon_x}\hat{x} \\ \sqrt{\varepsilon_x}\hat{p}_x \\ \sqrt{\varepsilon_y}\hat{y} \\ \sqrt{\varepsilon_y}\hat{p}_y \\ \sqrt{\varepsilon_\zeta}\hat{\zeta} \\ \sqrt{\varepsilon_\zeta}\hat{p}_\zeta \end{pmatrix} \tag{1.206}$$

where

$$\begin{pmatrix} \hat{x} & \hat{p}_x & \hat{y} & \hat{p}_y & \hat{\zeta} & \hat{p}_\zeta \end{pmatrix} \tag{1.207}$$

are normalized coordinates in sigmas and ε_x, ε_y and ε_ζ are the geometric emittances.

1.5.6 Crab dispersion

For a particle having no betatron amplitude ($\hat{x} = \hat{p}_x = \hat{y} = \hat{p}_y = 0$) we can write:

$$x = W_{15}\hat{\zeta} + W_{16}\hat{p}_\zeta \tag{1.208}$$

$$\zeta = W_{55}\hat{\zeta} + W_{56}\hat{p}_\zeta \tag{1.209}$$

$$p_\zeta = W_{65}\hat{\zeta} + W_{66}\hat{p}_\zeta \tag{1.210}$$

The crab dispersion is:

$$D_x^\zeta = \frac{dx}{dz} \quad \text{for } p_\zeta = 0 \tag{1.211}$$

By imposing $p_\zeta = 0$ in Eq. 1.210 we obtain:

$$\hat{p}_\zeta = -\frac{W_{65}}{W_{66}}\hat{\zeta} \tag{1.212}$$

We replace in Eq. 1.209:

$$\hat{\zeta} = \left(W_{55} - \frac{W_{56}W_{65}}{W_{66}}\right)^{-1}\zeta \tag{1.213}$$

From Eq. 1.212 we obtain:

$$\hat{p}_\zeta = -\frac{W_{65}}{W_{66}}\left(W_{55} - \frac{W_{56}W_{65}}{W_{66}}\right)^{-1}\zeta \tag{1.214}$$

Replacing the last two into Eq. 1.208 we obtain:

$$x = \left(W_{15} - \frac{W_{16}W_{65}}{W_{66}}\right)\left(W_{55} - \frac{W_{56}W_{65}}{W_{66}}\right)^{-1}\zeta \tag{1.215}$$

which gives the crab dispersion:

$$D_x^\zeta = \left(W_{15} - \frac{W_{16}W_{65}}{W_{66}}\right)\left(W_{55} - \frac{W_{56}W_{65}}{W_{66}}\right)^{-1} \tag{1.216}$$

1.6 Synchrotron motion

Definition of momentum compation factor:

$$\alpha_c = \frac{\Delta C/C}{\delta} \tag{1.217}$$

Slip factor:

$$\eta = -\frac{\Delta f/f_0}{\delta} = \alpha_c - \frac{1}{\gamma_0^2} = \frac{1}{\gamma_t^2} - \frac{1}{\gamma_0^2} \tag{1.218}$$

(positive above transition)
Slippage over a single turn:

$$\Delta\zeta = -\beta_0 c\Delta T = -\beta_0 c(T - T_0) = -\beta_0 c\left(\frac{1}{f} - \frac{1}{f_0}\right) \tag{1.219}$$

$$= -\frac{\beta_0 c}{f_0}\left(\frac{1}{1+\Delta f/f_0} - 1\right) \simeq \frac{\beta_0 c}{f_0}\frac{\Delta f}{f_0} = -\eta\frac{\beta_0 c}{f_0}\delta = -\eta C\delta \tag{1.220}$$

RF kick

$$\Delta E = qV_{RF}\sin\left(2\pi h_{RF}f_0 t + \phi_{RF}\right) \tag{1.221}$$

$$= qV_{RF}\sin\left(-2\pi h_{RF}\frac{\zeta}{C} + \phi_{RF}\right) \tag{1.222}$$

$$= qV_{RF}\sin\left(-2\pi f_{RF}\frac{\zeta}{\beta_0 c} + \phi_{RF}\right) \tag{1.223}$$

from which:

$$\Delta p_\zeta = \frac{\Delta E}{\beta_0^2 E_0} = \frac{qV_{RF}}{\beta_0^2 E_0}\sin\left(-2\pi f_{RF}\frac{\zeta}{\beta_0 c} + \phi_{RF}\right) \tag{1.224}$$

1.6.1 Linearized motion

We expand around the fixed point ζ_0:

$$\Delta p_\zeta \approx \frac{qV_{RF}}{\beta_0^2 E_0} \sin\left(-2\pi f_{RF}\frac{\zeta_0}{\beta_0 c} + \phi_{RF}\right) - \frac{2\pi q f_{RF} V_{RF}}{\beta_0^3 E_0 c}(\zeta - \zeta_0)\cos\left(-2\pi f_{RF}\frac{\zeta_0}{\beta_0 c} + \phi_{RF}\right) \tag{1.225}$$

We call synchronous phase:

$$\phi_s = -2\pi f_{RF}\frac{\zeta_0}{\beta_0 c} + \phi_{RF} \tag{1.226}$$

And we call

$$\hat{\zeta} = \zeta - \zeta_0 \tag{1.227}$$

obtaining:

$$\Delta p_\zeta \approx \frac{qV_{RF}}{\beta_0^2 E_0}\sin\phi_s - \frac{2\pi q f_{RF} V_{RF}}{\beta_0^3 E_0 c}\hat{\zeta}\cos\phi_s \tag{1.228}$$

We assume that that the energy deviation of the stable fixed point is zero:

$$\Delta p_\zeta \approx -\frac{2\pi q f_{RF} V_{RF}}{\beta_0^3 E_0 c}\cos\phi_s\hat{\zeta} \tag{1.229}$$

1.6.2 Smooth approximation

Assuming that the slippage and the energy kicks are uniformly distributed along the ring we have:

$$\frac{dp_\zeta}{ds} = \frac{\Delta p_\zeta}{C} = -\frac{2\pi q V_{RF}}{\beta_0^3 C E_0 c}\cos\phi_s\hat{\zeta} \tag{1.230}$$

$$\frac{d\hat{\zeta}}{ds} = \frac{\Delta\zeta}{C} = -\eta p_\zeta \tag{1.231}$$

where we have used the approximation:

$$\beta \simeq \beta_0 \Rightarrow \delta \simeq p_\zeta \tag{1.232}$$

We derive the second equation and replace the first:

$$\frac{d^2\hat{\zeta}}{ds^2} - \frac{2\pi q\eta f_{RF} V_{RF}}{\beta_0^3 C E_0 c}\cos\phi_s\hat{\zeta} = 0 \tag{1.233}$$

The motion is stable if

$$\eta\cos\phi_s < 0 \tag{1.234}$$

In that case the solution is in the form:

$$\hat{\zeta}(s) = A \sin\left(\sqrt{-\frac{2\pi q\eta f_{RF} V_{RF}}{\beta_0^3 C E_0 c}\cos\phi_s}\, s + B\right) = A\sin\left(2\pi Q_s s/C + B\right) \tag{1.235}$$

where the synchrotron tune is given by:

$$Q_s = \sqrt{-\frac{2\pi q\eta f_{RF} V_{RF}}{\beta_0^3 C E_0 c}\cos\phi_s}\frac{C}{2\pi} = \sqrt{-\frac{q\eta f_{RF} C V_{RF}}{2\pi\beta_0^3 E_0 c}\cos\phi_s} \tag{1.236}$$

We replace

$$f_{RF} = \frac{h_{RF}\beta_0 c}{C} \tag{1.237}$$

obtaining:

$$Q_s = \sqrt{-\frac{q\eta h_{RF} V_{RF}}{2\pi\beta_0^2 E_0}\cos\phi_s} \tag{1.238}$$

The solution can be written as:

$$\hat{\zeta}(s) = \hat{\zeta}_A \cos\left(2\pi Q_s s/C\right) + B\sin\left(2\pi Q_s s/C\right) \tag{1.239}$$

Replacing in Eq. 1.231:

$$p_\zeta = -\frac{2\pi Q_s}{\eta C}\left(-\zeta_A \sin\left(2\pi Q_s s/C\right) + B\cos\left(2\pi Q_s s/C\right)\right) \tag{1.240}$$

Replacing $s = 0$:

$$p_{\zeta_A} = -\frac{2\pi Q_s}{\eta C} B \tag{1.241}$$

from which:

$$B = -\frac{\eta C}{2\pi Q_s} p_{\zeta_A} = -\beta_\zeta p_{\zeta_A} \tag{1.242}$$

where we have defined:

$$\beta_\zeta = \frac{\eta C}{2\pi Q_s} \tag{1.243}$$

Replacing

$$\hat{\zeta}(s) = \hat{\zeta}_A \cos\left(2\pi Q_s \frac{s}{C}\right) - p_{\zeta_A}\beta_\zeta \sin\left(2\pi Q_s \frac{s}{C}\right) \tag{1.244}$$

$$p_\zeta(s) = \frac{\hat{\zeta}_A}{\beta_\zeta}\sin\left(2\pi Q_s \frac{s}{C}\right) + p_{\zeta_A}\cos\left(2\pi Q_s \frac{s}{C}\right) \tag{1.245}$$

For the kick-drift mode we want to rewrite the Eq. 1.229:

$$\Delta p_\zeta = -\frac{2\pi q f_{RF} V_{RF}}{\beta_0^3 E_0 c}\cos\phi_s \hat{\zeta} \tag{1.246}$$

Chapter 2

Xfields

2.1 Fields generated by a bunch of particles

We assume that the bunch travels rigidly along s with velocity $\beta_0 c$:

$$\rho\left(x,y,s,t\right) = \rho_0\left(x,y,s-\beta_0 ct\right) \tag{2.1}$$
$$\mathbf{J}\left(x,y,s,t\right) = \beta_0 c\,\rho_0\left(x,y,s-\beta_0 ct\right)\hat{\mathbf{i}}_s \tag{2.2}$$

We define an auxiliary variable ζ as the position along the bunch:

$$\zeta = s - \beta_0 ct\,. \tag{2.3}$$

We call K the lab reference frame in which we have defined all equations above, and we introduce a boosted frame K' moving rigidly with the reference particle. The coordinates in the two systems are related by a Lorentz transformation [**?**]:

$$ct' = \gamma_0\left(ct - \beta_0 s\right) \tag{2.4}$$
$$x' = x \tag{2.5}$$
$$y' = y \tag{2.6}$$
$$s' = \gamma_0\left(s - \beta_0 ct\right) = \gamma_0\zeta \tag{2.7}$$

The corresponding inverse transformation is:

$$ct = \gamma_0\left(ct' + \beta_0 s'\right) \tag{2.8}$$
$$x = x' \tag{2.9}$$
$$y = y' \tag{2.10}$$
$$s = \gamma_0\left(s' + \beta_0 ct'\right) \tag{2.11}$$

The quantities $\left(c\rho, J_x, J_y, J_s\right)$ form a Lorentz 4-vector and therefore they are transformed between K and K' by relationships similar to the Eqs. 2.4-2.6 [**?**]:

$$c\rho'\left(\mathbf{r'},t'\right) = \gamma_0\left[c\rho\left(\mathbf{r}\left(\mathbf{r'},t'\right),t\left(\mathbf{r'},t'\right)\right) - \beta_0 J_s\left(\mathbf{r}\left(\mathbf{r'},t'\right),t\left(\mathbf{r'},t'\right)\right)\right] \tag{2.12}$$
$$J_s'\left(\mathbf{r'},t'\right) = \gamma_0\left[J_s\left(\mathbf{r}\left(\mathbf{r'},t'\right),t\left(\mathbf{r'},t'\right)\right) - \beta_0 c\rho\left(\mathbf{r}\left(\mathbf{r'},t'\right),t\left(\mathbf{r'},t'\right)\right)\right] \tag{2.13}$$

where the transformations $\mathbf{r}\left(\mathbf{r'}, t'\right)$ and $t\left(\mathbf{r'}, t'\right)$ are defined by Eqs. 2.8 and 2.11 respectively. The transverse components J_x and J_y of the current vector are invariant for our transformation, and are anyhow zero in our case.
Using Eq. 2.2 these become:

$$\rho'\left(\mathbf{r'}, t'\right) = \frac{1}{\gamma_0}\rho\left(\mathbf{r}\left(\mathbf{r'}, t'\right), t\left(\mathbf{r'}, t'\right)\right) \tag{2.14}$$

$$J'_s\left(\mathbf{r'}, t'\right) = 0 \tag{2.15}$$

Using Eqs. 2.1 and 2.8-2.10, we obtain:

$$\rho\left(x', y', s(s', t'), t(s', t')\right) = \rho_0\left(x', y', s(s', t') - \beta_0 c\, t(s', t')\right) \tag{2.16}$$

From Eq. 2.7 we get:

$$s(s', t') - \beta_0 c\, t(s', t') = \frac{s'}{\gamma_0} \tag{2.17}$$

where the coordinate t' has disappeared.
We can therefore write:

$$\rho'\left(x', y', s', t'\right) = \frac{1}{\gamma_0}\rho_0\left(x', y', \frac{s'}{\gamma_0}\right) \tag{2.18}$$

The electric potential in the bunch frame is solution of Poisson's equation:

$$\frac{\partial^2\phi'}{\partial x'^2} + \frac{\partial^2\phi'}{\partial y'^2} + \frac{\partial^2\phi'}{\partial s'^2} = -\frac{\rho'(x', y', s')}{\varepsilon_0} \tag{2.19}$$

From Eq. 2.18 we can write:

$$\frac{\partial^2\phi'}{\partial x'^2} + \frac{\partial^2\phi'}{\partial y'^2} + \frac{\partial^2\phi'}{\partial s'^2} = -\frac{1}{\gamma_0\varepsilon_0}\rho_0\left(x', y', \frac{s'}{\gamma_0}\right) \tag{2.20}$$

We now make the substitution:

$$\zeta = \frac{s'}{\gamma_0} \tag{2.21}$$

obtained from Eq. 2.7, which allows to rewrite Eq. 2.20 as:

$$\frac{\partial^2\phi'}{\partial x^2} + \frac{\partial^2\phi'}{\partial y^2} + \frac{1}{\gamma_0^2}\frac{\partial^2\phi'}{\partial \zeta^2} = -\frac{1}{\gamma_0\varepsilon_0}\rho_0\left(x, y, \zeta\right) \tag{2.22}$$

Here we have dropped the "'" sign from x and y as these coordinates are unaffected by the Lorentz boost.
The quantities $\left(\frac{\phi}{c}, A_x, A_y, A_s\right)$ form a Lorentz 4-vector, so we can write:

$$\phi = \gamma_0\left(\phi' + \beta_0 c A'_s\right) \tag{2.23}$$

$$A_s = A'_s + \beta_0\frac{\phi'}{c} \tag{2.24}$$

In the bunch frame the charges are at rest therefore $A'_x = A'_y = A'_s = 0$ therefore:

$$\phi = \gamma_0 \phi' \tag{2.25}$$

$$A_s = \beta_0 \frac{\phi'}{c} = \frac{\beta_0}{\gamma_0 c} \phi \tag{2.26}$$

Combining Eq. 2.25 with Eq. 2.22 we obtain the equation in ϕ:

$$\boxed{\frac{\partial^2 \phi}{\partial x^2} + \frac{\partial^2 \phi}{\partial y^2} + \frac{1}{\gamma_0^2} \frac{\partial^2 \phi}{\partial \zeta^2} = -\frac{1}{\varepsilon_0} \rho_0 \left(x, y, \zeta\right)} \tag{2.27}$$

2.1.1 2.5D approximation

For large enough values of γ_0, Eq. 2.22 can be approximated by:

$$\boxed{\frac{\partial^2 \phi}{\partial x^2} + \frac{\partial^2 \phi}{\partial y^2} = -\frac{1}{\varepsilon_0} \rho_0 \left(x, y, \zeta\right)} \tag{2.28}$$

which means that we can solve a simple 2D problem for each beam slice (identified by its coordinate ζ).

2.1.2 Modulated 2D

Often the beam distribution can be factorized as:

$$\rho_0(x, y, \zeta) = q_0 \lambda_0(\zeta) \rho_\perp(x, y) \tag{2.29}$$

where:

$$\int \rho_\perp(x, y)\, dx\, dy = 1 \tag{2.30}$$

and $\lambda_0(z)$ is therefore the bunch line density.
For a bunched beam:

$$\int \lambda_0(z)\, dz = N \tag{2.31}$$

where N is the bunch population.
In this case the potential can be factorized as:

$$\phi(x, y, \zeta) = q_0 \lambda(\zeta) \phi_\perp(x, y) \tag{2.32}$$

where $\phi_\perp(x, y)$ is the solution of the following 2D Poisson equation:

$$\frac{\partial^2 \phi_\perp}{\partial x^2} + \frac{\partial^2 \phi_\perp}{\partial y^2} = -\frac{1}{\varepsilon_0} \rho_\perp \left(x, y\right) \tag{2.33}$$

2.2 Lorentz force

We now compute the Lorentz force on the particles moving in the longitudinal directions, including particles of the bunch itself (space charge forces) and particles of a colliding bunch moving in the opposite directions (beam-beam forces). The angles of such test particles are neglected as done in the usual thin-lens approximation. Therefore the velocity of a test particle can be written as:

$$\mathbf{v} = \beta c\, \hat{\mathbf{i}}_s \tag{2.34}$$

The Lorenz force can be written as:

$$\begin{aligned} \mathbf{F} &= q\left(-\nabla\phi - \frac{\partial \mathbf{A}}{\partial t} + \beta c\, \hat{\mathbf{i}}_s \times (\nabla \times \mathbf{A})\right) \\ &= q\left(-\nabla\phi - \frac{\beta_0}{\gamma_0 c}\frac{\partial \phi}{\partial t}\hat{\mathbf{i}}_s + \beta c\, \hat{\mathbf{i}}_s \times (\nabla \times \mathbf{A})\right) \end{aligned} \tag{2.35}$$

We compute the vector product:

$$\begin{aligned} \hat{\mathbf{i}}_s \times (\nabla \times \mathbf{A}) &= \left(\frac{\partial A_s}{\partial x} - \frac{\partial A_x}{\partial s}\right)\hat{\mathbf{i}}_x + \left(\frac{\partial A_s}{\partial y} - \frac{\partial A_y}{\partial s}\right)\hat{\mathbf{i}}_y \\ &= \left(\frac{\partial A_s}{\partial x} - \frac{\partial A_x}{\partial s}\right)\hat{\mathbf{i}}_x + \left(\frac{\partial A_s}{\partial y} - \frac{\partial A_y}{\partial s}\right)\hat{\mathbf{i}}_y + \underbrace{\left(\frac{\partial A_s}{\partial s} - \frac{\partial A_s}{\partial s}\right)}_{=0}\hat{\mathbf{i}}_s \\ &= \nabla A_s - \frac{\partial \mathbf{A}}{\partial s} \end{aligned} \tag{2.36}$$

We replace:

$$\mathbf{F} = q\left(-\nabla\phi - \frac{\beta_0}{\gamma_0 c}\frac{\partial \phi}{\partial t}\hat{\mathbf{i}}_s + \beta\beta_0\nabla\phi - \frac{\beta\beta_0}{\gamma_0}\frac{\partial \phi}{\partial s}\hat{\mathbf{i}}_s\right) \tag{2.37}$$

The potentials will have the same form as the sources (this can be shown explicitly using the Lorentz transformations):

$$\phi(x, y, s, t) = \phi\left(x, y, t - \frac{s}{\beta_0 c}\right) \tag{2.38}$$

For a function in this form we can write:

$$\frac{\partial \phi}{\partial s} = \frac{\partial}{\partial \zeta} = -\frac{1}{\beta_0 c}\frac{\partial \phi}{\partial t} \tag{2.39}$$

obtaining:

$$\mathbf{F} = q\left(-\nabla\phi + \frac{\beta_0^2}{\gamma_0}\frac{\partial \phi}{\partial \zeta}\hat{\mathbf{i}}_s + \beta\beta_0\nabla\phi - \frac{\beta\beta_0}{\gamma_0}\frac{\partial \phi}{\partial \zeta}\hat{\mathbf{i}}_s\right) \tag{2.40}$$

Reorganizing:

$$\mathbf{F} = -q(1 - \beta\beta_0)\nabla\phi - \frac{\beta_0(\beta - \beta_0)}{\gamma_0}\frac{\partial \phi}{\partial \zeta}\hat{\mathbf{i}}_s \tag{2.41}$$

Writing the dependencies explicitly:

$$F_x(x,y,\zeta(t)) = -q(1-\beta\beta_0)\frac{\partial\phi}{\partial x}(x,y,\zeta(t)) \tag{2.42}$$

$$F_y(x,y,\zeta(t)) = -q(1-\beta\beta_0)\frac{\partial\phi}{\partial y}(x,y,\zeta(t)) \tag{2.43}$$

$$F_z(x,y,\zeta(t)) = -q\left(1-\beta\beta_0-\frac{\beta_0(\beta-\beta_0)}{\gamma_0}\right)\frac{\partial\phi}{\partial\zeta}(x,y,\zeta(t)) \tag{2.44}$$

where $\zeta(t)$ is the position of the particle within the bunch.

2.3 Space charge

Over the single interaction we neglect the particle slippage[1]:

$$\beta = \beta_0 \tag{2.45}$$

$$\zeta(t) = \zeta \tag{2.46}$$

This gives the following simplification of Eqs. (2.42) - (2.44):

$$F_x(x,y,\zeta) = -q(1-\beta_0^2)\frac{\partial\phi}{\partial x}(x,y,\zeta) \tag{2.47}$$

$$F_y(x,y,\zeta) = -q(1-\beta_0^2)\frac{\partial\phi}{\partial y}(x,y,\zeta) \tag{2.48}$$

$$F_z(x,y,\zeta) = -q(1-\beta_0^2)\frac{\partial\phi}{\partial\zeta}(x,y,\zeta) \tag{2.49}$$

In this way the force over the single interaction becomes independent on time and therefore we can compute the kicks simply as:

$$\Delta\mathbf{P} = \frac{L}{\beta_0 c}\mathbf{F} \tag{2.50}$$

where L is the portion of the machine on which we want to compute the e-cloud interaction.
The kicks on the normalized momenta can be expressed as (recalling that $P_0 = m_0\beta_0\gamma_0 c$):

$$\boxed{\Delta p_x = \frac{m_0}{m}\frac{\Delta P_x}{P_0} = -\frac{qL(1-\beta_0^2)}{m\gamma_0\beta_0^2c^2}\frac{\partial\phi}{\partial x}(x,y,\zeta)} \tag{2.51}$$

$$\boxed{\Delta p_y = \frac{m_0}{m}\frac{\Delta P_y}{P_0} = -\frac{qL(1-\beta_0^2)}{m\gamma_0\beta_0^2c^2}\frac{\partial\phi}{\partial y}(x,y,\zeta)} \tag{2.52}$$

$$\boxed{\Delta\delta \simeq \Delta p_z = \frac{m_0}{m}\frac{\Delta P_z}{P_0} = -\frac{qL(1-\beta_0^2)}{m\gamma_0\beta_0^2c^2}\frac{\partial\phi}{\partial\zeta}(x,y,\zeta)} \tag{2.53}$$

[1] In any case one would need to take into account also the dispersion in order to have the right slippage.

If the beam includes particles of different species (tracking of fragments), note that here q and m refer to the individual particle while m_0 is the mass of the reference particle.
In the modulated 2D case (see Sec. 2.1.2 and in particular Eq. 2.32), the kick can be expressed as:

$$\boxed{\Delta p_x = \frac{m_0}{m}\frac{\Delta P_x}{P_0} = -\frac{qq_0L(1-\beta_0^2)}{m\gamma_0\beta_0^2c^2}\,\lambda_0(\zeta)\,\frac{\partial\phi_\perp}{\partial x}\,(x,y)} \tag{2.54}$$

$$\boxed{\Delta p_y = \frac{m_0}{m}\frac{\Delta P_y}{P_0} = -\frac{qq_0L(1-\beta_0^2)}{m\gamma_0\beta_0^2c^2}\,\lambda_0(\zeta)\,\frac{\partial\phi_\perp}{\partial y}\,(x,y)} \tag{2.55}$$

$$\boxed{\Delta\delta \simeq \Delta p_z = \frac{m_0}{m}\frac{\Delta P_z}{P_0} = -\frac{qq_0L(1-\beta_0^2)}{m\gamma_0\beta_0^2c^2}\,\frac{d\lambda_0}{d\zeta}(\zeta)\,\phi_\perp\,(x,y)} \tag{2.56}$$

2.4 Beam-beam interaction (4D model)

We consider a test particle moving in the opposite direction with velocity:

$$\mathbf{v}_W = -\beta_{0W}c\,\hat{\mathbf{i}}_s \tag{2.57}$$
$$s_W(t) = -\beta_{0W}ct \tag{2.58}$$

Equations (2.42) - (2.44) become:

$$F_x(x,y,\zeta_W(t)) = -q(1+\beta_{0W}\beta_{0s})\frac{\partial\phi}{\partial x}(x,y,\zeta_W(t)) \tag{2.59}$$
$$F_y(x,y,\zeta_W(t)) = -q(1+\beta_{0W}\beta_{0S})\frac{\partial\phi}{\partial y}(x,y,\zeta_W(t)) \tag{2.60}$$
$$F_z(x,y,\zeta_W(t)) = -q\left(1+\beta_{0W}\beta_{0S}-\frac{\beta_{0S}(\beta_{0W}+\beta_{0S})}{\gamma_0}\right)\frac{\partial\phi}{\partial\zeta}(x,y,\zeta_W(t)) \tag{2.61}$$

where we have used the the subscript S (strong) for the bunch generating the fields, and the subscript W (weak) for the test particle.
$\zeta_W(t)$ is the position of the test particle within the bunch generating the fields:

$$\zeta_W(t) = s_W(t) - \beta_{0S}ct = -(\beta_{0W}+\beta_{0S})ct \tag{2.62}$$

In modulated-2D case (Eq. 2.32), Eqs. (2.59) - (2.60) become:

$$F_x(x,y,\zeta_W(t)) = -qq_{0S}(1+\beta_{0W}\beta_{0s})\lambda_{0S}(\zeta_W(t))\frac{\partial\phi_\perp}{\partial x}(x,y) \tag{2.63}$$
$$F_y(x,y,\zeta_W(t)) = -qq_{0S}(1+\beta_{0W}\beta_{0s})\lambda_{0S}(\zeta_W(t))\frac{\partial\phi_\perp}{\partial y}(x,y) \tag{2.64}$$
$$F_z(x,y,\zeta_W(t)) = -qq_{0S}\left(1+\beta_{0W}\beta_{0S}-\frac{\beta_{0S}(\beta_{0W}+\beta_{0S})}{\gamma_0}\right)\frac{d\lambda_{0S}}{d\zeta}(\zeta_W(t))\phi_\perp(x,y) \tag{2.65}$$

The change in momentum for the test particle is given by:

$$\Delta \mathbf{P} = \int_{-\infty}^{+\infty} \mathbf{F}(t)\, dt \tag{2.66}$$

Therefore:

$$\Delta P_x(x,y,\zeta_W(t)) = -qq_{0S}N_S(1+\beta_{0W}\beta_{0s})\frac{\partial \phi_\perp}{\partial x}(x,y)\int_{-\infty}^{+\infty}\lambda_{0S}(\zeta_W(t))\, dt \tag{2.67}$$

$$\Delta P_y(x,y,\zeta_W(t)) = -qq_{0S}N_S(1+\beta_{0W}\beta_{0s})\frac{\partial \phi_\perp}{\partial y}(x,y)\int_{-\infty}^{+\infty}\lambda_{0S}(\zeta_W(t))\, dt \tag{2.68}$$

$$\Delta P_z(x,y,\zeta_W(t)) = -qq_{0S}\left(1+\beta_{0W}\beta_{0S}-\frac{\beta_{0S}(\beta_{0W}+\beta_{0S})}{\gamma_0}\right)\phi_\perp(x,y)\int_{-\infty}^{+\infty}\frac{d\lambda_{0S}}{d\zeta}(\zeta_W(t))\, dt \tag{2.69}$$

Using Eq. (2.62) and Eq. (2.31) we can write:

$$\int_{-\infty}^{+\infty}\lambda_{0S}(\zeta_W(t))\, dt = \frac{1}{(\beta_{0W}+\beta_{0S})c}\int_{-\infty}^{+\infty}\lambda_{0S}(\zeta)\, d\zeta = \frac{N_S}{(\beta_{0W}+\beta_{0S})c} \tag{2.70}$$

Similarly, for a bunched beam:

$$\int_{-\infty}^{+\infty}\frac{d\lambda_{0S}}{d\zeta}(\zeta_W(t))\, dt = \frac{1}{(\beta_{0W}+\beta_{0S})c}\int_{-\infty}^{+\infty}\frac{d\lambda_{0S}}{d\zeta}\, d\zeta = \frac{\lambda_{0S}(+\infty)-\lambda_{0S}(-\infty)}{(\beta_{0W}+\beta_{0S})c} = 0 \tag{2.71}$$

From which we can write:

$$\boxed{\Delta p_x = \frac{m_0}{m}\frac{\Delta P_x}{P_0} = -\frac{qq_{0S}N_S}{m\beta_{0W}\gamma_{0W}c^2}\frac{(1+\beta_{0W}\beta_{0s})}{(\beta_{0W}+\beta_{0S})}\frac{\partial \phi_\perp}{\partial x}(x,y)} \tag{2.72}$$

$$\boxed{\Delta p_y = \frac{m_0}{m}\frac{\Delta P_y}{P_0} = -\frac{qq_{0S}N_S}{m\beta_{0W}\gamma_{0W}c^2}\frac{(1+\beta_{0W}\beta_{0s})}{(\beta_{0W}+\beta_{0S})}\frac{\partial \phi_\perp}{\partial y}(x,y)} \tag{2.73}$$

$$\boxed{\Delta p_z = \frac{m_0}{m}\frac{\Delta P_z}{P_0} = 0} \tag{2.74}$$

2.5 Longitudinal profiles

2.5.1 Gaussian profile

The profile is in the form:

$$\lambda_0(z) = \frac{N}{\sqrt{2\pi}\sigma}e^{-\frac{(z-z_0)^2}{2\sigma^2}} \tag{2.75}$$

2.5.2 q-Gaussian

The profile is in the form:

$$\lambda_0(z) = \frac{N\sqrt{\beta}}{C_q}e_q\left(-\beta(z-z_0)^2\right) \tag{2.76}$$

where e_q is the q-exponential function:

$$e_q(x) = [1 + (1-q)x]_+^{\frac{1}{1-q}} \tag{2.77}$$

C_q is a normalization factor dependent on q alone:

$$C_q = \frac{\sqrt{\pi}\Gamma\left(\frac{3-q}{2(q-1)}\right)}{\sqrt{q-1}\Gamma\left(\frac{1}{q-1}\right)} \tag{2.78}$$

The parameter beta defines the standard deviation of the distribution:

$$\sigma = \sqrt{\frac{1}{\beta(5-3q)}} \iff \beta = \frac{1}{\sigma^2(5-3q)} \tag{2.79}$$

These expressions are valid for values of the parameter q is the range of interest:

$$1 < q < \frac{5}{3} \tag{2.80}$$

In general the q-Gaussian is defined outside this range, but for smaller values it has a limited support (not of interest) and for larger values has a not defined standard deviation.

2.6 FFT Poisson solver

2.6.1 Notation for Discrete Fourier Transform

We will use the following notation for the Discrete Fourier Transform of a sequence of length M:

$$\hat{a}_k = \mathrm{DFT}_M(a_m) = \sum_{m=0}^{M-1} a_m \, e^{-j2\pi\frac{km}{M}} \quad \text{for } k \in 0, ..., M \tag{2.81}$$

The corresponding inverse transform is defined as:

$$a_n = \mathrm{DFT}_M^{-1}(\hat{a}_k) = \frac{1}{M}\sum_{k=0}^{M-1} \hat{a}_k \, e^{j2\pi\frac{km}{M}} \quad \text{for } m \in 0, ..., M \tag{2.82}$$

Multidimensional Discrete Fourier Transforms are obtained by applying sequentially 1D DFTs.. For example, in two dimensions:

$$\begin{aligned}\hat{a}_{k_x k_y} &= \mathrm{DFT}_{M_x M_y}\left\{a_{m_x m_y}\right\} = \mathrm{DFT}_{M_y}\left\{\mathrm{DFT}_{M_x}\left\{a_{m_x m_y}\right\}\right\} \\ &= \sum_{m_x=0}^{M_x-1} e^{-j2\pi\frac{k_x m_x}{M_x}} \sum_{m_y=0}^{M_y-1} e^{-j2\pi\frac{k_y m_y}{M_y}} a_{m_x m_y}\end{aligned} \tag{2.83}$$

$$\begin{aligned}a_{n_x n_y} &= \mathrm{DFT}^{-1}_{M_x M_y}\left\{a_{k_x k_y}\right\} = \mathrm{DFT}^{-1}_{M_y}\left\{\mathrm{DFT}^{-1}_{M_x}\left\{\hat{a}_{k_x k_y}\right\}\right\} \\ &= \frac{1}{M_x M_y}\sum_{k_x=0}^{M_x-1} e^{j2\pi\frac{k_x m_x}{M_x}} \sum_{k_y=0}^{M_y-1} e^{j2\pi\frac{k_y m_y}{M_y}} \hat{a}_{k_x k_y}\end{aligned} \tag{2.84}$$

2.6.2 FFT convolution - 1D case

The potential can be written as the convolution of a Green function with the charge distribution:

$$\phi(x) = \int_{-\infty}^{+\infty} \rho(x')\, G(x - x')dx' \tag{2.85}$$

We assume that the source is limited to the region $[0, L]$:

$$\rho(x) = \rho(x)\, \Pi_{[0,L]}\,(x) \tag{2.86}$$

where $\Pi_{[a,b]}(x)$ is a rectangular window function defined as:

$$\Pi_{[a,b]}(x) = \begin{cases} 1 & \text{for } x \in [a, b] \\ 0 & \text{elsewhere} \end{cases} \tag{2.87}$$

We are interested in the electric potential only the region occupied by the sources, so we can compute:

$$\phi_L(x) = \phi(x)\Pi_{[0,L]}\,(x) \tag{2.88}$$

We replace Eq. (2.86) and Eq. (2.88) into Eq.(2.85), obtaining:

$$\phi_L(x) = \Pi_{[0,L]}\,(x) \int_{-\infty}^{+\infty} \Pi_{[0,L]}\,(x')\, \rho(x')\, G(x - x')dx' \tag{2.89}$$

We apply the change of variable $x'' = x - x'$:

$$\phi_L(x) = \int_{-\infty}^{+\infty} \Pi_{[0,L]}\,(x)\, \Pi_{[0,L]}\,(x - x'')\, \rho(x - x'')\, G(x'')\, dx'' \tag{2.90}$$

The integrand vanishes outside the set of the (x, x'') defined by:

$$\begin{cases} 0 < x < L \\ 0 < (x - x'') < L \end{cases} \tag{2.91}$$

We flip the signs in the second equation, obtaining:

$$\begin{cases} 0 < x < L \\ -L < (x'' - x) < 0 \end{cases} \tag{2.92}$$

Combining the two equations we obtain:

$$-L < -L + x < x'' < x < L \tag{2.93}$$

i.e. the integrand is zero for $-L < x'' < L$. Therefore in Eq. (2.90) we can replace $G(x'')$ with its truncated version:

$$G_{2L}(x'') = G(x'')\, \Pi_{[-L,L]}\,(x'') \tag{2.94}$$

obtaining:

$$\phi_L(x) = \int_{-\infty}^{+\infty} \Pi_{[0,L]}\,(x)\, \Pi_{[0,L]}\,(x - x'')\, \rho(x - x'')\, G_{2L}(x'')dx'' \tag{2.95}$$

Since the two window functions force the integrand to zero outside the region $|x''| < L$ we can replace $G_{2L}(x'')$ with its replicated version:

$$G_{2LR}(x'') = \sum_{n=-\infty}^{+\infty} G_{2L}(x'' - 2nL) = \sum_{n=-\infty}^{+\infty} G(x'' - 2nL)\, \Pi_{[-L,L]}\left(x'' - 2nL\right) \tag{2.96}$$

obtaining:

$$\phi_L(x) = \int_{-\infty}^{+\infty} \Pi_{[0,L]}\left(x\right) \Pi_{[0,L]}\left(x - x''\right) \rho(x - x'')\, G_{2LR}(x'')dx'' \tag{2.97}$$

We can go back to the initial coordinate by substituting $x'' = x - x'$:

$$\phi_L(x) = \Pi_{[0,L]}\left(x\right) \int_{-\infty}^{+\infty} \rho(x')\, G_{2LR}(x - x')dx' \tag{2.98}$$

This is a cyclic convolution, so we can proceed as follows. We split the integral:

$$\phi_L(x) = \Pi_{[0,L]}\left(x\right) \sum_{n=-\infty}^{+\infty} \int_{2nL}^{2(n+1)L} \rho(x')\, G_{2LR}(x - x')\, dx' \tag{2.99}$$

In each term we replace $x''' = x' + 2nL$:

$$\phi_L(x) = \Pi_{[0,L]}\left(x\right) \sum_{n=-\infty}^{+\infty} \int_{0}^{2L} \rho(x''' - 2nL)\, G_{2LR}(x - x''' - 2nL)\, dx''' \tag{2.100}$$

We use the fact that $G_{2LR}(x)$ is periodic:

$$\begin{aligned} \phi_L(x) &= \Pi_{[0,L]}\left(x\right) \sum_{n=-\infty}^{+\infty} \int_{0}^{2L} \rho(x''' - 2nL)\, G_{2LR}(x - x''')dx''' \\ &= \Pi_{[0,L]}\left(x\right) \int_{0}^{2L} \sum_{n=-\infty}^{+\infty} \rho(x''' - 2nL)\, G_{2LR}(x - x''')dx''' \end{aligned} \tag{2.101}$$

We can define a replicated version of $\rho(x)$:

$$\rho_{2LR}(x) = \sum_{n=-\infty}^{+\infty} \rho(x - 2nL) \tag{2.102}$$

noting that this implies:

$$\rho_{2LR}(x) = 0 \quad \text{for } x \in [L, 2L] \tag{2.103}$$

We obtain:

$$\phi_L(x) = \Pi_{[0,L]}\left(x\right) \int_{0}^{2L} \rho_{2LR}(x')\, G_{2LR}(x - x')dx' \tag{2.104}$$

The function:

$$\phi_{2LR}(x) = \int_{0}^{2L} \rho_{2LR}(x')\, G_{2LR}(x - x')dx' \tag{2.105}$$

is periodic of period $2L$. From it the potential of interest can be simply calculated by selecting the first half period $[0, L]$:

$$\phi_L(x) = \Pi_{[0,L]}(x)\,\phi_{2LR}(x) \tag{2.106}$$

To compute the convolution in Eq. 2.105 we expand $\phi_{2LR}(x)$ in Fourier series:

$$\phi_{2LR}(x) = \sum_{k=-\infty}^{+\infty} \tilde{\phi}_k\, e^{j2\pi k\frac{x}{2L}} \tag{2.107}$$

where the Fourier coefficients are given by:

$$\tilde{\phi}_k = \frac{1}{2L}\int_0^{2L} \phi_{2LR}(x)\, e^{-j2\pi k\frac{x}{2L}}\, dx \tag{2.108}$$

We replace Eq. (2.105) into Eq. (2.108) obtaining:

$$\hat{\phi}_k = \frac{1}{2L}\int_0^{2L}\int_0^{2L} \rho_{2LR}(x')\, G_{2LR}(x-x')\, e^{-j2\pi k\frac{x}{2L}}\, dx'\, dx \tag{2.109}$$

With the change of variable $x'' = x - x'$ we obtain:

$$\tilde{\phi}_k = \frac{1}{2L}\int_0^{2L} \rho_{2LR}(x')e^{-j2\pi k\frac{x'}{2L}}dx' \int_0^{2L} G_{2LR}(x'')e^{-j2\pi k\frac{x''}{2L}}\, dx'' \tag{2.110}$$

where we recognize the Fourier coefficients of $\rho_{2LR}(x)$ and $G_{2LR}(x)$:

$$\tilde{\rho}_k = \frac{1}{2L}\int_0^{2L} \rho_{2LR}(x)\, e^{-j2\pi k\frac{x}{2L}}\, dx \tag{2.111}$$

$$\tilde{G}_k = \frac{1}{2L}\int_0^{2L} G_{2LR}(x)\, e^{-j2\pi k\frac{x}{2L}}\, dx \tag{2.112}$$

obtaining simply:

$$\hat{\phi}_k = 2L\,\hat{G}_k\,\hat{\rho}_k \tag{2.113}$$

I assume to have the functions $\rho_{2LR}(x)$ and $G_{2LR}(x)$ sampled (or averaged) with step:

$$h_x = \frac{2L}{M} = \frac{L}{N} \tag{2.114}$$

I can approximate the integrals in Eqs. (2.111) and (2.112) as:

$$\tilde{\rho}_k = \frac{1}{M}\sum_{n=0}^{M-1} \rho_{2LR}(x_n)\, e^{-j2\pi\frac{kn}{M}} = \frac{1}{M}\hat{\rho}_k \tag{2.115}$$

$$\tilde{G}_k = \frac{1}{M}\sum_{n=0}^{M-1} G_{2LR}(x_n)\, e^{-j2\pi\frac{kn}{M}} = \frac{1}{M}\hat{G}_k \tag{2.116}$$

where we recognize the Discrete Fourier Transforms:

$$\hat{\rho}_k = \mathrm{DFT}_M\left\{\rho_{2LR}(x_n)\right\} \tag{2.117}$$

$$\hat{G}_k = \mathrm{DFT}_M\left\{G_{2LR}(x_n)\right\} \tag{2.118}$$

Using Eq. (2.107) we can obtain a sampled version of $\phi(x)$:

$$\phi_{2LR}(x_n) = \sum_{n=0}^{M-1} \tilde{\phi}_k \, e^{j2\pi \frac{kn}{M}} \tag{2.119}$$

where we have assumed that $\phi(x)$ is sufficiently smooth to allow truncating the sum. Using Eqs. (2.113), (2.115) and (2.116) we obtain:

$$\phi_{2LR}(x_n) = 2L \sum_{n=0}^{M-1} \tilde{G}_k \, \tilde{\rho}_k \, e^{j2\pi \frac{kn}{M}} = \frac{2L}{M^2} \sum_{n=0}^{M-1} \hat{G}_k \, \hat{\rho}_k \, e^{j2\pi \frac{kn}{M}} \tag{2.120}$$

This can be rewritten as:

$$\phi_{2LR}(x_n) = \frac{1}{M} \sum_{n=0}^{M-1} (h_x \hat{G}_k) \, \hat{\rho}_k \, e^{j2\pi \frac{kn}{M}} = \mathrm{DFT}_M^{-1} \{\phi_k\} \tag{2.121}$$

where

$$\hat{\phi}_k = h_x \hat{G}_k \, \hat{\rho}_k \tag{2.122}$$

We call "Integrated Green Function" the quantity:

$$G_{2LR}(x_n) = h_x G_{2LR}(x_n) \tag{2.123}$$

we introduce the corresponding Fourier transform:

$$\hat{G}_k^{\mathrm{int}} = \mathrm{DFT}_M \left\{ G_{2LR}^{\mathrm{int}}(x_n) \right\} \tag{2.124}$$

Eq. (2.122) can be rewritten as:

$$\boxed{\hat{\phi}_k = \hat{G}_k^{\mathrm{int}} \, \hat{\rho}_k} \tag{2.125}$$

In summary the potential at the grid nodes can be computed as follows:

1. We compute the Integrated Green function at the grid points in the range $[0, L]$:

$$G_{2LR}^{\mathrm{int}}(x_n) = \int_{x_n - \frac{h_x}{2}}^{x_n + \frac{h_x}{2}} G(x) dx \tag{2.126}$$

2. We extend to the interval $[L, 2L]$ using the fact that in this interval:

$$G_{2LR}^{\mathrm{int}}(x_n) = G_{2LR}^{\mathrm{int}}(x_n - 2L) = G_{2LR}^{\mathrm{int}}(2L - x_n) \tag{2.127}$$

   where the first equality comes from the periodicity of $G_{2LR}^{\mathrm{int}}(x)$ and the second from the fact that $G(x)$ is an even function (i.e. $G(x) = G(-x)$). Note that for $x_n \in [L, 2L]$ we have that $2L - x_n \in [0, L]$ so we can reuse the values computed at the previous step.

3. We transform it:

$$\hat{G}_k^{\mathrm{int}} = \mathrm{DFT}_{2N} \{G_{2LR}(x_n)\} \tag{2.128}$$

4. We assume that we are given $\rho(x_n)$ in the interval $[0, L]$. From this we can obtain $\rho_{2LR}(x_n)$ over the interval $[0, 2L]$ simply extending the sequence with zeros (see Eq. (2.103)).

5. We transform it:
$$\hat{\rho}_k = \mathrm{DFT}_{2N}\left\{\rho_{2LR}(x_n)\right\} \tag{2.129}$$

6. We compute the potential in the transformed domain:
$$\hat{\phi}_k = \hat{G}_k^{\mathrm{int}}\hat{\rho}_k \quad \text{for } k \in [0, 2N] \tag{2.130}$$

7. We inverse-transform:
$$\phi_{2LR}(x_n) = \mathrm{DFT}_{2N}^{-1}\left\{\hat{\phi}_k\right\} \tag{2.131}$$
which provides the physical potential in the range $[0, L]$:
$$\phi(x_n) = \phi_{2LR}(x_n) \quad \text{for } x_n \in [0, L] \tag{2.132}$$

2.6.3 Extension to multiple dimensionss

The procedure described above can be extended to multiple dimensions by applying the same reasoning for all coordinates. This gives the following procedure:

1. We compute the Integrated Green function at the grid points in the volume $[0, L_x] \times [0, L_y] \times [0, L_z]$:
$$G_{2LR}^{\mathrm{int}}(x_{n_x}, y_{n_y}, z_{n_z}) = \int_{x_{n_x}-\frac{h_x}{2}}^{x_{n_x}+\frac{h_x}{2}} dx \int_{y_{n_y}-\frac{h_y}{2}}^{y_{n_y}+\frac{h_y}{2}} dy \int_{z_{n_z}-\frac{h_z}{2}}^{z_{n_z}+\frac{h_z}{2}} dz\, G(x, y, z) \tag{2.133}$$

2. We extend to the region $[0, 2L_x] \times [0, 2L_y] \times [0, 2L_z]$ using the fact that:
$$G_{2LR}^{\mathrm{int}}(x_n, y_n, z_n) = G_{2LR}^{\mathrm{int}}(x_n - 2L_x, y_n, z_n) = G_{2LR}^{\mathrm{int}}(2L_x - x_n, y_n, z_n)$$
$$\text{for } x_n \in [L_x, 2L_x], y_n \in [0, 2L_y], z_n \in [0, 2L_z] \tag{2.134}$$

$$G_{2LR}^{\mathrm{int}}(x_n, y_n, z_n) = G_{2LR}^{\mathrm{int}}(x_n, y_n - 2L_y, z_n) = G_{2LR}^{\mathrm{int}}(x_n, 2L_y - y_n, z_n)$$
$$\text{for } y_n \in [L_y, 2L_y], x_n \in [0, 2L_x], z_n \in [0, 2L_z] \tag{2.135}$$

$$G_{2LR}^{\mathrm{int}}(x_n, y_n, z_n) = G_{2LR}^{\mathrm{int}}(x_n, y_n, z_n - 2L_z) = G_{2LR}^{\mathrm{int}}(x_n, y_n, 2L_z - z_n)$$
$$\text{for } z_n \in [L_z, 2L_z], x_n \in [0, 2L_x], y_n \in [0, 2L_y] \tag{2.136}$$

This allows reusing the values computed at the previous step.

3. We transform it:
$$\hat{G}_{k_x k_y k_z}^{\mathrm{int}} = \mathrm{DFT}_{2N_x 2N_y 2N_z}\left\{G_{2LR}(x_n, y_n, z_n)\right\} \tag{2.137}$$

4. We assume that we are given $\rho(x_n, y_n, z_n)$ in the region $[0, L_x] \times [0, L_y] \times [0, L_z]$. From this we can obtain $\rho_{2LR}(x_n)$ over the region $[0, 2L_x] \times [0, 2L_y] \times [0, 2L_z]$ simply extending the matrix with zeros (see Eq. (2.103)).

5. We transform it:

$$\hat{\rho}^{\text{int}}_{k_x k_y k_z} = \text{DFT}_{2N_x 2N_y 2N_z} \{\rho_{2LR}(x_n, y_n, z_n)\} \tag{2.138}$$

6. We compute the potential in the transformed domain:

$$\hat{\phi}_{k_x k_y k_z} = \hat{G}^{\text{int}}_{k_x k_y k_z} \hat{\rho}_{k_x k_y k_z} \quad \text{for } k_{x/y/z} \in [0, 2N_{x/y/z}] \tag{2.139}$$

7. We inverse-transform:

$$\phi_{2LR}(x_n, y_n, z_n) = \text{DFT}^{-1}_{2N_x 2N_y 2N_z} \left\{ \hat{\phi}_{k_x k_y k_z} \right\} \tag{2.140}$$

which provides the physical potential in the region $[0, L_x] \times [0, L_y] \times [0, L_z]$:

$$\phi(x_n, y_n, z_n) = \phi_{2LR}(x_n, y_n, z_n) \text{ for } (x_n, y_n, z_n) \in [0, L_x] \times [0, L_y] \times [0, L_z] \tag{2.141}$$

2.6.4 Green functions for 2D and 3D Poisson problems

2.6.4.1 3D Poisson problem, free space boundary conditions

For the equation:

$$\nabla^2 \phi(x, y, z) = -\frac{1}{\varepsilon_0} \rho(x, y, z) \tag{2.142}$$

where:

$$\nabla = \left(\frac{\partial}{\partial x}, \frac{\partial}{\partial y}, \frac{\partial}{\partial z} \right) \tag{2.143}$$

the solution can be written as

$$\phi(x, y, z) = \iiint_{-\infty}^{+\infty} \rho(x', y', z')\, G(x - x', y - y', z - z')\, dx'\, dy'\, dz' \tag{2.144}$$

where:

$$G(x, y, z) = \frac{1}{4\pi\varepsilon_0} \frac{1}{\sqrt{x^2 + y^2 + z^2}} \tag{2.145}$$

The corresponding integrated Green function can be written as:

$$G^{\text{int}}_{2LR}(x_{n_x}, y_{n_y}, z_{n_z}) = \int_{x_{n_x}-\frac{h_x}{2}}^{x_{n_x}+\frac{h_x}{2}} dx \int_{y_{n_y}-\frac{h_y}{2}}^{y_{n_y}+\frac{h_y}{2}} dy \int_{z_{n_z}-\frac{h_z}{2}}^{x_{n_z}+\frac{h_z}{2}} dz\, G(x,y,z) \tag{2.146}$$

$$= + F\left(x_{n_x}+\frac{h_x}{2}, y_{n_x}+\frac{h_y}{2}, z_{n_x}+\frac{h_z}{2}\right) \tag{2.147}$$

$$- F\left(x_{n_x}+\frac{h_x}{2}, y_{n_x}+\frac{h_y}{2}, z_{n_x}-\frac{h_z}{2}\right) \tag{2.148}$$

$$- F\left(x_{n_x}+\frac{h_x}{2}, y_{n_x}-\frac{h_y}{2}, z_{n_x}+\frac{h_z}{2}\right) \tag{2.149}$$

$$+ F\left(x_{n_x}+\frac{h_x}{2}, y_{n_x}-\frac{h_y}{2}, z_{n_x}-\frac{h_z}{2}\right) \tag{2.150}$$

$$- F\left(x_{n_x}-\frac{h_x}{2}, y_{n_x}+\frac{h_y}{2}, z_{n_x}+\frac{h_z}{2}\right) \tag{2.151}$$

$$+ F\left(x_{n_x}-\frac{h_x}{2}, y_{n_x}+\frac{h_y}{2}, z_{n_x}-\frac{h_z}{2}\right) \tag{2.152}$$

$$+ F\left(x_{n_x}-\frac{h_x}{2}, y_{n_x}-\frac{h_y}{2}, z_{n_x}+\frac{h_z}{2}\right) \tag{2.153}$$

$$- F\left(x_{n_x}-\frac{h_x}{2}, y_{n_x}-\frac{h_y}{2}, z_{n_x}-\frac{h_z}{2}\right) \tag{2.154}$$

where $F(x,y,z)$ is a primitive of $G(x,y,z)$, which can be obtained as:

$$F(x,y,z) = \int_{x_0}^{x} dx \int_{y_0}^{y} dy \int_{z_0}^{x} dz\, G(x,y,z) \tag{2.155}$$

with (x_0, y_0, z_0) being an arbitrary starting point.
An expression for $F(x,y,z)$ is the following

$$F(x,y,z) = \frac{1}{4\pi\varepsilon_0} \iiint \frac{1}{\sqrt{x^2+y^2+z^2}} dxdydz \tag{2.156}$$

$$= \frac{1}{4\pi\varepsilon_0}\left[-\frac{z^2}{2}\arctan\left(\frac{xy}{z\sqrt{x^2+y^2+z^2}}\right) - \frac{y^2}{2}\arctan\left(\frac{xz}{y\sqrt{x^2+y^2+z^2}}\right)\right. \tag{2.157}$$

$$- \frac{x^2}{2}\arctan\left(\frac{yz}{x\sqrt{x^2+y^2+z^2}}\right) + yz\ln\left(x+\sqrt{x^2+y^2+z^2}\right) \tag{2.158}$$

$$\left. + xz\ln\left(y+\sqrt{x^2+y^2+z^2}\right) + xy\ln\left(z+\sqrt{x^2+y^2+z^2}\right)\right] \tag{2.159}$$

Note that we need to choose the first cell center to be in (0,0,0) for evaluation of the integrated Green function. Therefore the cell edges have non zero coordinates and the denominators in the formula will always be non-vanishing.

2.6.4.2 2D Poisson problem, free space boundary conditions

For the equation:

$$\nabla_{\perp}^2 \phi(x,y) = -\frac{1}{\varepsilon_0}\rho(x,y) \tag{2.160}$$

where:

$$\nabla = \left(\frac{\partial}{\partial x}, \frac{\partial}{\partial y}\right) \tag{2.161}$$

the solution can be written as

$$\phi(x,y) = \iint_{-\infty}^{+\infty} \rho(x',y')\, G(x-x', y-y')\, dx'\, dy' \tag{2.162}$$

where:

$$G(x,y) = -\frac{1}{4\pi\varepsilon_0} \log\left(\frac{x^2+y^2}{r_0^2}\right) \tag{2.163}$$

where r_0 is arbitrary constant which has no effect on the evaluated fields (changes the potential by an additive constant).
The corresponding integrated Green function can be written as:

$$G_{2LR}^{\text{int}}(x_{n_x}, y_{n_y}) = \int_{x_{n_x}-\frac{h_x}{2}}^{x_{n_x}+\frac{h_x}{2}} dx \int_{y_{n_y}-\frac{h_y}{2}}^{y_{n_y}+\frac{h_y}{2}} dy\, G(x,y,z) \tag{2.164}$$

$$= + F\left(x_{n_x} + \frac{h_x}{2}, y_{n_x} + \frac{h_y}{2}\right) \tag{2.165}$$

$$- F\left(x_{n_x} + \frac{h_x}{2}, y_{n_x} - \frac{h_y}{2}\right) \tag{2.166}$$

$$- F\left(x_{n_x} - \frac{h_x}{2}, y_{n_x} + \frac{h_y}{2}\right) \tag{2.167}$$

$$+ F\left(x_{n_x} - \frac{h_x}{2}, y_{n_x} - \frac{h_y}{2}\right) \tag{2.168}$$

$$\tag{2.169}$$

where $F(x,y)$ is a primitive of $G(x,y)$, which can be obtained as:

$$F(x,y) = \int_{x_0}^{x} dx \int_{y_0}^{y} dy\, G(x,y) \tag{2.170}$$

where (x_0, y_0) is an arbitrary starting point.
An expression for $F(x,y)$ is the following (where we have chosen $r_0 = 1$):

$$F(x,y) = -\frac{1}{4\pi\varepsilon_0} \iint \ln\left(x^2+y^2\right) dx/, dy \tag{2.171}$$

$$= \frac{1}{4\pi\varepsilon_0}\left[3xy - x^2 \arctan(y/x) - y^2 \arctan(x/y) - xy \ln\left(x^2+y^2\right)\right] \tag{2.172}$$

Note that we need to choose the first cell center to be in (0,0) for evaluation of the integrated Green function. Therefore the cell edges have non zero coordinates and the denominators in the formula will always be non-vanishing.

Chapter 3

"6D" beam-beam interaction

3.1 Introduction

This chapter describes in detail the numerical method used in different codes, and in particular in SixTrack [11] and Xsuite, for the simulation of beam-beam interactions in the weak-strong framework using the "Synchro Beam Mapping" approach [12]. This allows correctly modeling the coupling introduced by beam-beam between the longitudinal and transverse planes. The goal of this document is in particular to provide in a compact, complete and self-consistent manner, the set of equations that are needed for the implementation in a numerical code. Complementary information can be found in [13], including graphical representations of the procedure presented in this note and several validation tests.
The effect of a "crossing angle" in an arbitrary "crossing plane" with respect to the assigned reference frame is taken into account with a suitable coordinate transformation following the approach described in [12, 6]. The employed description of the strong beam allows the correct inclusion of the hour-glass effect as well as the linear coupling at the interaction point, following the treatment presented in [6].
If not differently stated in an explicit way in the following, all coordinates are given in the reference system defined by the closed orbit of the weak beam, which is traveling with positive speed along the s direction. The Interaction Point (IP) is located at s=0 and the crossing plane is defined by as the angle that the strong beam forms with the s-axis. In the presence of an offset between the beams (separation), the orientation of the reference system is defined by the closed orbit of the weak beam and the system is centered at the IP location as defined for the strong beam. Therefore the strong beam passes always through the origin of the reference frame.

3.2 Direct Lorentz boost (for the weak beam)

We want to transform the coordinates by moving to a Lorentz boosted frame in which the collision is head-on (i.e. $p_x = p_y = 0$ for the strong beam and for the reference particle of the weak beam). We call ϕ the half crossing angle and α the angle that the crossing plane makes with respect to the $x - z$ plane. For this purpose, we perform a transformation which actually includes four operations (more details can be found in

Appendix A1 and in [13, 6]):

- Transform the accelerator positions and momenta into Cartesian coordinates (which can then be Lorentz boosted);
- Rotate particle coordinates to the "barycentric" reference frame;
- Perform the Lorentz boost;
- Drift all the particles back to $s = 0$ (as not all particles with $s = 0$ are fixed points of the transformation, and we are tracking with respect to s and not with respect to time).

We name the original accelerator coordinates (as defined in the SixTrack Physics Manual [11]):

$$\left(x, p_x, y, p_y, \sigma, \delta\right) \tag{3.1}$$

and the transformed coordinates:

$$\left(x^*, p_x^*, y^*, p_y^*, \sigma^*, \delta^*\right) \tag{3.2}$$

We start by computing the drift Hamiltonian in the original coordinates (we are doing a Lorentz transformation, therefore constants matter as we are assuming that h is the total energy of the particle):

$$h = \delta + 1 - \sqrt{(1+\delta)^2 - p_x^2 - p_y^2} \tag{3.3}$$

We transform the momenta:

$$p_x^* = \frac{p_x}{\cos\phi} - h\cos\alpha\frac{\tan\phi}{\cos\phi} \tag{3.4}$$

$$p_y^* = \frac{p_y}{\cos\phi} - h\sin\alpha\frac{\tan\phi}{\cos\phi} \tag{3.5}$$

$$\delta^* = \delta - p_x\cos\alpha\tan\phi - p_y\sin\alpha\tan\phi + h\tan^2\phi \tag{3.6}$$

In order to calculate the angles in the transformed frame, we evaluate:

$$p_z^* = \sqrt{(1+\delta^*)^2 - p_x^{*2} - p_y^{*2}} \tag{3.7}$$

We can now evaluate the following derivatives of the transformed Hamiltonian (from Hamilton's equations it can be easily seen that these are the angles in the boosted frame):

$$h_x^* = \frac{\partial h^*}{\partial p_x^*} = \frac{p_x^*}{p_z^*} \tag{3.8}$$

$$h_y^* = \frac{\partial h^*}{\partial p_y^*} = \frac{p_y^*}{p_z^*} \tag{3.9}$$

$$h_\sigma^* = \frac{\partial h^*}{\partial \delta} = 1 - \frac{\delta^* + 1}{p_z^*} \tag{3.10}$$

These can be used to build the following matrix:

$$L = \begin{pmatrix} (1 + h_x^* \cos\alpha \sin\phi) & h_x^* \sin\alpha \sin\phi & \cos\alpha \tan\phi \\ h_y^* \cos\alpha \sin\phi & \left(1 + h_y^* \sin\alpha \sin\phi\right) & \sin\alpha \tan\phi \\ h_\sigma^* \cos\alpha \sin\phi & h_\sigma^* \sin\alpha \sin\phi & \frac{1}{\cos\phi} \end{pmatrix} \tag{3.11}$$

which can then be used to transform the test-particle positions:

$$\begin{pmatrix} x^* \\ y^* \\ \sigma^* \end{pmatrix} = L \begin{pmatrix} x \\ y \\ \sigma \end{pmatrix} \tag{3.12}$$

3.3 Syncrho-beam mapping

Following the approach introduced in [12], the strong beam is sliced along z. A common approach is to use constant-charge slices (see Appendix A2). For each particle in the weak beam and for each slice in the strong beam we perform the following.

We identify the position of the Collision Point (CP):

$$S = \frac{\sigma^* - \sigma_{\text{sl}}^*}{2} \tag{3.13}$$

Here σ^* is defined in the reference system of the weak beam ($\sigma^* > 0$ for particles at the head of the weak bunch) while σ_{sl}^* is defined in the reference system of the strong beam ($\sigma_{\text{sl}}^* > 0$ for particles at the head of the strong bunch). S is the coordinate of the collision point in the reference system of the weak beam (from Eq. 3.13, we can see that particles at the head of the weak bunch, collide with particles at the tail of the strong bunch at $S > 0$).

N.B. Here we are making an approximation since we are assuming that particles are moving at the speed of light along z independently on their angles. This means that the presented approach works only for small particle angles. It is for this reason that we need to Lorentz boost to get rid of the crossing angle and we cannot just move to the reference of the strong beam using a rotation (in this case the weak beam would have large angles).

We now evaluate the transverse position of the particle at the CP, with respect to the centroid of the slice, taking into account the particle angles :

$$\overline{x}^* = x^* + p_x^* S - (x_{\text{sl}}^* - p_{x,\text{sl}}^* S) \tag{3.14}$$

$$\overline{y}^* = y^* + p_y^* S - (y_{\text{sl}}^* - p_{y,\text{sl}}^* S) \tag{3.15}$$

Here x_{sl}^*, y_{sl}^*, $p_{x,\text{sl}}^*$ and $p_{y,\text{sl}}^*$ are defined in the coordinate system of the weak beam. The momenta of the strong slice appear with a negative sign since in the weak frame the strong slice is travelling "backwards".

3.3.1 Propagation of the strong beam to the collision point

The distribution of the strong beam in the transverse phase-space can be written using the Σ-matrix [14]:

$$f(\eta) = f_0 e^{-\eta^{\mathrm{T}}\Sigma^{-1}\eta} \tag{3.16}$$

where:

$$\eta = \begin{pmatrix} x \\ p_x \\ y \\ p_y \end{pmatrix} \tag{3.17}$$

Points having same phase space density lie on hyper-elliptic manifolds defined by the equation:

$$\eta^{\mathrm{T}}\Sigma^{-1}\eta = \text{const.} \tag{3.18}$$

Further considerations on the Σ-matrix can be found in Appendix A3.
We transform the Σ-matrix at the Interaction Point to take into account the Lorentz Boost:

$$\Sigma^{*0}_{11} = \Sigma^{0}_{11} \tag{3.19}$$
$$\Sigma^{*0}_{12} = \Sigma^{0}_{12}/\cos\phi \tag{3.20}$$
$$\Sigma^{*0}_{13} = \Sigma^{0}_{13} \tag{3.21}$$
$$\Sigma^{*0}_{14} = \Sigma^{0}_{14}/\cos\phi \tag{3.22}$$
$$\Sigma^{*0}_{22} = \Sigma^{0}_{22}/\cos^2\phi \tag{3.23}$$
$$\Sigma^{*0}_{23} = \Sigma^{0}_{23}/\cos\phi \tag{3.24}$$
$$\Sigma^{*0}_{24} = \Sigma^{0}_{24}/\cos^2\phi \tag{3.25}$$
$$\Sigma^{*0}_{33} = \Sigma^{0}_{33} \tag{3.26}$$
$$\Sigma^{*0}_{34} = \Sigma^{0}_{34}/\cos\phi \tag{3.27}$$
$$\Sigma^{*0}_{44} = \Sigma^{0}_{44}/\cos^2\phi \tag{3.28}$$
$$\tag{3.29}$$

We transport the position part of the boosted Σ-matrix to the CP (here we are taking into account hourglass effect, assuming that we are in a drift space):

$$\Sigma^{*}_{11} = \Sigma^{*0}_{11} + 2\Sigma^{*0}_{12}S + \Sigma^{*0}_{22}S^2 \tag{3.30}$$
$$\Sigma^{*}_{33} = \Sigma^{*0}_{33} + 2\Sigma^{*0}_{34}S + \Sigma^{*0}_{44}S^2 \tag{3.31}$$
$$\Sigma^{*}_{13} = \Sigma^{*0}_{13} + \left(\Sigma^{*0}_{14} + \Sigma^{*0}_{23}\right)S + \Sigma^{*0}_{24}S^2 \tag{3.32}$$

The Σ-matrix is given in the reference system of the weak beam.

For singular cases we will also need to transport the other terms:

$$\Sigma^*_{12} = \Sigma^{*0}_{12} + \Sigma^{*0}_{22} S \tag{3.33}$$
$$\Sigma^*_{14} = \Sigma^{*0}_{14} + \Sigma^{*0}_{24} S \tag{3.34}$$
$$\Sigma^*_{22} = \Sigma^{*0}_{22} \tag{3.35}$$
$$\Sigma^*_{23} = \Sigma^{*0}_{23} + \Sigma^{*0}_{24} S \tag{3.36}$$
$$\Sigma^*_{24} = \Sigma^{*0}_{24} \tag{3.37}$$
$$\Sigma^*_{34} = \Sigma^{*0}_{34} + \Sigma^{*0}_{44} S \tag{3.38}$$
$$\Sigma^*_{44} = \Sigma^{*0}_{44} \tag{3.39}$$

We introduce the following three auxiliary quantities:

$$R(S) = \Sigma^*_{11} - \Sigma^*_{33} \tag{3.40}$$
$$W(S) = \Sigma^*_{11} + \Sigma^*_{33} \tag{3.41}$$
$$T(S) = R^2 + 4{\Sigma^*_{13}}^2 \tag{3.42}$$

The following derivatives will be needed in the following:

$$\frac{\partial R}{\partial S} = 2\left(\Sigma^0_{12} - \Sigma^0_{34}\right) + 2S\left(\Sigma^0_{22} - \Sigma^0_{44}\right) \tag{3.43}$$
$$\frac{\partial W}{\partial S} = 2\left(\Sigma^0_{12} + \Sigma^0_{34}\right) + 2S\left(\Sigma^0_{22} + \Sigma^0_{44}\right) \tag{3.44}$$
$$\frac{\partial \Sigma^*_{13}}{\partial S} = \Sigma^0_{14} + \Sigma^0_{23} + 2\Sigma^0_{24} S \tag{3.45}$$
$$\frac{\partial T}{\partial S} = 2R\frac{\partial R}{\partial S} + 8\Sigma^*_{13}\frac{\partial \Sigma^*_{13}}{\partial S} \tag{3.46}$$

We will now compute, at the location of the CP, the coupling angle θ, defining a reference frame in which the beam is decoupled. We will call $\hat{x}$ and $\hat{y}$ the coordinates in the decoupled frame and $\hat{\Sigma}^*_{11}$, $\hat{\Sigma}^*_{33}$ the corresponding squared beam sizes. The angle θ is defined as the angle between the $\hat{x}$-axis and the x-axis.
These quantities can be found by diagonalizing the $x-y$ block of the Σ-matrix. We will make determination choices (Eqs. 3.49, 3.52 and 3.56) so that the set $(\theta, \hat{\Sigma}^*_{11}, \hat{\Sigma}^*_{33})$ is uniquely defined and the coupling angle θ lies in the interval:

$$-\frac{\pi}{4} < \theta < \frac{\pi}{4} \tag{3.47}$$

Different cases need to be treated separately:

Case T>0, $\left|\Sigma^*_{13}\right|$>0

We evaluate the coupling angle at the position of the CP in the boosted frame:

$$\cos 2\theta = \mathrm{sgn}\left(\Sigma^*_{11} - \Sigma^*_{33}\right) \frac{\Sigma^*_{11} - \Sigma^*_{33}}{\sqrt{\left(\Sigma^*_{11} - \Sigma^*_{33}\right)^2 + 4{\Sigma^*_{13}}^2}} \tag{3.48}$$

Or more synthetically:

$$\cos 2\theta = \mathrm{sgn}(R)\frac{R}{\sqrt{T}} \tag{3.49}$$

In the following we will need also the derivative of this quantity:

$$\frac{\partial}{\partial S}\left[\cos 2\theta\right] = \mathrm{sgn}(R)\left(\frac{\partial R}{\partial S}\frac{1}{\sqrt{T}} - \frac{R}{2\left(\sqrt{T}\right)^3}\frac{\partial T}{\partial S}\right) \tag{3.50}$$

It can be proved that [6]:

$$\cos\theta = \sqrt{\frac{1}{2}\left(1+\cos 2\theta\right)} \tag{3.51}$$

$$\sin\theta = \mathrm{sgn}(R)\mathrm{sgn}(\Sigma^*_{13})\sqrt{\frac{1}{2}\left(1-\cos 2\theta\right)} \tag{3.52}$$

The corresponding derivatives are given by (see Eq. 2.64 in [**?**]):

$$\frac{\partial}{\partial S}\cos\theta = \frac{1}{4\cos\theta}\frac{\partial}{\partial S}\cos 2\theta \tag{3.53}$$

$$\frac{\partial}{\partial S}\sin\theta = -\frac{1}{4\sin\theta}\frac{\partial}{\partial S}\cos 2\theta \tag{3.54}$$

The squared beam sizes in the rotated (un-coupled) boosted frame are given by:

$$\hat{\Sigma}^*_{11} = \frac{1}{2}\left[\left(\Sigma^*_{11}+\Sigma^*_{33}\right) + \mathrm{sgn}\left(\Sigma^*_{11}-\Sigma^*_{33}\right)\sqrt{\left(\Sigma^*_{11}-\Sigma^*_{33}\right)^2 + 4{\Sigma^*_{13}}^2}\right] \tag{3.55}$$

$$\hat{\Sigma}^*_{33} = \frac{1}{2}\left[\left(\Sigma^*_{11}+\Sigma^*_{33}\right) - \mathrm{sgn}\left(\Sigma^*_{11}-\Sigma^*_{33}\right)\sqrt{\left(\Sigma^*_{11}-\Sigma^*_{33}\right)^2 + 4{\Sigma^*_{13}}^2}\right] \tag{3.56}$$

Equation 3.56 can be written in a compact form as:

$$\hat{\Sigma}^*_{11} = \frac{1}{2}\left(W + \mathrm{sgn}(R)\sqrt{T}\right) \tag{3.57}$$

$$\hat{\Sigma}^*_{33} = \frac{1}{2}\left(W - \mathrm{sgn}(R)\sqrt{T}\right) \tag{3.58}$$

The corresponding derivatives, which will be needed in the following, are given by:

$$\frac{\partial}{\partial S}\left[\hat{\Sigma}^*_{11}\right] = \frac{1}{2}\left(\frac{\partial W}{\partial S} + \mathrm{sgn}(R)\frac{1}{2\sqrt{T}}\frac{\partial T}{\partial S}\right) \tag{3.59}$$

$$\frac{\partial}{\partial S}\left[\hat{\Sigma}^*_{33}\right] = \frac{1}{2}\left(\frac{\partial W}{\partial S} - \mathrm{sgn}(R)\frac{1}{2\sqrt{T}}\frac{\partial T}{\partial S}\right) \tag{3.60}$$

Case T>0, $\left|\Sigma^*_{13}\right|$=0:

The treatment of the previous case is still applicable with the exception of Eq. 3.54 in which the denominator becomes zero. This happens when Σ^*_{13}=0, which implies $\sqrt{T} = |R|$ and therefore $\cos 2\theta = 1$. The case $T = 0$ will be treated separately later, therefore here we can assume $|R| > 0$. We can expand with respect to Σ^*_{13}/R obtaining:

$$\cos 2\theta = \frac{|R|}{\sqrt{R^2 + 4{\Sigma^*_{13}}^2}} = \frac{1}{\sqrt{1 + 4\frac{{\Sigma^*_{13}}^2}{R^2}}} \simeq \frac{1}{1 + 2\frac{{\Sigma^*_{13}}^2}{R^2}} \simeq 1 - 2\frac{{\Sigma^*_{13}}^2}{R^2} \tag{3.61}$$

Replacing these result in Eq. 3.52 we obtain:

$$\sin\theta = \mathrm{sgn}(R)\mathrm{sgn}(\Sigma^*_{13})\frac{|\Sigma^*_{13}|}{|R|} = \frac{\Sigma^*_{13}}{R} \tag{3.62}$$

We call S_0 the location at which $\Sigma^*_{13} = 0$. At this location we define the auxiliary quantities:

$$c = \Sigma^*_{14} + \Sigma^*_{23} \tag{3.63}$$
$$d = \Sigma^*_{24} \tag{3.64}$$

We introduce $\Delta S = S - S_0$ and we can write using Eqs. 3.30–3.32:

$$\Sigma^*_{13} = c\Delta S + d\Delta S^2 \tag{3.65}$$

By taking the derivative of Eq. 3.62 and using Eq. 3.65 we obtain:

$$\frac{\partial}{\partial S}\sin\theta = \frac{1}{R^2}\left[(c + 2d\Delta S)\,R\; - \frac{\partial R}{\partial S}\left(c\Delta S + d\Delta S^2\right)\right] \tag{3.66}$$

In the implementation we need only the value for ΔS=0, which is simply given by:

$$\frac{\partial}{\partial S}\sin\theta = \frac{c}{R} \tag{3.67}$$

Case T=0, $|c|$>0

Special care has to be taken at sections S_0 at which $\Sigma^*_{11} = \Sigma^*_{33}$ and $\Sigma^*_{13} = 0$ as Eqs. 3.49 and 3.60 cannot be evaluated directly. Also in this case we define:

$$\Delta S = S - S_0 \tag{3.68}$$

At the location of the apparent singularity (ΔS=0) we define the auxiliary quantities:

$$a = \Sigma^*_{12} - \Sigma^*_{34} \tag{3.69}$$
$$b = \Sigma^*_{22} - \Sigma^*_{44} \tag{3.70}$$
$$c = \Sigma^*_{14} + \Sigma^*_{23} \tag{3.71}$$
$$d = \Sigma^*_{24} \tag{3.72}$$

and therefore, using Eqs. 3.30–3.32, we can write:

$$R = 2a\Delta S + b\Delta S^2 \tag{3.73}$$

$$\Sigma^*_{13} = c\Delta S + d\Delta S^2 \tag{3.74}$$

With these definitions the function T (defined by Eq. 3.42) can be expanded around $\Delta S = 0$ (using the Eqs. 3.30, 3.31, 3.32):

$$T = \Delta S^2 \left[(2a + b\Delta S)^2 + 4\,(c + d\Delta S)^2 \right] \tag{3.75}$$

Replacing Eq. 3.75 in Eq. 3.49 allows removing the apparent singularity:

$$\cos 2\theta = \frac{|2a + b\Delta S|}{\sqrt{(2a + b\Delta S)^2 + 4\,(c + d\Delta S)^2}} \tag{3.76}$$

This can be derived obtaining:

$$\frac{\partial}{\partial S}\left[\cos 2\theta\right] = \mathrm{sgn}(2a + b\Delta S) \left[\frac{b}{\sqrt{(2a + b\Delta S)^2 + 4\,(c + d\Delta S)^2}} - \frac{(2a + b\Delta S)(2ab + b^2\Delta s + 4cd + 4d^2\Delta S)}{\left(\sqrt{(2a + b\Delta S)^2 + 4\,(c + d\Delta S)^2}\right)^3} \right] \tag{3.77}$$

Similarly, replacing Eq. 3.75 in Eq. 3.58 we obtain:

$$\hat{\Sigma}^*_{11} = \frac{W}{2} + \frac{1}{2}\mathrm{sgn}\left(2a\Delta S + b\Delta S^2\right) |\Delta S| \sqrt{(2a + b\Delta S)^2 + 4\,(c + d\Delta S)^2} \tag{3.78}$$

$$\hat{\Sigma}^*_{33} = \frac{W}{2} - \frac{1}{2}\mathrm{sgn}\left(2a\Delta S + b\Delta S^2\right) |\Delta S| \sqrt{(2a + b\Delta S)^2 + 4\,(c + d\Delta S)^2} \tag{3.79}$$

This can be derived obtaining:

$$\frac{\partial}{\partial S}\left[\hat{\Sigma}^*_{11}\right] = \frac{1}{2}\frac{\partial W}{\partial S} + \frac{1}{2}\mathrm{sgn}\left(2a\Delta S + b\Delta S^2\right) \mathrm{sgn}(\Delta S) \left[\sqrt{(2a + b\Delta S)^2 + 4\,(c + d\Delta S)^2} + \frac{\Delta S\left(2ab + b^2\Delta s + 4cd + 4d^2\Delta S\right)}{\sqrt{(2a + b\Delta S)^2 + 4\,(c + d\Delta S)^2}} \right] \tag{3.80}$$

$$\frac{\partial}{\partial S}\left[\hat{\Sigma}^*_{33}\right] = \frac{1}{2}\frac{\partial W}{\partial S} - \frac{1}{2}\mathrm{sgn}\left(2a\Delta S + b\Delta S^2\right) \mathrm{sgn}(\Delta S) \left[\sqrt{(2a + b\Delta S)^2 + 4\,(c + d\Delta S)^2} + \frac{\Delta S\left(2ab + b^2\Delta s + 4cd + 4d^2\Delta S\right)}{\sqrt{(2a + b\Delta S)^2 + 4\,(c + d\Delta S)^2}} \right] \tag{3.81}$$

In the implementation only the values at ΔS=0 are needed. For this case the obtained results above can be simplified as:

$$\cos 2\theta = \frac{|2a|}{2\sqrt{a^2+c^2}} \tag{3.82}$$

$$\frac{\partial}{\partial S}\left[\cos 2\theta\right] = \mathrm{sgn}(2a)\left[\frac{b}{2\sqrt{a^2+c^2}} - \frac{a(ab+2cd)}{2\left(\sqrt{a^2+c^2}\right)^3}\right] \tag{3.83}$$

$$\hat{\Sigma}^*_{11} = \frac{W}{2} \tag{3.84}$$

$$\hat{\Sigma}^*_{33} = \frac{W}{2} \tag{3.85}$$

$$\frac{\partial}{\partial S}\left[\hat{\Sigma}^*_{11}\right] = \frac{1}{2}\frac{\partial W}{\partial S} + \mathrm{sgn}(2a)\sqrt{a^2+c^2} \tag{3.86}$$

$$\frac{\partial}{\partial S}\left[\hat{\Sigma}^*_{33}\right] = \frac{1}{2}\frac{\partial W}{\partial S} - \mathrm{sgn}(2a)\sqrt{a^2+c^2} \tag{3.87}$$

Eqs. 3.52 and 3.54 can still be used to evaluate $\sin\theta$ and $\cos\theta$ and the corresponding derivatives, once we assume that $\mathrm{sgn}(0) = 1$ and noticing from Eqs. 3.73 and 3.74 that for small ΔS:

$$\mathrm{sgn}(R)\mathrm{sgn}(\Sigma^*_{13}) = \mathrm{sgn}(a)\mathrm{sgn}(c) \tag{3.88}$$

Case T=0, c=0, $|a|$>0

The treatment of the previous case is still applicable with the exception of Eq. 3.54 in which the denominator becomes zero.
For this case we can write (from Eq. 3.76) around the point where this condition is verified:

$$\cos 2\theta = \frac{1}{\sqrt{1+\frac{4d^2\Delta S^2}{(2a+b\Delta S)^2}}} \simeq 1 - \frac{2d^2\Delta S^2}{(2a+b\Delta S)^2} \tag{3.89}$$

We notice from Eqs. 3.73 and 3.74 that for small ΔS:

$$\mathrm{sgn}(R)\mathrm{sgn}(\Sigma^*_{13}) = \mathrm{sgn}(a)\mathrm{sgn}(d)\mathrm{sgn}(\Delta S) \tag{3.90}$$

Replacing Eq. 3.89 and 3.90 into in Eq. 3.52 we obtain:

$$\sin\theta = \frac{d\Delta S}{2a}\left|1 - \frac{b\Delta S}{2a}\right| \tag{3.91}$$

which can be derived in $\Delta S = 0$ obtaining:

$$\frac{\partial}{\partial S}\sin\theta = \frac{d}{2a} \tag{3.92}$$

The case in which also $d = 0$ is (or is equivalent to) the uncoupled case as Σ^*_{13} is zero for all S.

Case T=0, c=0, a=0

Around the apparently singular point we can write:

$$R = b\Delta S^2 \tag{3.93}$$
$$\Sigma^*_{13} = d\Delta S^2 \tag{3.94}$$

Therefore:

$$T = S^4\left(b^2 + 4d^2\right) \tag{3.95}$$

and:

$$\cos 2\theta = \frac{|b|}{\sqrt{b^2 + 4d^2}} \tag{3.96}$$

which is a constant. Eqs. 3.52 and 3.54 can still be used to evaluate $\sin\theta$ and $\cos\theta$ while the corresponding derivatives vanish:
This can be derived obtaining:

$$\frac{\partial}{\partial S}\cos\theta = 0 \tag{3.97}$$
$$\frac{\partial}{\partial S}\sin\theta = 0 \tag{3.98}$$

Replacing $a = c = 0$ into Eq 3.79 we obtain:

$$\hat{\Sigma}^*_{11} = \frac{W}{2} + \frac{1}{2}\mathrm{sgn}(b)\Delta S^2\sqrt{b^2 + 4d^2} \tag{3.99}$$
$$\hat{\Sigma}^*_{33} = \frac{W}{2} - \frac{1}{2}\mathrm{sgn}(b)\Delta S^2\sqrt{b^2 + 4d^2} \tag{3.100}$$

and:

$$\frac{\partial}{\partial S}\left[\hat{\Sigma}^*_{11}\right] = \frac{1}{2}\frac{\partial W}{\partial S} \tag{3.101}$$
$$\frac{\partial}{\partial S}\left[\hat{\Sigma}^*_{33}\right] = \frac{1}{2}\frac{\partial W}{\partial S} \tag{3.102}$$

The case in which also $d = 0$ is (or is equivalent to the uncoupled case) as Σ^*_{13} is zero for all S.

3.3.2 Forces and kicks on weak beam particles

The positions of the weak beam particle in the un-coupled boosted frame are given by:

$$\hat{\bar{x}}^* = \bar{x}^*\cos\theta + \bar{y}^*\sin\theta \tag{3.103}$$
$$\hat{\bar{y}}^* = -\bar{x}^*\sin\theta + \bar{y}^*\cos\theta \tag{3.104}$$

In the following we will also need to evaluate:

$$\frac{\partial}{\partial S}\left[\hat{\overline{x}}^*\left(\theta(S)\right)\right] = \frac{\partial \overline{x}^*}{\partial S}\cos\theta + \overline{x}^*\frac{\partial}{\partial S}\left[\cos\theta\right] + \frac{\partial \overline{y}^*}{\partial S}\sin\theta + \overline{y}^*\frac{\partial}{\partial S}\left[\sin\theta\right] \tag{3.105}$$

$$\frac{\partial}{\partial S}\left[\hat{\overline{y}}^*\left(\theta(S)\right)\right] = -\frac{\partial \overline{x}^*}{\partial S}\sin\theta - \overline{x}^*\frac{\partial}{\partial S}\left[\sin\theta\right] + \frac{\partial \overline{y}^*}{\partial S}\cos\theta + \overline{y}^*\frac{\partial}{\partial S}\left[\cos\theta\right] \tag{3.106}$$

In this boosted, rotated and re-centered frame, closed formulas exist to evaluate the following quantities:

$$\hat{F}_x^* = -K_{sl}\frac{\partial \hat{U}^*}{\partial \hat{\overline{x}}^*}\left(\hat{\overline{x}}^*, \hat{\overline{y}}^*, \hat{\Sigma}_{11}^*, \hat{\Sigma}_{33}^*\right) \tag{3.107}$$

$$\hat{F}_y^* = -K_{sl}\frac{\partial \hat{U}^*}{\partial \hat{\overline{y}}^*}\left(\hat{\overline{x}}^*, \hat{\overline{y}}^*, \hat{\Sigma}_{11}^*, \hat{\Sigma}_{33}^*\right) \tag{3.108}$$

$$\hat{G}_x^* = -K_{sl}\frac{\partial \hat{U}^*}{\partial \hat{\Sigma}_{11}^*}\left(\hat{\overline{x}}^*, \hat{\overline{y}}^*, \hat{\Sigma}_{11}^*, \hat{\Sigma}_{33}^*\right) \tag{3.109}$$

$$\hat{G}_y^* = -K_{sl}\frac{\partial \hat{U}^*}{\partial \hat{\Sigma}_{33}^*}\left(\hat{\overline{x}}^*, \hat{\overline{y}}^*, \hat{\Sigma}_{33}^*, \hat{\Sigma}_{33}^*\right) \tag{3.110}$$

where $\hat{U}^*$ is the electric potential associated to the normalized transverse distribution and:

$$K_{sl} = \frac{N_{sl} q_{sl} q_0}{P_0 c} \tag{3.111}$$

where N_{sl} is the number of particles in the strong-beam slice, q_{sl} and q_0 are the particle charges for the strong and weak beam respectively, P_0 is the reference momentum of the weak beam.

The minus sign in the Eqs. 3.107-3.110 comes from the definition of electric potential, i.e. $E = -\nabla U$.

For a bi-Gaussian beam (elliptic) [12]:

$$\hat{f}_x^* = -\frac{\partial \hat{U}^*}{\partial \hat{\bar{x}}^*} = \frac{1}{2\epsilon_0\sqrt{2\pi\left(\hat{\Sigma}_{11}^* - \hat{\Sigma}_{33}^*\right)}}\mathrm{Im}\left[w\left(\frac{\hat{\bar{x}}^* + i\hat{\bar{y}}^*}{\sqrt{2\left(\hat{\Sigma}_{11}^* - \hat{\Sigma}_{33}^*\right)}}\right)\right. \\ \left. - \exp\left(-\frac{(\hat{\bar{x}}^*)^2}{2\hat{\Sigma}_{11}^*} - \frac{(\hat{\bar{y}}^*)^2}{2\hat{\Sigma}_{33}^*}\right) w\left(\frac{\hat{\bar{x}}^*\sqrt{\frac{\hat{\Sigma}_{33}^*}{\hat{\Sigma}_{11}^*}} + i\hat{\bar{y}}^*\sqrt{\frac{\hat{\Sigma}_{11}^*}{\hat{\Sigma}_{33}^*}}}{\sqrt{2\left(\hat{\Sigma}_{11}^* - \hat{\Sigma}_{33}^*\right)}}\right)\right] \tag{3.112}$$

$$\hat{f}_y^* = -\frac{\partial \hat{U}^*}{\partial \hat{\bar{x}}^*} = \frac{1}{2\epsilon_0\sqrt{2\pi\left(\hat{\Sigma}_{11}^* - \hat{\Sigma}_{33}^*\right)}}\mathrm{Re}\left[w\left(\frac{\hat{\bar{x}}^* + i\hat{\bar{y}}^*}{\sqrt{2\left(\hat{\Sigma}_{11}^* - \hat{\Sigma}_{33}^*\right)}}\right)\right. \\ \left. - \exp\left(-\frac{(\hat{\bar{x}}^*)^2}{2\hat{\Sigma}_{11}^*} - \frac{(\hat{\bar{y}}^*)^2}{2\hat{\Sigma}_{33}^*}\right) w\left(\frac{\hat{\bar{x}}^*\sqrt{\frac{\hat{\Sigma}_{33}^*}{\hat{\Sigma}_{11}^*}} + i\hat{\bar{y}}^*\sqrt{\frac{\hat{\Sigma}_{11}^*}{\hat{\Sigma}_{33}^*}}}{\sqrt{2\left(\hat{\Sigma}_{11}^* - \hat{\Sigma}_{33}^*\right)}}\right)\right] \tag{3.113}$$

$$\hat{g}_x^* = -\frac{\partial \hat{U}^*}{\partial \hat{\Sigma}_{11}^*} = -\frac{1}{2\left(\hat{\Sigma}_{11}^* - \hat{\Sigma}_{33}^*\right)}\left\{\hat{\bar{x}}^*\hat{E}_x^* + \hat{\bar{y}}^*\hat{E}_y^* + \frac{1}{2\pi\epsilon_0}\left[\sqrt{\frac{\hat{\Sigma}_{33}^*}{\hat{\Sigma}_{11}^*}}\exp\left(-\frac{(\hat{\bar{x}}^*)^2}{2\hat{\Sigma}_{11}^*} - \frac{(\hat{\bar{y}}^*)^2}{2\hat{\Sigma}_{33}^*}\right) - 1\right]\right\} \tag{3.114}$$

$$\hat{g}_y^* = -\frac{\partial \hat{U}^*}{\partial \hat{\Sigma}_{33}^*} = \frac{1}{2\left(\hat{\Sigma}_{11}^* - \hat{\Sigma}_{33}^*\right)}\left\{\hat{\bar{x}}^*\hat{E}_x^* + \hat{\bar{y}}^*\hat{E}_y^* + \frac{1}{2\pi\epsilon_0}\left[\sqrt{\frac{\hat{\Sigma}_{11}^*}{\hat{\Sigma}_{33}^*}}\exp\left(-\frac{(\hat{\bar{x}}^*)^2}{2\hat{\Sigma}_{11}^*} - \frac{(\hat{\bar{y}}^*)^2}{2\hat{\Sigma}_{33}^*}\right) - 1\right]\right\} \tag{3.115}$$

where w is the Faddeeva function.
For a round beam, i.e. $\hat{\Sigma}_{11}^* = \hat{\Sigma}_{33}^* = \hat{\Sigma}^*$:

$$\hat{f}_x^* = -\frac{\partial \hat{U}^*}{\partial \hat{\bar{x}}^*} = \frac{1}{2\pi\epsilon_0}\left[1 - \exp\left(-\frac{(\hat{\bar{x}}^*)^2 + (\hat{\bar{y}}^*)^2}{2\hat{\Sigma}^*}\right)\right]\frac{x}{(\hat{\bar{x}}^*)^2 + (\hat{\bar{y}}^*)^2} \tag{3.116}$$

$$\hat{f}_y^* = -\frac{\partial \hat{U}^*}{\partial \hat{\bar{x}}^*} = \frac{1}{2\pi\epsilon_0}\left[1 - \exp\left(-\frac{(\hat{\bar{x}}^*)^2 + (\hat{\bar{y}}^*)^2}{2\hat{\Sigma}^*}\right)\right]\frac{y}{(\hat{\bar{x}}^*)^2 + (\hat{\bar{y}}^*)^2} \tag{3.117}$$

$$\hat{g}_x^* = -\frac{\partial \hat{U}^*}{\partial \hat{\Sigma}_{11}^*} = \frac{1}{2\left[(\hat{\bar{x}}^*)^2 + (\hat{\bar{y}}^*)^2\right]}\left[\hat{\bar{y}}^*\hat{E}_y^* - \hat{\bar{x}}^*\hat{E}_x^* + \frac{1}{2\pi\epsilon_0}\frac{\left(\hat{\bar{x}}^*\right)^2}{\hat{\Sigma}^*}\exp\left(-\frac{(\hat{\bar{x}}^*)^2 + (\hat{\bar{y}}^*)^2}{2\hat{\Sigma}^*}\right)\right] \tag{3.118}$$

$$\hat{g}_y^* = -\frac{\partial \hat{U}^*}{\partial \hat{\Sigma}_{33}^*} = \frac{1}{2\left[(\hat{\bar{x}}^*)^2 + (\hat{\bar{y}}^*)^2\right]}\left[\hat{\bar{x}}^*\hat{E}_x^* - \hat{\bar{y}}^*\hat{E}_y^* + \frac{1}{2\pi\epsilon_0}\frac{\left(\hat{\bar{y}}^*\right)^2}{\hat{\Sigma}^*}\exp\left(-\frac{(\hat{\bar{x}}^*)^2 + (\hat{\bar{y}}^*)^2}{2\hat{\Sigma}^*}\right)\right] \tag{3.119}$$

We have used lower-case symbols to indicate that the factor given by Eq. 3.111 is not yet applied.

The transverse kicks in the coupled (but still boosted) reference frame are given by:

$$F_x^* = \hat{F}_x^* \cos\theta - \hat{F}_y^* \sin\theta \tag{3.120}$$

$$F_y^* = \hat{F}_x^* \sin\theta + \hat{F}_y^* \cos\theta \tag{3.121}$$

To compute the longitudinal kick we notice from Eq. 3.13 that:

$$\frac{\partial}{\partial z} = \frac{1}{2}\frac{\partial}{\partial S} \tag{3.122}$$

Therefore:

$$F_z^* = \frac{1}{2}\frac{\partial}{\partial S}\left[\hat{U}^*\left(\hat{\bar{x}}^*\left(\theta(S)\right), \hat{\bar{y}}^*\left(\theta(S)\right), \hat{\Sigma}_{11}^*(S), \hat{\Sigma}_{33}^*(S)\right)\right] \tag{3.123}$$

This can be rewritten as:

$$F_z^* = \frac{1}{2}\left(\hat{F}_x^*\frac{\partial}{\partial S}\left[\hat{\bar{x}}^*\left(\theta(S)\right)\right] + \hat{F}_y^*\frac{\partial}{\partial S}\left[\hat{\bar{y}}^*\left(\theta(S)\right)\right] + \hat{G}_x^*\frac{\partial}{\partial S}\left[\hat{\Sigma}_{11}^*(S)\right] + \hat{G}_y^*\frac{\partial}{\partial S}\left[\hat{\Sigma}_{33}^*(S)\right]\right) \tag{3.124}$$

where all the terms have been evaluated before.
The quantities evaluated so far can be used to compute the effect of the beam-beam interaction on the particles coordinates and momenta [12]:

$$x_{new}^* = x^* - SF_x^* \tag{3.125}$$

$$p_{x,new}^* = p_x^* + F_x^* \tag{3.126}$$

$$y_{new}^* = y^* - SF_y^* \tag{3.127}$$

$$p_{y,new}^* = p_y^* + F_y^* \tag{3.128}$$

$$z_{new}^* = z^* \tag{3.129}$$

$$\delta_{new}^* = \delta^* + F_z^* + \frac{1}{2}\left[F_x^*\left(p_x^* + \frac{1}{2}F_x^* + p_{x,\mathrm{sl}}^*\right) + F_y^*\left(p_y^* + \frac{1}{2}F_y^* + p_{y,\mathrm{sl}}^*\right)\right] \tag{3.130}$$

The physical meaning of the different terms in these equations is illustrated in [13].

3.4 Inverse Lorentz boost (for the weak beam)

Now we need to go back to the accelerator coordinates by undoing the transformation described in Sec. 3.2.
As before we evaluate:

$$p_z^* = \sqrt{(1+\delta^*)^2 - p_x^{*2} - p_y^{*2}} \tag{3.131}$$

and then:

$$h_x^* = \frac{p_x^*}{p_z^*} \tag{3.132}$$

$$h_y^* = \frac{p_y^*}{p_z^*} \tag{3.133}$$

$$h_\sigma^* = 1 - \frac{\delta^* + 1}{p_z^*} \tag{3.134}$$

We invert the matrix (3.11) using Cramer's rule:

$$\mathrm{Det}\,(L) = \frac{1}{\cos\phi} + \left(h_x^* \cos\alpha + h_y^* \sin\alpha - h_\sigma^* \sin\phi\right) \tan\phi \tag{3.135}$$

$$L^{\mathrm{inv}} = \frac{1}{\mathrm{Det}\,(L)} \times \begin{pmatrix} \left(\frac{1}{\cos\phi} + \sin\alpha\tan\phi\left(h_y^* - h_\sigma^*\sin\alpha\sin\phi\right)\right) & \sin\alpha\tan\phi\left(h_\sigma^*\cos\alpha\sin\phi - h_x^*\right) & -\tan\phi\left(\cos\alpha - h_x^*\sin^2\alpha\sin\phi + h_y^*\cos\alpha\sin\alpha\sin\phi\right) \\ \cos\alpha\tan\phi\left(-h_y^* + h_\sigma^*\sin\alpha\sin\phi\right) & \left(\frac{1}{\cos\phi} + \cos\alpha\tan\phi\left(h_x^* - h_\sigma^*\cos\alpha\sin\phi\right)\right) & -\tan\phi\left(\sin\alpha - h_y^*\cos^2\alpha\sin\phi + h_x^*\cos\alpha\sin\alpha\sin\phi\right) \\ -h_\sigma^*\cos\alpha\sin\phi & -h_\sigma^*\sin\alpha\sin\phi & \left(1 + h_x^*\cos\alpha\sin\phi + h_y^*\sin\alpha\sin\phi\right) \end{pmatrix} \tag{3.136}$$

This can be used to transform the positions:

$$\begin{pmatrix} x \\ y \\ \sigma \end{pmatrix} = L^{\mathrm{inv}} \begin{pmatrix} x^* \\ y^* \\ \sigma^* \end{pmatrix} \tag{3.137}$$

The Hamiltonian can be transformed with a re-scaling:

$$h = h^* \cos^2\phi = \left(\delta^* + 1 - \sqrt{(1+\delta^*)^2 - p_x^{*2} - p_y^{*2}}\right)\cos^2\phi \tag{3.138}$$

This can be used to transform the transverse momenta (inverting Eqs. 3.4 and following):

$$p_x = p_x^* \cos\phi + h\cos\alpha\tan\phi \tag{3.139}$$
$$p_y = p_y^* \cos\phi + h\sin\alpha\tan\phi \tag{3.140}$$

The longitudinal momentum can be calculated using directly Eq. 3.6:

$$\delta = \delta^* + p_x\cos\alpha\tan\phi + p_y\sin\alpha\tan\phi - h\tan^2\phi \tag{3.141}$$

3.5 Bhabha scattering

In quantum electrodynamics (QED), the Coulomb attraction of two opposite charges (e.g. an electron and a positron) is called Bhabha scattering [15]. The mathematical treatment of Bhabha scattering can be done using the method of equivalent photons (Weizsäcker-Williams approach) [16, 17]. The essence of this method lies in the fact that the electromagnetic field of a relativistic charged particle, say the positron, is almost transversal and can therefore accurately be substituted by an appropriately chosen equivalent radiation field of photons. Thus, the cross section for the scattering of an electron with this positron (Bhabha scattering) can be approximated by that of the electron and an "equivalent" photon (Compton scattering). In this case, the equivalent photon corresponds to the exchanged virtual photon between the scattering primaries. The whole process, including the subsequent emission of bremsstrahlung photons can be treated in a numerical simulation as an inverse Compton scattering process [18]. In this, the virtual photons emitted by the positron will collide with the

electron. Due to the relativistic dynamics of the participating leptons, the virtual photons have an energy which is often negligible compared to that of the leptons, thus we can treat them as real. The process is called inverse since here the electron will lose energy while the photons will gain energy, contrary to standard Compton scattering. The scattered photons are real and typically end up with an energy E'_γ comparable to the initial lepton energy E_e [19].
The generation of photons from radiative Bhabha scattering in Xsuite can be divided into 3 steps. First, the charge density of the opposite bunch slice at the location of the macroparticle in the soft-Gaussian approximation is computed [20]. From this one computes the integrated luminosity of the collision of the macroparticle with the virtual photons represented by the slice, integrated over the time of passing through the slice. Second, a set of virtual photons is generated corresponding to the total energy of the opposite slice. Third, the code iterates over these virtual photons and simulates the bremsstrahlung process as a series of inverse Compton scattering events between the macroparticle and each virtual photon.

3.5.1 Luminosity Computation

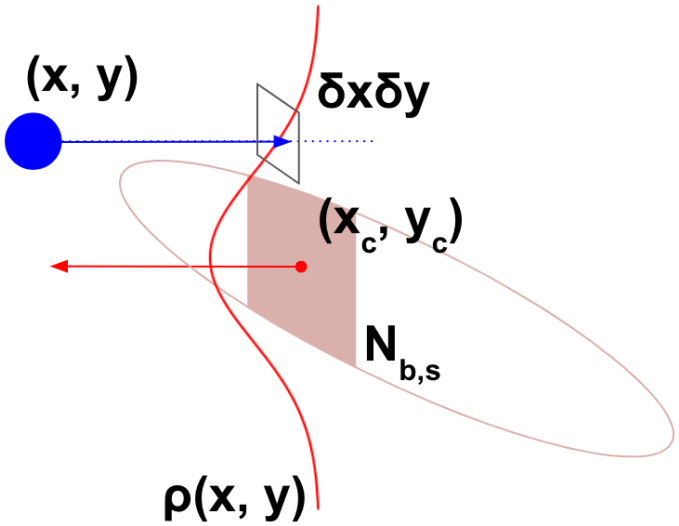

Figure 3.1: Schematic illustration of a single macroparticle from bunch 1 (blue) colliding with a single longitudinal slice of the opposing bunch 2 (red).

Figure 3.1 illustratres how `Xfields` computes the integrated luminosity in a collision of a single macroparticle from one beam with a single slice of the opposing beam[1]. On the figure x, y denote the transverse coordinates of a macroparticle in the boosted and uncoupled frame, at the collision point with a slice of the opposing bunch, cor-

[1]Note that this luminosity can be recorded in a table with the **flag_luminosity** flag of the `BeamBeamGaussian3D` element and **lumitable** keyword in the `Xline` internal log. The recorded entries must be summed up to get the total integrated luminosity of the collision. This method has an uncertainty of $\pm 10\%$ compared to the analytical formula.

responding to the notation $\hat{\hat{x}}^*, \hat{\hat{y}}^*$ in the previous sections. The centroid (mean) coordinate of the opposing slice, with a bunch intensity of $N_{b,s}$, is denoted by x_c, y_c, in the boosted, uncoupled, transported reference frame of its own bunch. `Xfields` models the charge density of a longitudinal slice as a 2D Gaussian distribution $\rho(x, y)$. Considering an infinitesimal area $\delta x \delta y$ around the transverse position x, y of a given macroparticle at the collision point with the slice, one can write the number of charges with which this macroparticle will interact:

$$N_e(x, y) = N_{b,s}\rho(x, y)\delta x \delta y, \tag{3.142}$$

and the integrated luminosity of the macroparticle-slice collision:

$$L = \frac{N_{b,m} \cdot N_e(x, y)}{\delta x \delta y} = N_{b,m} N_{b,s} \rho(x, y), \tag{3.143}$$

where $N_{b,m}$ denotes the number of elementary charges per macroparticle.

3.5.2 Virtual Photon Generation

Equation (3.143) describes the integrated luminosity of primary-primary collisions. In order to simulate the collision of the primaries with virtual photons instead, `Xfields` uses the assumption that the virtual photon distribution $N_\gamma(x, y)$ is proportional to that of the primary charges:

$$N_\gamma(x, y) = n N_e(x, y), \tag{3.144}$$

where n is a proportionality factor denoting the number of virtual photons corresponding to one elementary charge. The number density spectrum of virtual photons is given by:

$$\frac{dn}{dx dQ^2} = \frac{\alpha}{2\pi} \frac{1 + (1 - x)^2}{x} \frac{1}{Q^2}, \tag{3.145}$$

where $x = \dfrac{\hbar\omega}{E_e} = \dfrac{E_\gamma}{E_e}$ is the total energy of the virtual photon normalized to the primary energy and Q^2 is the squared virtuality of the virtual photon [21].
The virtual photon energies and virtualities can be drawn using the method of inverse CDF (Cumulative Distribution Function) sampling. The sampling algorithm in `Xsuite` has been adapted from `GUINEA-PIG` [22], a Particle In Cell (PIC) based single beam-beam collision simulation software. For each macroparticle in the beam, we first compute the total amount of equivalent photons using the energy of the opposite bunch slice. Subsequently, the energy and virtuality of each photon will be sampled. In the current implementation all virtual photons inherit the dynamical variables of the strong bunch slice centroid. Note that the virtual photons sampled this way will also be "macroparticles" in the sense that they represent the dynamics of all virtual photons generated by all charges in a primary macroparticle.

3.5.3 Inverse Compton Scattering of Virtual Photons

We account for the proportionality of the primary charge and virtual photon distributions described by Eq. (3.144) by resampling the virtual photons for each macroparticle. With each photon, we simulate the bremsstrahlung process in the form of a set of inverse Compton scattering events. The number of Compton events can be described as:

$$R = \sigma_{C,tot}(s)L = \sigma_{C,tot}(s)N_{b,m}N_{b,s}\rho(x,y), \tag{3.146}$$

where $s \approx \frac{4E_\gamma E_e}{m_e^2 c^4}$ is the center of mass energy squared of the photon-primary Compton interaction, normalized to the rest mass of the primary [23], and $\sigma_{C,tot}(s)$ denotes the total Compton scattering cross section, given by:

$$\sigma_{C,tot}(s) = \frac{2\pi r_e^2}{s}\left[\ln(s+1)\left(1-\frac{4}{s}-\frac{8}{s^2}\right).+\frac{1}{2}+\frac{8}{s}-\frac{1}{2(s+1)^2}\right], \tag{3.147}$$

with r_e being the classical electron radius. For each event, we sample the scattered photon energy from the differential cross section:

$$\frac{d\sigma_C}{dy} = \frac{2\pi r_e^2}{s}\left[\frac{1}{1-y}+1-y-\frac{4y}{s(1-y)}+\frac{4y^2}{s^2(1-y)^2}\right], \tag{3.148}$$

which describes the scattering of a beam of unpolarized photons on the primary charge [18]. Here $y = \frac{\hbar\omega'}{E_e} = \frac{E'_\gamma}{E_e}$ is the energy of the scattered photon in units of the total energy of the colliding primary. Given the energy E'_γ, we can compute the scattering angle of the primary and the photon as well as their momenta, using the constraints given by energy and momentum conservation. While the emitted photon spectrum corresponds to the sum of all charges represented by a macroparticle, a given macroparticle should represent the dynamics of a single primary charge. Thus, the dynamical variables of the macroparticles are updated according to energy and momentum conservation accounting for the emission of only a fraction of the photons. The latter are picked randomly based on a probability corresponding to the inverse of the number of charges per macroparticle.

3.6 Beamstrahlung

The implementation of beamstrahlung in `Xfields` is based on `GUINEA-PIG` [22]. In this section a high level summary of the modeling is presented. Further details can be found in [24].
`Xfields` samples the quantum theoretical synchrotron radiation spectrum $G(v,\xi)$:

$$G(v,\xi) = \frac{v^2}{(1-(1-\xi)v^3)^2}\left(G_1(y)+\frac{\xi^2 y^2}{1+\xi y}G_2(y)\right), \tag{3.149}$$

which is normalized such that $G(v=0,\xi)=1$ and $G(v,\xi)\leq 1$ for all v and ξ. The variable ξ is defined as:

$$\xi = \frac{E_{crit}}{E} \tag{3.150}$$

and denotes the magnitude of the quantum correction, i.e. the critical energy normalized to the energy E of the primary particle in GeV undergoing the beamstrahlung process. The critical beamstrahlung energy is defined in the classical way as:

$$E_{crit} = \frac{3\hbar c\gamma^3}{2\rho} \tag{3.151}$$

The unitless variable y is related to the energy of the emitted beamstrahlung photon E_γ:

$$y = \frac{E_\gamma}{E_{crit}} \frac{1}{1 - \frac{E_\gamma}{E}}. \tag{3.152}$$

Equation 3.152 can be expressed with the help of a uniform random variable v as follows:

$$y = \frac{v^3}{1 - v^3};\ v \in U[0, 1]. \tag{3.153}$$

With these the number of beamstrahlung photons emitted in the interval $[v,\ v + \Delta v]$ during a time interval δ_t can be given as:

$$\Delta N_\gamma = p_0 G(v, \xi) \Delta v, \tag{3.154}$$

where

$$p_0 = \frac{2^{\frac{2}{3}}}{\Gamma(\frac{4}{3})} \frac{\alpha\gamma\delta_t}{\rho} \approx 25.4 \cdot \frac{E\delta_t}{\rho} \tag{3.155}$$

is a scaling factor dependent on the relativistic γ of the primary, the instantaneous bending radius ρ and the fine structure constant α. The bending radius of each macroparticle in the electromagnetic field of a given longitudinal slice of the opposite bunch is obtained from the radial kick:

$$F_r^* = r_{pp} \sqrt{F_x^{*2} + F_y^{*2}}, \tag{3.156}$$

$$\rho = \frac{1}{F_r^*}, \tag{3.157}$$

with $r_{pp} = \frac{1}{1+\delta} = \frac{p}{p_0}$. In the `Xfields` `BeamBeamGaussian3D` element the time interval δ_t is expressed as a longitudinal distance Δz, which is the distance the macroparticle travels between two consecutive longitudinal slices and it corresponds to the bin width of the longitudinal slicing.
Figure 3.2 shows the beamstrahlung photon number density $p_0 G(v, \xi)$ for a fixed value of p_0 and ξ. The area in the region C is the mean number of beamstrahlung photons emitted during an interval δ_t, i.e. a passage through one longitudinal slice of width Δz.

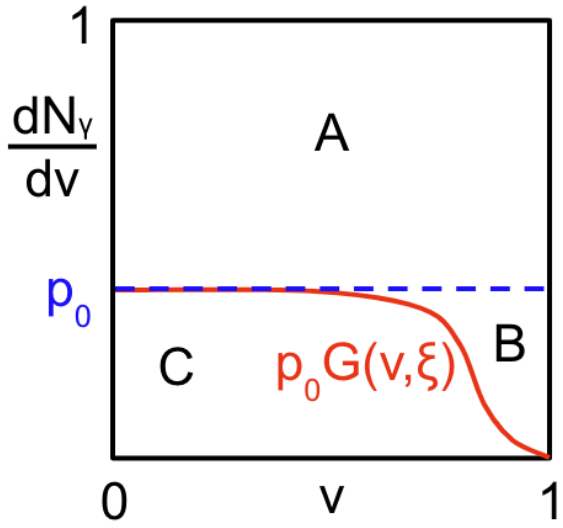

Figure 3.2: Schematic illustration of the number density function of beamstrahlung photons $p_0 G(v,\xi)$ (red curve) for a given p_0 (blue dashed line) and ξ, as a function of v.

The functions $G_1(y)$ and $G_2(y)$ are defined as follows:

$$\begin{aligned} G_1(y) &= \frac{\sqrt{3}\Gamma(\frac{1}{3})}{2^{\frac{5}{3}}\pi} \int_y^\infty K_{\frac{5}{3}}(x)dx, \\ G_2(y) &= \frac{\sqrt{3}\Gamma(\frac{1}{3})}{2^{\frac{5}{3}}\pi} K_{\frac{2}{3}}(y). \end{aligned} \tag{3.158}$$

Equations 3.158 are evaluated numerically with the below approximate formulas:

$0 \leq y \leq 1.54$

$$\begin{aligned} G_1(y) &= y^{-\frac{2}{3}}(1 - 0.8432885317 \cdot y^{\frac{2}{3}} + 0.1835132767 \cdot y^2 \\ &\quad - 0.0527949659 \cdot y^{\frac{10}{3}} + 0.0156489316 \cdot y^4) \\ G_2(y) &= y^{-\frac{2}{3}}(0.4999456517 - 0.5853467515 \cdot y^{\frac{4}{3}} \\ &\quad + 0.3657833336 \cdot y^2 - 0.0695055284 \cdot y^{\frac{10}{3}} + 0.0191803860 \cdot y^4) \end{aligned} \tag{3.159}$$

$1.54 < y \leq 4.48$

$$\begin{aligned} G_1(y) &= \frac{2.066603927 - 0.5718025331 \cdot y + 0.04243170587 \cdot y^2}{-0.9691386396 + 5.651947051 \cdot y - 0.6903991322 \cdot y^2 + y^3} \\ G_2(y) &= \frac{1.8852203645 - 0.5176616313 \cdot y + 0.03812218492 \cdot y^2}{-0.4915880600 + 6.1800441958 \cdot y - 0.6524469236 \cdot y^2 + y^3} \end{aligned} \tag{3.160}$$

$$4.48 < y \leq 165.0$$

$$G_1(y) = \frac{e^{-y}}{\sqrt{y}} \cdot \frac{1.0174394594 + 0.5831679349 \cdot y}{0.9949036186 + y} \tag{3.161}$$

$$G_2(y) = \frac{e^{-y}}{\sqrt{y}} \cdot \frac{0.2847316689 + 0.5830684600 \cdot y}{0.3915531539 + y}.$$

For $y > 165$ the model assumes no radiation. With these one can simulate beamstrahlung emission by first drawing a random uniform number p. The condition $p > p_0$ corresponds to region A on Fig. 3.2, therefore no photons are emitted. In the other case a second random uniform number v is drawn, and Eq. 3.149 is computed. If $p < p_0 G(v, \xi)$ is satisfied (region C) a photon is emitted with an energy

$$\frac{E_\gamma}{E} = \frac{\xi v^3}{1 - (1 - \xi)v^3}, \tag{3.162}$$

otherwise no photon is emitted (region B). The generated beamstrahlung photons are themselves macroparticles in the sense that they represent the dynamics of all photons generated by all charges in a primary macroparticle.

Appendices

A1 Detailed explanation of "the boost" transformation

The reference frame transformation used in Sec. 3.2 can be written as [12, 6]:

$$\begin{pmatrix} \sigma^* \\ x^* \\ s^* \\ y^* \end{pmatrix} = A^{-1} {R_{\mathrm{CP}}}^{-1} L_{\mathrm{boost}} R_{\mathrm{CA}} R_{\mathrm{CP}} A \begin{pmatrix} \sigma \\ x \\ s \\ y \end{pmatrix} \tag{163}$$

Here A is the matrix transforming the accelerator coordinates (Courant-Snyder) to Cartesian coordinates:

$$\begin{pmatrix} ct \\ X \\ Z \\ Y \end{pmatrix} = A \begin{pmatrix} \sigma \\ x \\ s \\ y \end{pmatrix} = \begin{pmatrix} -1 & 0 & 1 & 0 \\ 0 & 1 & 0 & 0 \\ 0 & 0 & 1 & 0 \\ 0 & 0 & 0 & 1 \end{pmatrix} \begin{pmatrix} \sigma \\ x \\ s \\ y \end{pmatrix} \tag{164}$$

R_{CP} is a rotation matrix bringing the crossing plane to the $X - Z$ plane:

$$R_{\mathrm{CP}} = \begin{pmatrix} 1 & 0 & 1 & 0 \\ 0 & \cos\alpha & 0 & \sin\alpha \\ 0 & 0 & 1 & 0 \\ 0 & -\sin\alpha & 0 & \cos\alpha \end{pmatrix} \tag{165}$$

R_{CA} is a rotation matrix moving to the barycentric reference frame (in which the two beams are symmetric with respect to the s-axis):

$$R_{\mathrm{CA}} = \begin{pmatrix} 1 & 0 & 0 & 0 \\ 0 & \cos\phi & \sin\phi & 0 \\ 0 & -\sin\phi & \cos\phi & 0 \\ 0 & 0 & 0 & 1 \end{pmatrix} \tag{166}$$

L_{boost} is the matrix defining a Lorentz boost in the direction of the rotated X-axis:

$$L_{\mathrm{boost}} = \begin{pmatrix} 1/\cos\phi & -\tan\phi & 0 & 0 \\ -\tan\phi & 1/\cos\phi & 0 & 0 \\ 0 & 0 & 1 & 0 \\ 0 & 0 & 0 & 1 \end{pmatrix} \tag{167}$$

The momenta are transformed similarly [6]:

$$\begin{pmatrix} \delta^* \\ p_x^* \\ h^* \\ p_y^* \end{pmatrix} = B^{-1} {R_{\mathrm{CP}}}^{-1} L_{\mathrm{boost}} R_{\mathrm{CA}} R_{\mathrm{CP}} B \begin{pmatrix} \delta \\ p_x \\ h \\ p_y \end{pmatrix} \tag{168}$$

where the transformation from accelerator to Cartesian coordinates given by:

$$\begin{pmatrix} E/c - p_0 \\ P_x \\ P_z - p_0 \\ P_y \end{pmatrix} = p_0 \begin{pmatrix} 1 & 0 & 0 & 0 \\ 0 & 1 & 0 & 0 \\ 0 & 0 & -1 & 0 \\ 0 & 0 & 0 & 1 \end{pmatrix} \begin{pmatrix} \delta \\ p_x \\ h \\ p_y \end{pmatrix} \tag{169}$$

As explaned in Sec.3.2 not all particles with $s = 0$ are fixed points of the transformation, therefore a drift back to s=0 needs to be performed as we are tracking w.r.t. s and not w.r.t. time. The net effect of the transformation is to move from the reference frame of the weak beam to the boosted barycentric frame.

A2 Constant charge slicing

We consider a Gaussian longitudinal bunch distribution:

$$\lambda(z) = \frac{1}{\sigma_z \sqrt{2\pi}} e^{-\frac{z^2}{2\sigma_z^2}} \tag{170}$$

We introduce the cumulative distribution function:

$$Q(z) = \int_{-\infty}^{z} \lambda(z')dz' = \frac{1}{2} + \frac{1}{2}\mathrm{erf}\left(\frac{z}{\sqrt{2}\sigma_z}\right) \tag{171}$$

We define longitudinal cuts z_n^{cut} such that the bunch is sliced in N sections having the same charge:

$$Q(z_n^{\mathrm{cut}}) = \frac{n}{N} \tag{172}$$

Replacing 172 in 171 we obtain:

$$z_n^{\mathrm{cut}} = \sqrt{2}\sigma_z \mathrm{erf}^{-1}\left(\frac{2n}{N} - 1\right) \tag{173}$$

For each slice we need to find the longitudinal centroid position. For generic slice having edges z_1 and z_2 the centroid position can be written as:

$$z^{centroid} = \frac{1}{Q(z_2) - Q(z_1)} \int_{z_1}^{z_2} z\lambda(z)dz = \frac{\sigma_z}{\sqrt{2\pi}\,(Q(z_2) - Q(z_1))} \left(e^{-\frac{z_1^2}{2\sigma_z^2}} - e^{-\frac{z_2^2}{2\sigma_z^2}} \right) \tag{174}$$

A3 Considerations on the Σ-matrix description

Given the reduced Σ-matrix of the beam (including only position terms, no momenta):

$$\Sigma = \begin{pmatrix} \Sigma_{11} & \Sigma_{13} \\ \Sigma_{13} & \Sigma_{33} \end{pmatrix} \tag{175}$$

the distribution for a Gaussian beam can be written as:

$$\rho(\mathbf{x}) = \rho_0 e^{-\mathbf{x}^{\mathrm{T}}\Sigma^{-1}\mathbf{x}} \tag{176}$$

Points having same density lie con ellipses defined by the equation:

$$\mathbf{x}^{\mathrm{T}}\Sigma^{-1}\mathbf{x} = \text{const.} \tag{177}$$

As Σ is symmetric, it can be diagonalized:

$$\Sigma = \mathbf{V}\mathbf{W}\mathbf{V}^{T} \tag{178}$$

where the matrix **V** has in its columns the eigenvectors of Σ and **W** is a diagonal matrix with the corresponding eigenvalues:

$$W = \begin{pmatrix} \hat{\Sigma}_{11} & 0 \\ 0 & \hat{\Sigma}_{33} \end{pmatrix} \tag{179}$$

V is a unitary matrix (eigenvectors are ortho-normal):

$$\mathbf{V}\mathbf{V}^{T} = \mathbf{I} \Rightarrow \mathbf{V}^{-1} = \mathbf{V}^{T} \tag{180}$$

V can be used to transform coordinates from the initial frame to the de-coupled frame: where $\hat{\mathbf{x}}$ are the coordinates in the decoupled frame, i.e. the projections of of **x** on the eigenvectors:

$$\hat{\mathbf{x}} = \mathbf{V}^{T}\mathbf{x} \tag{181}$$

Combining Eqs. 178 and 180 we can write:

$$\Sigma^{-1} = \mathbf{V}\mathbf{W}^{-1}\mathbf{V}^{T} \tag{182}$$

This can be replaced in Eq. 177, re-writing the equation of the ellipse as:

$$\mathbf{x}^{\mathrm{T}}\mathbf{V}\mathbf{W}^{-1}\mathbf{V}^{T}\mathbf{x} = \text{const.} \tag{183}$$

Using Eq. 181 we obtain the equation of the ellipse in the reference system of the eigenvectors:

$$\hat{\mathbf{x}}^{\mathrm{T}}\mathbf{W}^{-1}\hat{\mathbf{x}} = \text{const.} \tag{184}$$

which can be rewritten in the familiar form:

$$\frac{\hat{x}^2}{\hat{\Sigma}_{11}} + \frac{\hat{y}^2}{\hat{\Sigma}_{33}} = \text{const.} \tag{185}$$

Once the Σ-matrix is assigned, the one-sigma ellipse can be drawn by the following procedure:

- We diagonalize Σ and we generate an auxiliary matrix defined as:

$$\mathbf{A} = \mathbf{V}\sqrt{\mathbf{W}}\mathbf{V}^T \tag{186}$$

- We generate a set of points in the unitary circle

$$\mathbf{z} = \begin{bmatrix} \cos t \\ \sin t \end{bmatrix} \tag{187}$$

- We apply $\mathbf{A}$ to t to generate points on the one-sigma ellipse:

$$\mathbf{x}_{1\sigma} = \mathbf{A}\mathbf{z} \tag{188}$$

This can be verified as follows:

$$\begin{aligned} {\mathbf{x}_{1\sigma}}^{\mathrm{T}}\Sigma^{-1}\mathbf{x}_{1\sigma} &= \mathbf{z}^{\mathrm{T}}\mathbf{A}^{\mathrm{T}}\Sigma^{-1}\mathbf{A}\mathbf{z} = \mathbf{z}^{\mathrm{T}}(\mathbf{V}\sqrt{\mathbf{W}}\mathbf{V})(\mathbf{V}^T\mathbf{W}^{-1}\mathbf{V}^T)(\mathbf{V}\sqrt{\mathbf{W}}\mathbf{V}^T)\mathbf{z} \\ &= \mathbf{z}^{\mathrm{T}}\mathbf{V}\sqrt{\mathbf{W}}\mathbf{W}^{-1}\sqrt{\mathbf{W}}\mathbf{V}^T\mathbf{z} = \mathbf{z}^{\mathrm{T}}\mathbf{V}\mathbf{V}^T\mathbf{z} = \mathbf{z}^{\mathrm{T}}\mathbf{z} = 1 \end{aligned} \tag{189}$$

Chapter 4

Configuration of beam-beam lenses

4.1 Introduction

The effects of the non-linear forces introduced by beam-beam interactions in the Large Hadron Collider (LHC) are studied with tracking simulations using, for example, the SixTrack and sixtracklib codes [11, 25]. In these simulations the beam-beam interactions are modeled by a set of "thin" non-linear lenses around the collision points. "6D beam-beam lenses" based on Hirata's synchro-beam method [12, 26, 13] are used to model the Head-On (HO) interactions at the for interaction points (IPs) while simpler "4D lenses" are used to model parasitic Long-Range encounters [27].
This document describes a method to configure the beam-beam lenses in tracking simulations based on the MAD-X model of the accelerator, as it has been implemented in the pymask configuration tool [28], which has been recently developed as an evolution of existing tools in MAD-X scripting language [29]. In particular, in Sec. 4.2, we discuss how to reconstruct the absolute position of the two beams with respect to the lab frame using the MAD-X twiss and survey tables; in Sec. 4.3 we discuss how to compute the separation between the two beams; in Sec. 4.4 we describe how to identify the crossing plane and crossing angle; in Sec. 4.5 we describe how to configure the anticlockwise beam (conventionally called beam 4) from the MAD-X model based on two clockwise-oriented sequences; in Sec. 4.6 we introduce the effect of crab cavities on the beam-beam configuration.

4.2 Identification of the beam position and direction

The position and orientation of the beams at a certain machine element can be obtained from MAD-X combining the information from the survey and twiss tables.
We assume that:

- The sequences start from an element at which the reference trajectories of the two beams are known to be parallel;
- Both beams (B1 and B2) have the same orientation (clockwise);
- Markers or beam-beam lenses are installed at the s-locations of the beam-beam interactions.

The MAD-X survey provides the coordinates in the lab frame of the two beams:

$$\mathbf{P}^{\mathrm{su}} = \begin{pmatrix} x^{\mathrm{su}} \\ y^{\mathrm{su}} \\ s^{\mathrm{su}} \end{pmatrix} \tag{4.1}$$

and the corresponding set of angles $(\theta^{\mathrm{su}}, \phi^{\mathrm{su}}, \psi^{\mathrm{su}})$ defining the orientation of the local reference system used by the twiss [30]. The origin and the orientation of the lab frame are defined by the the first element in the sequence.
The components of the unit vectors defining the local reference frame with respect to the lab frame can be obtained from the following relationship:

$$\begin{aligned} &(\hat{\mathbf{e}}_x, \hat{\mathbf{e}}_y, \hat{\mathbf{e}}_s) = \\ &\begin{pmatrix} \cos\theta^{\mathrm{su}} & 0 & \sin\theta^{\mathrm{su}} \\ 0 & 1 & 0 \\ -\sin\theta^{\mathrm{su}} & 0 & \cos\theta^{\mathrm{su}} \end{pmatrix} \times \begin{pmatrix} 1 & 0 & 0 \\ 0 & \cos\phi^{\mathrm{su}} & \sin\phi^{\mathrm{su}} \\ 0 & -\sin\phi^{\mathrm{su}} & \cos\phi^{\mathrm{su}} \end{pmatrix} \times \begin{pmatrix} \cos\psi^{\mathrm{su}} & -\sin\psi^{\mathrm{su}} & 0 \\ \sin\psi^{\mathrm{su}} & \cos\psi^{\mathrm{su}} & 0 \\ 0 & 0 & 1 \end{pmatrix}. \end{aligned} \tag{4.2}$$

The MAD-X twiss provides the transverse position of the beam in the local reference frame $(x^{\mathrm{tw}}, y^{\mathrm{tw}})$, so that the absolute position of the beam in the lab frame can written as

$$\mathbf{P} = \mathbf{P}^{\mathrm{su}} + x^{\mathrm{tw}}\hat{\mathbf{e}}_x + y^{\mathrm{tw}}\hat{\mathbf{e}}_y\,. \tag{4.3}$$

At the beam-beam locations the local reference frames for the two beams are assumed to be aligned. This is not strictly the case in the regions between the separation-recombination magnets (D1 and D2), but also in that case that case the existing small divergence can be considered negligible. The beam-beam module of pymask checks the conditions:

$$||\hat{\mathbf{e}}_x^{\mathrm{b1}} - \hat{\mathbf{e}}_x^{\mathrm{b2}}|| \ll 1\,, \tag{4.4}$$

$$||\hat{\mathbf{e}}_y^{\mathrm{b1}} - \hat{\mathbf{e}}_y^{\mathrm{b2}}|| \ll 1\,. \tag{4.5}$$

Therefore we will simply define:

$$\hat{\mathbf{e}}_x = \hat{\mathbf{e}}_x^{\mathrm{b1}} = \hat{\mathbf{e}}_x^{\mathrm{b2}}\,, \tag{4.6}$$

$$\hat{\mathbf{e}}_y = \hat{\mathbf{e}}_y^{\mathrm{b1}} = \hat{\mathbf{e}}_y^{\mathrm{b2}}\,. \tag{4.7}$$

4.3 Computation of beam-beam separations

The beam-beam separations are defined as the transverse coordinates of the strong beam with respect to the weak beam. They can be computed as:

$$\Delta x = \hat{\mathbf{e}}_x \cdot \left(\mathbf{P}^S - \mathbf{P}^W\right)\,, \tag{4.8}$$

$$\Delta y = \hat{\mathbf{e}}_y \cdot \left(\mathbf{P}^S - \mathbf{P}^W\right)\,, \tag{4.9}$$

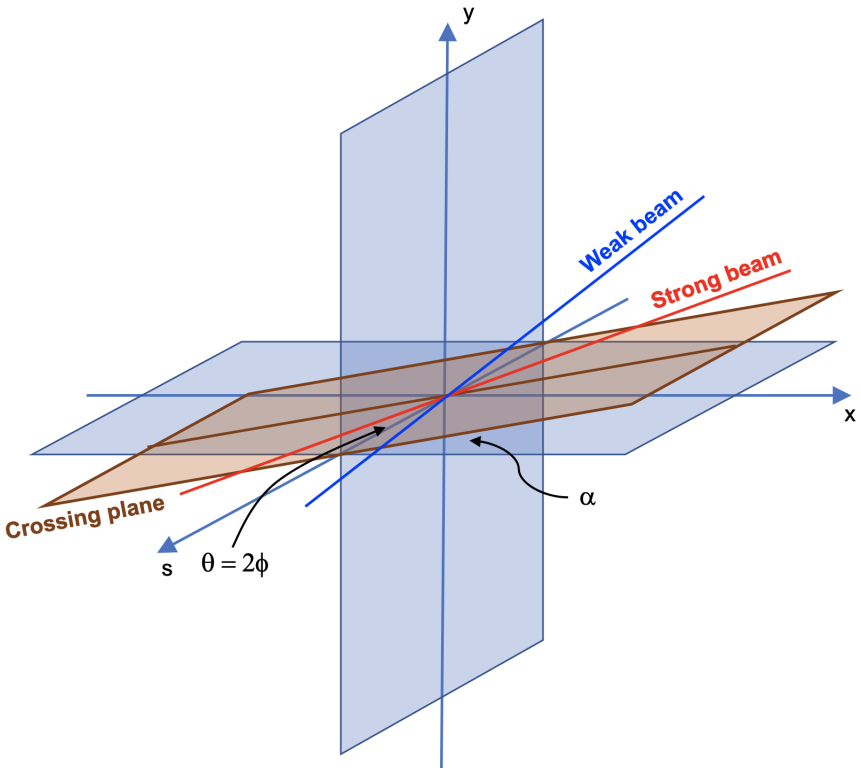

Figure 4.1: Schematic illustration of the crossing plane.

where the superscripts identify the weak (W) and the strong (S) beam.
Typically the accuracy of the survey table is insufficient to computed the separations correctly, especially for elements that are too far from the first element in the sequence, due to accumulation of errors along the sequence. A correction can be computed looking as the apparent displacement of the closest Interaction Point (IP) between the two surveys, as the IPs are supposed to coincide.

4.4 Crossing plane and crossing angle

At the beam-beam encounters the local reference frames for the two beams share the same orientation. Therefore the elevation angle α of the crossing plane and the crossing angle θ can be computed in the local reference frame, as will be illustrated in the following.

4.4.1 The crossing plane

The directions defined by the local trajectories of the two beams are identified by the unit vectors

$$\hat{\mathbf{p}}^W = \left(p_x^W, p_y^W, p_s^W\right) , \tag{4.10}$$

$$\hat{\mathbf{p}}^S = \left(p_x^S, p_y^S, p_s^S\right) , \tag{4.11}$$

containing the angles of the closed orbit obtained from the twiss of the two beams. The plane defined by these two directions is called Crossing Plane (XP), as illustrated in Fig. 4.1, and its equation is given by:

$$\mathbf{v}_{\mathrm{XP}}(w_1, w_2) = w_1 \hat{\mathbf{p}}^W + w_2 \hat{\mathbf{p}}^S \,. \tag{4.12}$$

The line defined by the intersection of the crossing plane and the transverse plane identified by the unit vectors $\hat{\mathbf{e}}_x$ and $\hat{\mathbf{e}}_y$ is given by the condition:

$$\mathbf{v}_{\mathrm{XP}}(w_1, w_2) \cdot \hat{\mathbf{e}}_s = 0 \,. \tag{4.13}$$

Replacing Eq. (4.12) into Eq. (4.13) we obtain:

$$w_1 p_s^W + w_2 p_s^S = 0 \,, \tag{4.14}$$

and replacing this condition in Eq. (4.12) we obtain the equation of the intersection line

$$\mathbf{v}_{\mathrm{T}}(w_1) = w_1 \left(\hat{\mathbf{p}}^W - \frac{p_s^W}{p_s^S} \hat{\mathbf{p}}^S \right) . \tag{4.15}$$

The elevation angle α of the intersection line with respect to the local x-direction ($\hat{\mathbf{e}}_x$) can be written as:

$$\alpha = \arctan \frac{\mathbf{v}_{\mathrm{T}} \cdot \hat{\mathbf{e}}_y}{\mathbf{v}_{\mathrm{T}} \cdot \hat{\mathbf{e}}_x} \,. \tag{4.16}$$

Using Eq. (4.15) we obtain:

$$\alpha = \arctan \frac{\left(p_y^W - \frac{p_s^W}{p_s^S} p_y^S \right)}{\left(p_x^W - \frac{p_s^W}{p_s^S} p_x^S \right)} . \tag{4.17}$$

In the paraxial approximation ($p_s^S \simeq p_s^W \simeq 1$) this simply becomes:

$$\alpha = \arctan \frac{\Delta p_y}{\Delta p_x} , \tag{4.18}$$

where we have defined:

$$\Delta p_x = p_x^W - p_x^S \,, \tag{4.19}$$

$$\Delta p_y = p_y^W - p_y^S \,. \tag{4.20}$$

In the legacy beam-beam macros as well as in the configuration pymask tool, the following logic is implemented

$$\alpha = \begin{cases} \arctan \left(\dfrac{\Delta p_y}{\Delta p_x} \right) & \text{if } |\Delta p_x| \geq |\Delta p_y| \\ \dfrac{\pi}{2} - \arctan \left(\dfrac{\Delta p_x}{\Delta p_y} \right) & \text{if } |\Delta p_x| < |\Delta p_y| \end{cases} , \tag{4.21}$$

for which α is limited to the range:

$$-\frac{\pi}{4} \leq \alpha \leq \frac{3}{4}\pi\,. \tag{4.22}$$

In particular, for a purely horizontal crossing we have $\alpha = 0$ and for a purely vertical crossing we have $\alpha = \frac{\pi}{2}$.

4.4.2 The crossing angle

The crossing angle θ between the two beams can be found from the relation:

$$\cos\theta = \hat{\mathbf{p}}^W \cdot \hat{\mathbf{p}}^S\,. \tag{4.23}$$

The half crossing angle

$$\phi = \frac{\theta}{2} \tag{4.24}$$

is often used instead of θ.
In the paraxial approximation

$$p_x \ll 1\,, \tag{4.25}$$
$$p_y \ll 1\,, \tag{4.26}$$
$$\tag{4.27}$$

the scalar product in Eq. (4.23) can be rewritten as

$$\begin{aligned}
\hat{\mathbf{p}}^W \cdot \hat{\mathbf{p}}^S &= p_x^W p_x^S + p_y^W p_y^S + p_s^W p_s^S \\
&= p_x^W p_x^S + p_y^W p_y^S + \sqrt{1-\left(p_x^W\right)^2 - \left(p_y^W\right)^2}\sqrt{1-\left(p_x^S\right)^2 - \left(p_y^S\right)^2} \\
&\simeq p_x^W p_x^S + p_y^W p_y^S + \left(1 - \frac{\left(p_x^W\right)^2}{2} - \frac{\left(p_y^W\right)^2}{2}\right)\left(1 - \frac{\left(p_x^S\right)^2}{2} - \frac{\left(p_y^S\right)^2}{2}\right) \\
&\simeq p_x^W p_x^S + p_y^W p_y^S + 1 - \frac{\left(p_x^W\right)^2}{2} - \frac{\left(p_y^W\right)^2}{2} - \frac{\left(p_x^S\right)^2}{2} - \frac{\left(p_y^S\right)^2}{2},
\end{aligned} \tag{4.28}$$

which can be written in compact form as:

$$\hat{\mathbf{p}}^W \cdot \hat{\mathbf{p}}^S \simeq 1 - \frac{\left(p_x^W - p_x^S\right)^2 + \left(p_y^W - p_y^S\right)^2}{2}. \tag{4.29}$$

For small crossing angle we can write:

$$\cos\theta \simeq 1 - \frac{\theta^2}{2}. \tag{4.30}$$

Replacing Eqs. (4.29) and (4.30) into Eq. (4.23) we obtain

$$|\theta| = \sqrt{\Delta p_x^2 + \Delta p_y^2}\,. \tag{4.31}$$

The sign of θ is defined positive when the weak beam needs to rotate in the clockwise sense in the crossing plane in order to be brought on the strong beam. This corresponds to the following sign choices:

	$\lvert\Delta p_x\rvert > \lvert\Delta p_y\rvert$	$\lvert\Delta p_x\rvert < \lvert\Delta p_y\rvert$
$\Delta p_x \geq 0,\ \Delta p_y \geq 0$	$\theta > 0$	$\theta > 0$
$\Delta p_x < 0,\ \Delta p_y \geq 0$	$\theta < 0$	$\theta > 0$
$\Delta p_x < 0,\ \Delta p_y < 0$	$\theta < 0$	$\theta < 0$
$\Delta p_x \geq 0,\ \Delta p_y < 0$	$\theta > 0$	$\theta < 0$

which are consistent with the sign convention used in LHC operation.

4.5 Transformations for the counterclockwise beam (B4)

The typically used MAD-X model of the LHC consists of two sequences both having clockwise (CW) orientation, conventionally called Beam 1 and Beam 2. To perform tracking simulations of the anticlockwise (ACW) beam, an anticlockwise sequence needs to be generated, which is conventionally called Beam 4. The beam-beam lenses in the Beam 4 sequence can be configured based on the beam-beam lenses defined in Beam 2, taking into account that the two are related by the following change of coordinates:

$$x^{\mathrm{ACW}} = -x^{\mathrm{CW}}, \tag{4.32}$$
$$y^{\mathrm{ACW}} = +y^{\mathrm{CW}}, \tag{4.33}$$
$$s^{\mathrm{ACW}} = -s^{\mathrm{CW}}. \tag{4.34}$$

The corresponding transformation for the transverse momenta is:

$$p_x^{\mathrm{ACW}} = +p_x^{\mathrm{CW}}, \tag{4.35}$$
$$p_y^{\mathrm{ACW}} = -p_y^{\mathrm{CW}}. \tag{4.36}$$

This can be easily seen from the fact that:

$$p_x \simeq \frac{dx}{ds}, \tag{4.37}$$
$$p_y \simeq \frac{dy}{ds}. \tag{4.38}$$

Additionally, from Eqs. (4.32) - (4.36) it is possible to derive the following relations to

transform the Σ-matrix [26] of the strong beam:

$$\Sigma_{11}^{\mathrm{ACW}} = +\Sigma_{11}^{\mathrm{CW}}\,, \tag{4.39}$$
$$\Sigma_{12}^{\mathrm{ACW}} = -\Sigma_{12}^{\mathrm{CW}}\,, \tag{4.40}$$
$$\Sigma_{13}^{\mathrm{ACW}} = -\Sigma_{13}^{\mathrm{CW}}\,, \tag{4.41}$$
$$\Sigma_{14}^{\mathrm{ACW}} = +\Sigma_{14}^{\mathrm{CW}}\,, \tag{4.42}$$
$$\Sigma_{22}^{\mathrm{ACW}} = +\Sigma_{22}^{\mathrm{CW}}\,, \tag{4.43}$$
$$\Sigma_{23}^{\mathrm{ACW}} = +\Sigma_{23}^{\mathrm{CW}}\,, \tag{4.44}$$
$$\Sigma_{24}^{\mathrm{ACW}} = -\Sigma_{24}^{\mathrm{CW}}\,, \tag{4.45}$$
$$\Sigma_{33}^{\mathrm{ACW}} = +\Sigma_{33}^{\mathrm{CW}}\,, \tag{4.46}$$
$$\Sigma_{34}^{\mathrm{ACW}} = -\Sigma_{34}^{\mathrm{CW}}\,, \tag{4.47}$$
$$\Sigma_{44}^{\mathrm{ACW}} = +\Sigma_{44}^{\mathrm{CW}}\,. \tag{4.48}$$
$$\tag{4.49}$$

4.6 Crab crossing

To discuss the effect of crab cavities, we define along the bunches of Beam 1 and Beam 2 (sharing the same s coordinate as in the MAD-X model), the longitudinal coordinates z_1 and z_2, oriented like s.
Assuming that the slices with $z_1 = z_2 = 0$ collide at s=0, the collision point (CP) for two generic slices z_1 and z_2 is at the location:

$$s_{\mathrm{CP}} = \frac{z_1 + z_2}{2}\,. \tag{4.50}$$

In the absence of crab crossing, the transverse position of the two beams is independent from z:

$$x_1 = +\phi s\,, \tag{4.51}$$
$$x_2 = -\phi s\,. \tag{4.52}$$

Ideal crab cavities, in the linear approximation, introduce a z-dependent orbit correction such that:

$$x_1(s) = +\phi s + \phi_c z_1\,, \tag{4.53}$$
$$x_2(s) = -\phi s - \phi_c z_2\,, \tag{4.54}$$

where ϕ_c is the crabbing angle and we assume, without loss of generality, horizontal crabbing plane.
The separation of the two slices at their collision point is obtained replacing (4.50) into (4.53) and (4.54):

$$\Delta x(s_{\mathrm{CP}}) = x_2(s_{\mathrm{CP}}) - x_1(s_{\mathrm{CP}}) = -(\phi + \phi_c)(z_1 + z_2)\,. \tag{4.55}$$

If $\phi_c = -\phi$, the separation is zero independently of z_1 and z_2 (perfect crabbing).
The crab crossing in the IPs of the HL-LHC for the clockwise and anticlockwise beams is illustrated with the relevant sign conventions in Figs. 4.2 - 4.5.

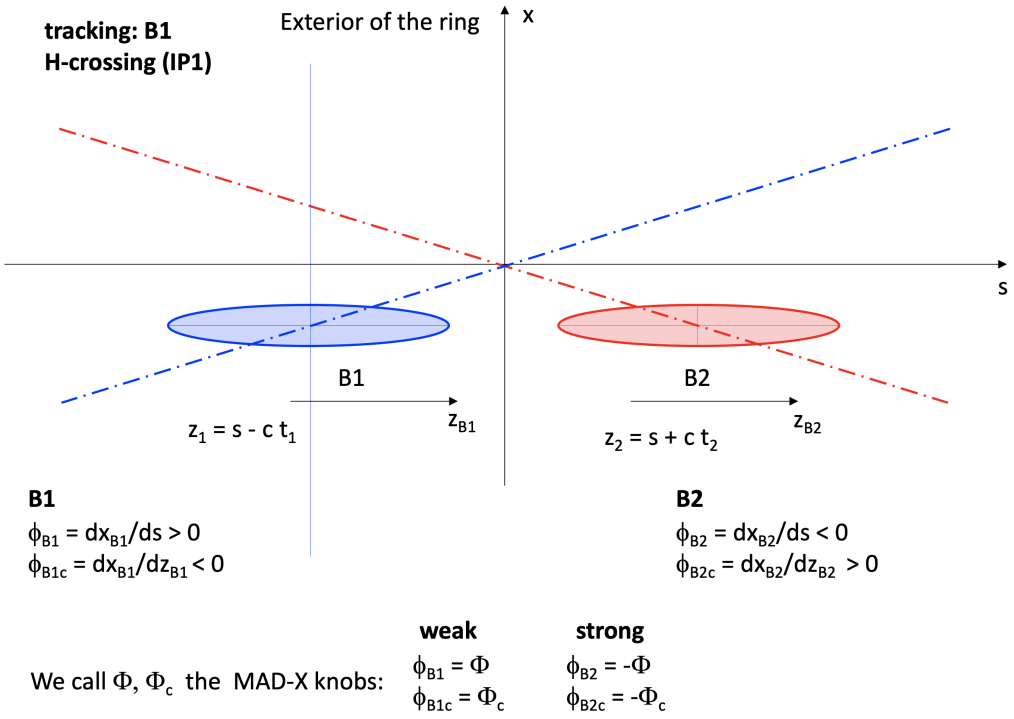

Figure 4.2: Crab crossing in the IP1 of the HL-LHC modeled for the tracking of the clockwise beam (beam 1).

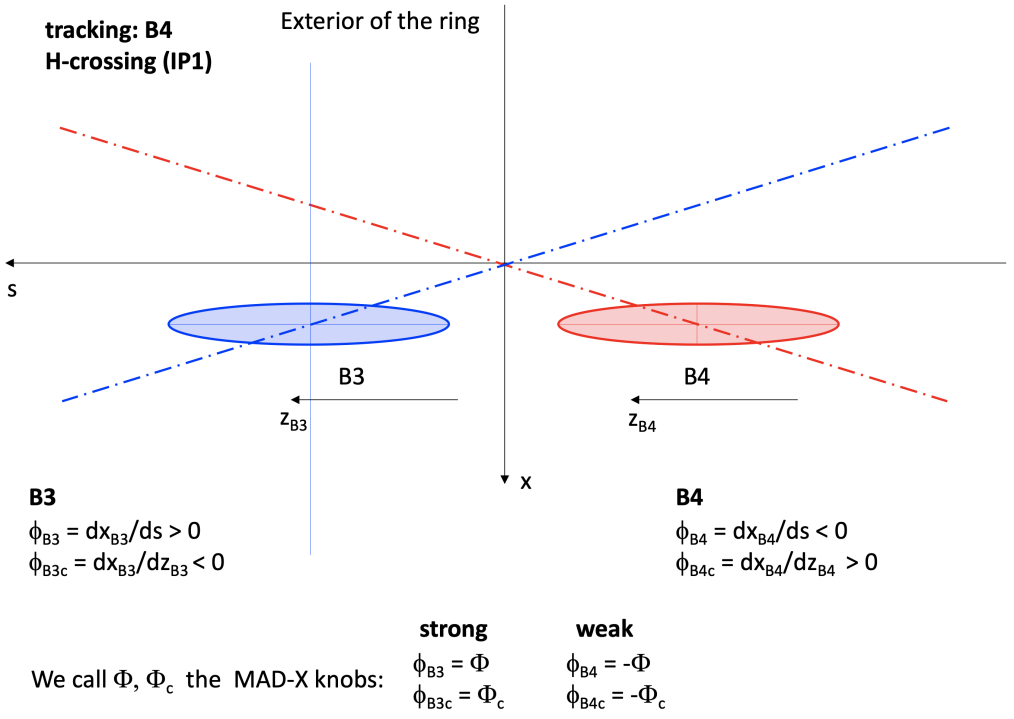

Figure 4.3: Crab crossing in the IP1 of the HL-LHC modeled for the tracking of the anticlockwise beam (beam 4).

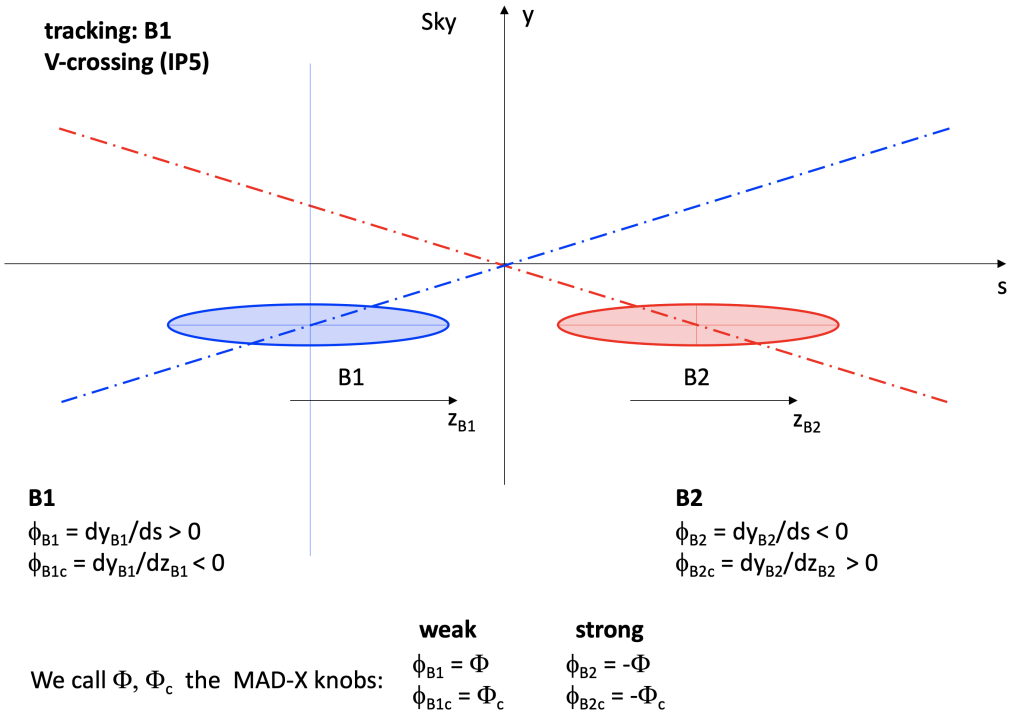

Figure 4.4: Crab crossing in the IP5 of the HL-LHC modeled for the tracking of the clockwise beam (beam 1).

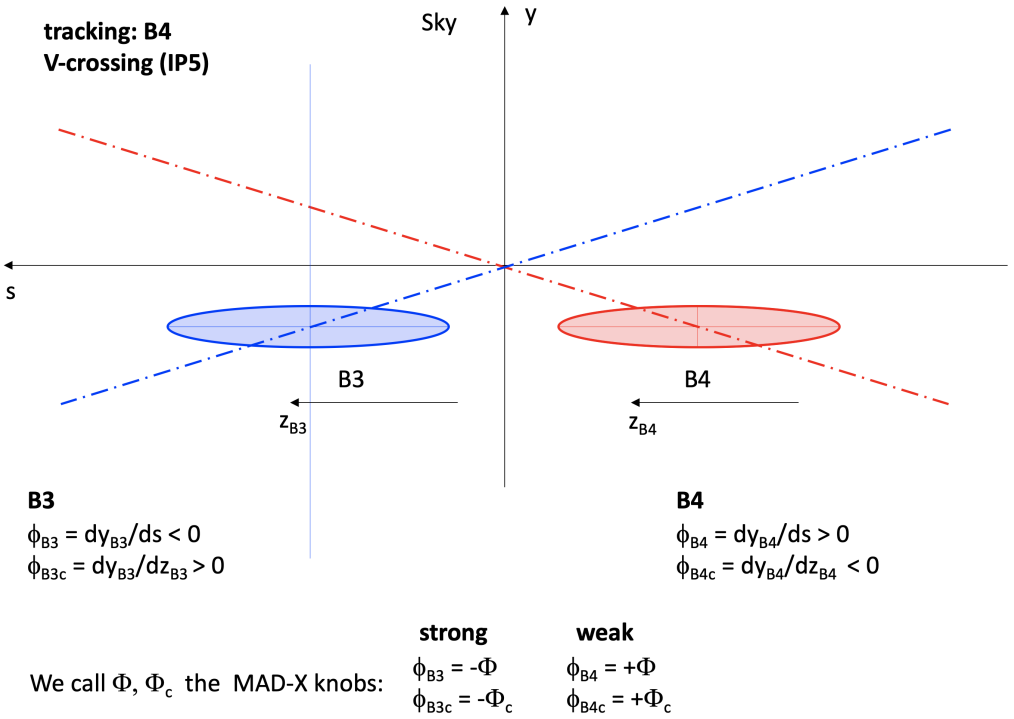

Figure 4.5: Crab crossing in the IP5 of the HL-LHC modeled for the tracking of the anticlockwise beam (beam 4).

4.6.1 Configuration of beam-beam lenses for beam 1

In order to model the HO interaction for a crab crossing, the "strong bunch" is sliced longitudinally using the constant charge method, and one beam-beam lens for each slice is installed in the sequence.
In particular, in the sequence of beam 1, the lens corresponding to a slice of the strong beam (beam 2) having longitudinal coordinate $z_2 = Z_2$ is installed at the location where the slice encounters the synchronous particle of the weak beam (see Eq. (4.50) with $z_1 = 0$):

$$s_{\text{lens}} = +\frac{Z_2}{2}\,. \tag{4.56}$$

The position of the strong beam at the lens can be found replacing Eq. (4.56) into Eq. (4.54):

$$X_2 = -s_{\text{lens}}(\phi + 2\phi_c)\,. \tag{4.57}$$

The effect of the crab bump alone is given by:

$$X_2^{\text{crab}} = -2\phi_c s_{\text{lens}} = -\phi_c Z_2\,. \tag{4.58}$$

Taking into account the RF curvature coming from the crab cavity frequency, the position of the slice at the beam-beam lens can be written as:

$$X_2^{\text{crab}} = -\phi_c \frac{L_{\text{ring}}}{2\pi h_{\text{CC}}} \sin\left(\frac{2\pi h_{\text{CC}}}{L_{\text{ring}}} Z_2\right) = -\phi_c \frac{L_{\text{ring}}}{2\pi h_{\text{CC}}} \sin\left(\frac{2\pi h_{\text{CC}}}{L_{\text{ring}}} 2s_{\text{lens}}\right)\,, \tag{4.59}$$

where h_{CC} is the harmonic number of the crab cavity and L_{ring} is the circumference of the ring.

4.6.2 Configuration of beam-beam lenses for beam 2

In the sequence of beam 2, we install the beam-beam lens for a slice of the strong beam (beam 1) having longitudinal coordinate $z_1 = Z_1$ at the location where the slice encounters the synchronous particle of the weak beam, (see Eq. (4.50) with $z_2 = 0$):

$$s_{\text{lens}} = \frac{Z_1}{2}\,. \tag{4.60}$$

The position of the strong beam at the lens can be found replacing Eq. (4.60) into Eq. (4.53):

$$X_1 = s_{\text{lens}}(\phi + 2\phi_c)\,. \tag{4.61}$$

The effect of the crab bump alone is given by:

$$X_1^{\text{crab}} = 2\phi_c s_{\text{lens}} = \phi_c Z_1\,. \tag{4.62}$$

Taking into account the RF curvature coming from the crab cavity frequency, the position of the slice at the beam-beam lens can be written as:

$$X_1^{\text{crab}} = \phi_c \frac{L_{\text{ring}}}{2\pi h_{\text{CC}}} \sin\left(\frac{2\pi h_{\text{CC}}}{L_{\text{ring}}} Z_1\right) = \phi_c \frac{L_{\text{ring}}}{2\pi h_{\text{CC}}} \sin\left(\frac{2\pi h_{\text{CC}}}{L_{\text{ring}}} 2s_{\text{lens}}\right)\,. \tag{4.63}$$

From Eqs. (4.59) and (4.63), we find that for lenses at the same longitudinal position s_{lens} the corresponding slices of the two beams $Z_1 = Z_2 = 2s_{\text{lens}}$ have opposite transverse coordinates:

$$X_1^{\text{crab}} = -X_2^{\text{crab}}\,. \tag{4.64}$$

4.6.3 Crab bump from MAD-X twiss

For a non-ideal crabbing, for example in the presence of a non-closure of the crab-bump, the realistic z-dependent orbit distortion introduced by the crab cavities can be characterized using the MAD-X twiss, by installing orbit correctors at the position of the crab cavities that introduce the crab cavity deflection as seen at a certain reference position along the bunch z_{ref}. To obtain the effect on particles at different positions along bunch it is possible to apply the following scaling:

$$x\left(z\right) = x\left(z_{\text{ref}}\right) \frac{\sin\left(\frac{2\pi h_{\text{CC}}}{L_{\text{ring}}} z\right)}{\sin\left(\frac{2\pi h_{\text{CC}}}{L_{\text{ring}}} z_{\text{ref}}\right)}. \tag{4.65}$$

4.7 Step-by-step configuration procedure

Based on the method introduced in the previous sections, the following procedure has been implemented in pymask to configure the beam-beam lenses in the sixtrack and sixtracklib tracking model:

1. Inactive beam-beam lenses (not configured) are installed in both clockwise sequences (Beam 1 and Beam 2) at the locations of the HO and LR beam-beam encounters. As discussed in Sec. 4.6, at each IP a set of lenses is installed to model the HO, one corresponding to each bunch slice.

2. The MAD-X twiss and survey tables are computed for both clockwise sequences.

3. The transverse beam shapes (Σ-matrix) are extracted from the twiss table for all beam-beam lenses.

4. The positions of the beams at the beam-beam lenses in the lab frame are computed combining the information from the survey and twiss tables, as discussed in Sec. 4.2.

5. The beam-beam separations are computed, as discussed in Sec. 4.3.

6. For all HO interactions, the crossing plane and the crossing angle are identified, as discussed in Sec. 4.4.

7. The relevant quantities for the beam-beam lenses in the anticlockwise sequences (Beam 3 and Beam 4) are obtained from the data computed for the lenses in the clockwise sequences (Beam 1 and Beam 2), using the transformations described in Sec. 4.5.

8. The effect of the crab cavities is introduced by using the shape of the crab bumps obtained from twiss tables computed with orbit correctors at the locations of the cavities, as discussed in Sec. 4.6.

9. The information computed before is used to configure the beam-beam lenses in the MAD-X model of the sequence for which the tracking simulation will be performed, typically either Beam 1 or Beam 4.

10. The SixTrack input and the pysixtrack/sixtracklib input files are generated using the MAD-X model and the additional information computed as described above.

11. The closed orbit as computed from the MAD-X sequences is saved on file, for the generation of matched beam distributions and for the computation of the beam-beam dipolar kicks on the closed orbit, which are usually subtracted in weak-strong tracking simulations.

Acknowledgments

The authors would like to thank all the colleagues who have contributed to the development of the MAD-X tools for the configuration of tracking simulations, on which the present work is largely based, and have provided important input and support, in particular G. Arduini, J. Barranco Garcia, R. De Maria, S. Fartoukh, M. Giovannozzi, S. Kostoglou, E. Métral, Y. Papaphippou, D. Pellegrini, T. Pieloni and F. Van Der Veken.

Bibliography

[1] G. Ripken. Non-linear canonical equations of coupled synchro-betatron motion and their solutions within the framework of a non-linear six-dimensional (symplectic) tracking program for ultrarelativistic protons. Technical Report 85-084, DESY, 1985.

[2] D.P. Barber, G. Ripken, and F. Schmidt. A non-linear canonical formalism for the coupled synchro-betatron motion of protons with arbitrary energy. Technical Report 87-36, DESY, 1987.

[3] G. Ripken and F. Schmidt. A symplectic six-dimensional thin-lens formalism for tracking. Technical Report DESY 95-63 and CERN/SL/95-12(AP), DESY, CERN, 1995.

[4] K. Heinemann, G. Ripken, and F. Schmidt. Construction of nonlinear symplectic six-dimensional thin-lens maps by exponentiation. Technical Report 95-189, DESY, 1995.

[5] D.P. Barber, K. Heinemann, G. Ripken, and F. Schmidt. Symplectic thin-lens transfer maps for SIXTRACK: Treatment of bending magnets in terms of the exact hamiltonian. Technical Report 96-156, DESY, 1996.

[6] L.H.A. Leunissen, F. Schmidt, and G. Ripken. 6D beam-beam kick including coupled motion. Technical report, 2001.

[7] A. Latina and R. De Maria. RF multipole implementation. Technical report, CERN-ATS. 2012-088.

[8] E. Forest. *Beam Dynamics: A New Attitude and Framework*. Harcourt Academic Publisher, 1999.

[9] F. Willeke and G. Ripken. Methods of beam optics. Technical Report 88-114, DESY, 1988.

[10] F. C. Iselin. The mad program (methodical accelerator design) - physics methods manual. Technical Report CERN/SL/92-?? (AP), CERN, 1992.

[11] SixTrack Project website. `http://cern.ch/sixtrack`.

[12] K Hirata, H Moshammer, and F Ruggiero. A Symplectic Beam-Beam Interaction with Energy Change. *SLAC-PUB-10055*, Dec 2017.

[13] G Iadarola, R De Maria, and Y Papaphilippou. Modelling and implementation of the "6D" beam-beam interaction. *CERN-ACC- SLIDES-2018-001*, Dec 2017.

[14] Andrzej Wolski. *Beam dynamics in high energy particle accelerators*. World Scientific, 2014.

[15] D. Griffiths. *Introduction to elementary particles*. 2nd rev. version, Wiley, 2008.

[16] C. Weizsäcker. Ausstrahlung bei Stössen sehr schneller Elektronen. *in Zeitschrift Für Physik, vol. 88, Sep. 1934, pp. 612-625.* https://doi.org/10.1007/BF01333110.

[17] E. Williams. Correlation of certain collision problems with radiation theory. *in Kong. Dan. Vid. Sel. Mat. Fys. Med., vol. 13N4, 1935, pp. 1-50.* https://inspirehep.net/literature/1377275.

[18] D. Schulte. Study of electromagnetic and hadronic background in the interaction region of the TESLA collider. Apr. 1997. https://cds.cern.ch/record/331845.

[19] F. Arutyunian and V. Tumanian. The Compton effect on relativistic electrons and the possibility of obtaining high energy beams. *in Physics Letters, vol. 4, 1963, pp. 176-178.* https://doi.org/10.1016/0031-9163(63)90351-2.

[20] M. Bassetti and G. Erskine. Closed expression for the electrical field of a two-dimensional Gaussian charge. 1980. https://cds.cern.ch/record/122227.

[21] F. Halzen and A. Martin. *Quarks and Leptons: An Introductory Course in Modern Particle Physics*. 1984. http://www.gammaexplorer.com/wp-content/uploads/2014/03/Quarks-and-Leptons-An-Introductory-Course-in-Modern-Particle-Physics.pdf.

[22] GUINEA-PIG repository. https://gitlab.cern.ch/clic-software/guinea-pig-legacy.

[23] I. Ginzburg, G. Kotkin, V. Serbo, and V. Telnov. Colliding ge and gg beams based on the single-pass e±e- colliders (VLEPP type). *in Nuclear Instruments And Methods In Physics Research, vol. 205, pp. 47-68.*, 1983. https://www.sciencedirect.com/science/article/pii/0167508783901734.

[24] Kaoru Yokoya. A Computer Simulation Code for the Beam-beam Interaction in Linear Colliders. 10 1985. https://inspirehep.net/literature/218375.

[25] SixTrackLib source code repository. http://github.com/SixTrack/SixTrackLib.

[26] G Iadarola, R De Maria, and Y Papaphilippou. 6D beam-beam interaction step-by-step. *CERN-ACC-NOTE-2018-0023*, Dec 2017.

[27] W Herr and T Pieloni. Beam-Beam Effects. *in Proceedings of CAS - CERN Accelerator School: Advanced Accelerator Physics Course, 18 - 29 Aug 2013, Trondheim, Norway, CERN-2014-009*, 2014.

[28] LHC Mask Project webstite. `http://lhcmaskdoc.web.cern.ch`.

[29] Mad-X beam-beam macros, source code repository. `https://github.com/lhcopt/beambeam_macros`.

[30] MAD-X Project website. `http://cern.ch/madx`.